A ZERO-ASSIGNMENT APPROACH TO TWO-CHANNEL FILTER BANKS AND WAVELETS

A THESIS

SUBMITTED TO THE DEPARTMENT OF ELECTRICAL AND

ELECTRONICS ENGINEERING

AND THE INSTITUTE OF ENGINEERING AND SCIENCES

OF BILKENT UNIVERSITY

IN PARTIAL FULFILLMENT OF THE REQUIREMENTS

FOR THE DEGREE OF

MASTER OF SCIENCE

By

Mustafa Akbaş

September 2001

I certify that I have read this thesis and that in my opinion it is fully adequate, in scope and in quality, as a thesis for the degree of Master of Science.

Prof. Dr. A. Bülent Özgüler(Supervisor)

I certify that I have read this thesis and that in my opinion it is fully adequate, in scope and in quality, as a thesis for the degree of Master of Science.

Prof. Dr. Enis Çetin

I certify that I have read this thesis and that in my opinion it is fully adequate, in scope and in quality, as a thesis for the degree of Master of Science.

Prof. Dr. Erol Sezer

Approved for the Institute of Engineering and Sciences:

Prof. Dr. Mehmet Baray
Director of Institute of Engineering and Sciences

ABSTRACT

A ZERO-ASSIGNMENT APPROACH TO TWO-CHANNEL FILTER BANKS AND WAVELETS

Mustafa Akbaş
M.S. in Electrical and Electronics Engineering
Supervisor: Prof. Dr. A. Bülent Özgüler
September 2001

It is well-known that subband decomposition and perfect reconstruction of an arbitrary input signal is possible by a proper design of four filters. Besides having a wide range of applications in signal processing, perfect reconstruction filter banks have a strong connection with wavelets as pointed out by Mallat. Daubechies managed to design minimal order, maximally flat filters and she proposed a cascade algorithm to construct compactly supported orthogonal wavelets from the orthogonal perfect reconstruction filter banks. The convergence of the cascade algorithm requires at least one zero at $z = -1$ and $z = 1$ for the lowpass and the highpass filters, respectively. This thesis focuses on the design of two-channel filter banks with assigned zeros. The fact that causal, stable and rational transfer functions form a Euclidean domain is used to pose the problem in an abstract setup. A polynomial algorithm is proposed to design filter banks with filters having assigned zeros and a characterization of all solutions having the same zeros in terms of a free, even, causal, stable and rational transfer function is obtained. A generalization of Daubechies design of orthogonal filter banks is given. The free parameter can be used to improve the filter bank design and the design of

corresponding orthogonal or biorthogonal wavelets. The results also find an application in examining the robustness of regularity of minimal length compactly supported wavelets with respect to perturbation of filter zeros at 1 and -1.

Keywords: filter banks, perfect reconstruction, wavelets, zero assignment, Euclidean domain, polynomial algorithm.

ÖZET

MÜKEMMEL-YENİDEN-İNŞA SÜZGEÇ KÜMESİ VE DALGACIKLARDA SIFIR ATAMA

Mustafa Akbaş
Elektrik ve Elektronik Mühendisliği Bölümü Yüksek Lisans
Tez Yöneticisi: Prof. Dr. A. Bülent Özgüler
Eylül 2001

Herhangi bir giriş sinyali için bantlara ayrıştırma ve mükemmel-yeniden-inşanın mümkün olduğu bilinen bir gerçektir. Sinyal işleme alanındaki uygulamalara ek olarak Mallat tarafından gösterildiği gibi iki-kanallı süzgeç kümeleri dalgacık dönüşümü ile de yakından alakalıdır. Daubechies minimum derece, maksimum düz süzgeçler tasarladı ve dikgen mükemmel-yeniden-inşa süzgeç kümelerini kullanarak cascade algoritmasıyla dikgen dalgacıklar üretti. Cascade algoritmasının yakınsaması alçak geçirgen süzgecin $z = -1$'de ve yüksek geçirgen süzgecin $z = 1$'de en az birer sıfırlarının olmasına bağlıdır. Bu tez belli sıfırları haiz süzgeçlerden oluşan iki-kanallı mükemmel-yeniden-inşa süzgeç kümelerinin tasarımına odaklanmaktadır. Nedensel, kararlı ve rasyonel dönüşüm fonksiyonlarının bir Öklid alanı (domain) oluşturması gerçeği kullanılarak cebirsel bir metod önerilmiştir. Belli sıfırları olan süzgeçleri tasarlamak için bir polinom algoritması ortaya atılmıştır. Serbest çift, nedensel, kararlı ve rasyonel bir dönüşüm fonksiyonu yardımıyla aynı sıfırları haiz bütün çözümler elde edilmiştir. Bu yeni metod aynı zamanda Daubechies'nin tasarımının da bir genellemesidir. Serbest parametre kullanılarak daha gelişmiş süzgeçler ve bunlara karşılık gelen dikgen

veya çift dikgen dalgacıklar üretmek mümkündür. Sıfırlar üzerindeki kontrol kullanılarak -1 ve 1'deki sıfırların yerinden oynatılması durumunda dalgacıkların ne kadar değiştiği de incelenmiştir.

Anahtar kelimeler: süzgeç kümeleri, mükemmel-yeniden-inşa, dalgacık dönüşümü, sıfır atama, Öklid alanı, polinom algoritması.

ACKNOWLEDGMENTS

I gratefully thank my supervisor Prof. Dr. A. Bülent Özgüler for his supervision, guidance, and suggestions throughout the development of this thesis.

Contents

List of Figures

List of Tables

To whom it may concern . . .

Chapter 1

INTRODUCTION

A filter bank is a set of filters and multirate operators. It is used to split an arbitrary signal into different frequency bands and to process each band independently. A two-channel filter bank as the one in Figure 2.1 consists of two main parts called the analysis part and the synthesis part. The analysis part is used for decomposition whereas the synthesis part is used for reconstruction. There are four basic types of errors created in a filter bank during the reconstruction process: Aliasing, imaging, magnitude distortion and phase distortion. All these errors can be removed by a proper choice of the analysis and the synthesis filters. Filter banks finds applications in speech and image compression [1], the digital audio industry, statistical and adaptive signal processing, and in many other fields [20]. Filter bank like decompositions are very popular in image and speech processing, since such decompositions emulate human auditory and vision system [21]. Filter banks are also closely related to some time-frequency representations such as the wavelet transform [20].

The wavelet transform was introduced at the beginning of eighties. First, a French geophysicist Morlet used it as tool for an analysis of seismic data. Later, it was started to be widely used in all areas of signal processing. The

wavelet transform is a new tool for time-frequency analysis. It generalizes the *short-time Fourier transform* (STFT). In STFT, translations and modulations of a fixed window function is used. This leads to the same resolution at all frequencies. However, good time locality is needed at high frequencies and good frequency localization is needed at low frequencies. This is achieved by the wavelet transform. What made the wavelet transform popular is the existence of efficient and fast algorithms to compute wavelet coefficients. The theory of *multiresolution analysis* (MRA) combines the wavelet transform and the two-channel filter banks within the same framework [21]. MRA has a wide range of applications. According to Daubechies: "The history of the formulation of MRA is a beautiful example of applications stimulating theoretical development", [6]. Among the applications of the wavelet transform, there are subband coding, speech, image and video compression, denoising, feature detection, etc. Today, subband coding is one of the most successful technique for image coding [19]. Therefore, FBI uses the wavelet scalar quantization algorithm to store digitized fingerprints. It was initially expected that the JPEG standard would win, but the wavelet scalar quantization happened to be the winning algorithm [19].

Two-channel filter banks were first studied by Croiser, Esteban and Galland (1976) [3] who showed that it is possible to achieve perfect reconstruction (PR) by a proper design of analysis and synthesis filters. Their design used a certain type of quadrature mirror filters (QMF) which resulted in FIR filters of only two nonzero coefficients and, hence, poor frequency responses. In 1986 Smith and Barnwell [17] and in 1985 Mintzer [15] independently showed that it is possible to have FIR filters with more satisfactory frequency responses if the filters are selected so that they satisfy conjugate quadrature property. Their design is called alternating flip design. The resulting filters also satisfy orthogonality conditions.

After Mallat discovered the relation between orthogonal wavelets and PR orthogonal filter banks, the latter gained importance as it became possible to

implement a fast algorithm for discrete wavelet transform via filter banks [13]. PR filter bank theory was further improved by biorthogonal filter banks proposed by Vetterli [21] and general paraunitary matrix theory introduced by Vaidyanathan [20]. One of the most important works on the relation of filter banks and wavelets was performed by Daubechies. She proposed a method to design an orthogonal PR system with filters that are flat to any degree [6]. She also determined the minimum order filter that satisfy a specified degree of flatness.

Design of filter banks of increasing sophistication is of course possible due to the large degree of freedom one has in designing the analysis and synthesis filters. Even after satisfying the PR condition, a large degree of freedom still remains. Most desirable filter properties such as flatness, minimal-length, etc., all directly relate to number and location of the zeros in the filter transfer function. FIR filters can be thought of as all-zero filters so that they are completely characterized by their zeros.

In this thesis, we study the problem of assigning zeros to the filters that satisfy perfect reconstruction property. The problem is posed and solved in an algebraic framework which allows considering various different classes of filters at the same time. Our approach is similar in technique to the recent study of Sweldens and Daubechies [7] in which the fact that the Laurent polynomials form a Euclidean domain is exploited to construct increasingly sophisticated wavelets with various properties. The approach in this thesis differs significantly from that of [7] in that, here, the filters with *pre-assigned zeros* are constructed.

The main result of the thesis is stated in Theorem 1 which shows that (i) it is possible to design a PR filter bank with any assigned zeros and with poles in any desired region of the complex plane and (ii) all such filter banks can be characterized (described) based on a free parameter which consists of an even filter transfer function. The construction of a filter bank with assigned zeros is given in

an algorithm which uses polynomial algebra and spectral factorization. Theorem 1, when specialized to FIR filters, can be used to characterize minimal-length, conjugate quadrature (or QMF) filters with assigned zeros. This result is stated in Theorem 2. When the assigned zeros are fixed at $z = -1$ for lowpass filters and at $z = 1$ for highpass filters, Theorem 2 gives rise to Daubechies maximally flat filters and to the associated minimal length orthonormal wavelets, a celebrated result of [6]. The result of Theorem 2 is further applied in investigating the robustness with respect to perturbations in filter zeros of the regularity of minimal-length compactly supported wavelets of Daubechies.

The outline of the thesis is as follows. We begin with the structure of a two-channel filter bank in Chapter 2, where we introduce multirate operators and analysis and synthesis filters. In addition to traditional building blocks, in filter banks two new building blocks are used. These are downsamplers and upsamplers which are called multirate operators. They are linear but time varying systems. Both time and frequency domain characterization of them are given in the chapter. In Chapter 3, the definition of PR and some simple PR filter banks are given. In Chapter 4, continuous and discrete-time wavelet transform and the relation between the wavelet transform and two channel filter banks are explained. The axiomatic definition of the *multiresolution analysis* (MRA) is also given in the chapter. The cascade algorithm discovered by Daubechies [6] is explained and used to construct compactly supported wavelets from the orthogonal FIR filter banks. The main results of this thesis are in Chapter 5, where a method of constructing filter banks with filters having assigned zeros is given. Applications of the main result to Daubechies' wavelets are also given in this chapter.

In order to make this thesis accessible to system and control theorists as well as to researchers in signal processing, the introductory chapters on filter banks

and wavelets and the algebraic preliminaries in Chapter 5 are presented in as much detail as possible.

Chapter 2

STRUCTURE OF A FILTER BANK

In traditional single rate digital signal processing, building blocks are adders, multipliers (multiplication of two or more signals and multiplication by a scalar), delay elements and filters. In multirate signal processing, in addition to single rate operators, there are two new building blocks called M-fold downsampler and L-fold upsampler. This chapter concerns the structure of a filter bank which is a simple system for multirate signal processing. A brief review of all building blocks of a filter bank is given.

This chapter is organized as follows: Section 2.1 gives a brief information on how filter banks operate. In Section 2.2, upsamplers and downsamplers, the basic operators of multirate signal processing, are explained. The input-output relation both in frequency-domain and in time-domain is stated. Section 2.3 deals with analysis and synthesis filters and their properties.

2.1 Introduction

Filter banks are used to separate an arbitrary signal into different frequency bands and then process each individual band independently. Figure 2.1 shows the general structure of a two-channel maximally decimated filter bank. An input signal is usually first filtered with a lowpass filter and a highpass filter in the two-channel filter banks. Analysis filters $H_1(z)$, $H_2(z)$ and 2-fold downsamplers form the analysis section. Maximally decimated means that the sum of reciprocals of downsampling ratios equals to 1. In the synthesis section there are upsamplers and synthesis filters $K_1(z)$ and $K_2(z)$. Subband signals $v_1[n]$ and $v_2[n]$ are in general further processed (quantization, subband coding) before entering the synthesis part. As a result of this further processing disturbances $d_1[n]$ and $d_2[n]$ are often created. In the literature both two-channel and M-channel filter banks are studied. However in this thesis we will concentrate on two-channel filter banks only. Moreover, we will assume throughout the thesis that disturbances $d_1[n]$ and $d_2[n]$ are both zero.

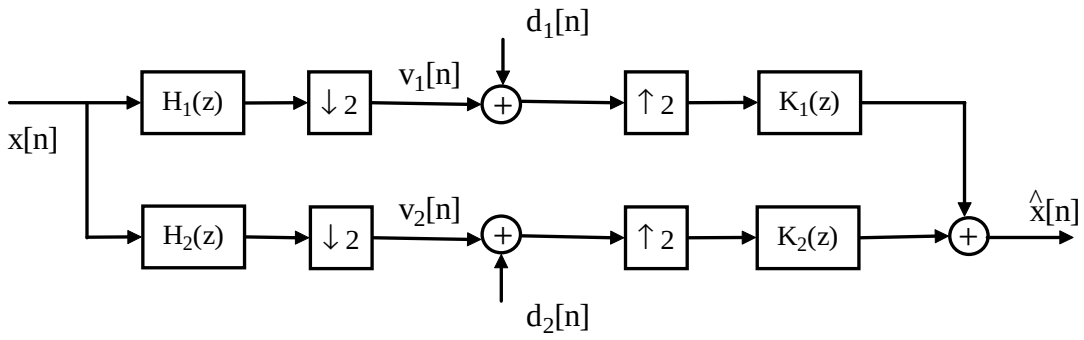

Figure 2.1: Two-channel maximally decimated filter bank structure.

2.2 Multirate Operators

The most basic operations in multirate signal processing are downsampling and upsampling. They are used to change the sampling rate. We will analyze upsampling and downsampling both in time-domain and in frequency-domain. Time domain analysis is useful to understand how they operate. Frequency domain analysis provides a simpler analysis of the overall filter bank.

2.2.1 Downsampling

Downsampling, which is also called subsampling or decimation, is used to decrease number of samples in subband signals $v_k[n]$. Figure 2.2 shows an M-fold downsampler.

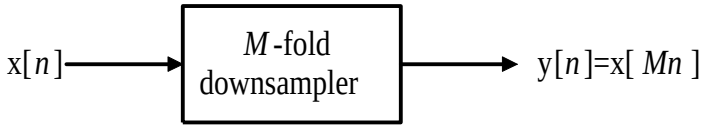

Figure 2.2: M-fold downsampler.

Downsampling in Time Domain

An M-fold downsampler keeps every M^{th} sample of its input and discards the rest. Therefore, in time domain we can express it as follows:

$$y[n] = x[Mn] \tag{2.1}$$

Obviously, downsampling is not causal. Moreover it is not time invariant. Figure 2.3 illustrates decimation for $M = 2$. The most obvious result of downsampling is a decrease in the number of samples. Therefore, for $M = 2$ unless the input is constructed from samples of a continuous time signal with sampling rate more

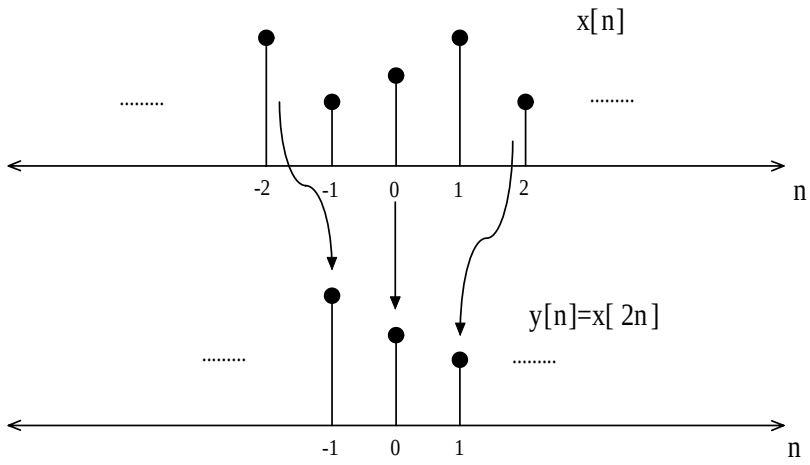

Figure 2.3: Downsampling for M=2 in time domain.

than twice the Nyquist rate [1], the basic consequence of downsampling operation is aliasing. This is more obvious in frequency domain.

Downsampling in Frequency Domain

Frequency domain relation between input and the output for an M-fold downsampler is

$$Y(e^{jw}) = \frac{1}{M}\sum_{k=0}^{M-1} X(e^{j(w-2\pi k)/M}), \tag{2.2}$$

which means that the input spectrum is expanded by a factor of M and then it is shifted by an amount of $2\pi k$ for $k = 0, 1, ..., M-1$. The final spectrum of the output is constructed as the superposition of all expanded and shifted spectra. Sometimes it is better to write the input-output relation in the z-domain. In that case we have

$$Y(z) = \frac{1}{M}\sum_{k=0}^{M-1} X(z^{1/M} W_M^k), \tag{2.3}$$

where $W_M^k = e^{-j2\pi k/M}$. Figure 2.4 illustrates downsampling in frequency domain for M=2. Downsamplers are in general sources of aliasing in a filter bank. The

[1] Nyquist rate is the minimum sampling frequency that prevents aliasing and allows reconstruction of a bandlimited signal from its samples. It is twice the maximum frequency that the continuous signal contains.

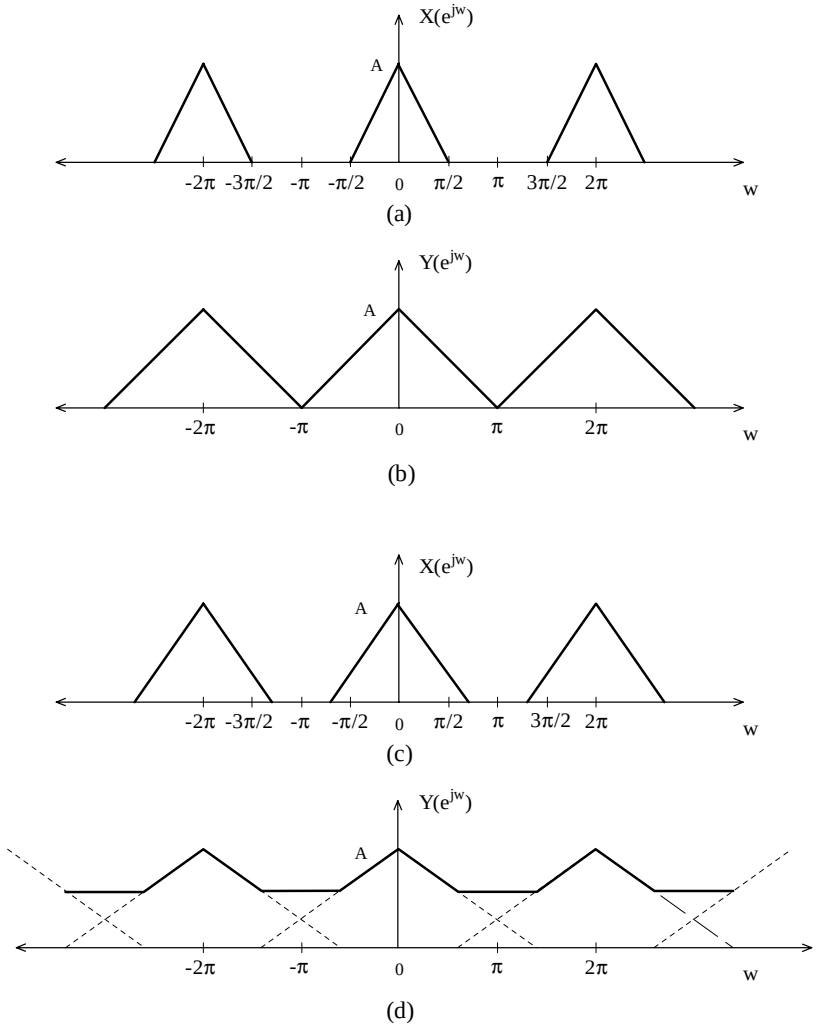

Figure 2.4: Downsampling for $M = 2$ in frequency domain. Figures a, b show a case of no aliasing, whereas c, d show aliasing.

necessary and sufficient condition for no aliasing is that the input signal must be band limited to a frequency band of $\frac{\pi}{M}$, that is, the input spectrum is nonzero for only $w_i \leq |w| \leq w_i + \frac{\pi}{M}$ where $w_i \geq 0$ [20].

2.2.2 Upsampling

Upsampling is the inverse of downsampling in the sense that it increases the number of samples. An L-fold upsampler simply puts $L - 1$ zeros between each samples of the input. Figure 2.5 shows the block diagram of an upsampler.

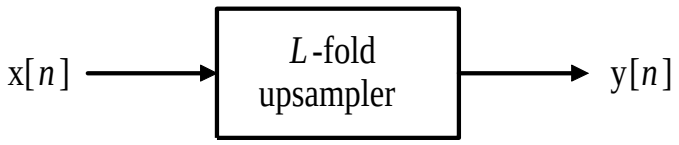

Figure 2.5: L-fold upsampler.

Upsampling in Time Domain

Mathematical relation between input and output in time domain is

$$y[n] = \begin{cases} x[n/L] & \text{if } n = kL, k \in Z \\ 0 & o/w \end{cases} \tag{2.4}$$

Upsampling is not causal and not time invariant, either. Figure 2.6 illustrates upsampling for $L = 2$.

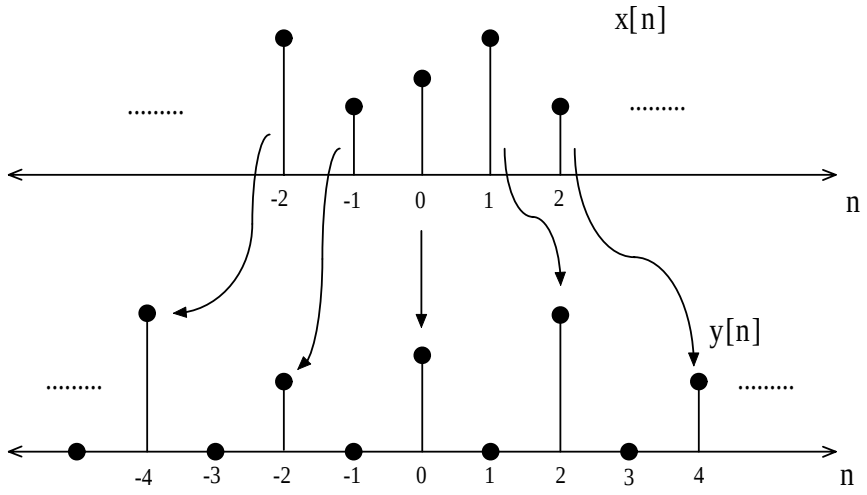

Figure 2.6: Upsampling for $L = 2$.

Upsampling in Frequency Domain

Frequency domain relation between input and the output of an L-fold upsampler is

$$Y(e^{jw}) = X(e^{jwL}) \quad \text{or} \quad Y(z) = X(z^L). \tag{2.5}$$

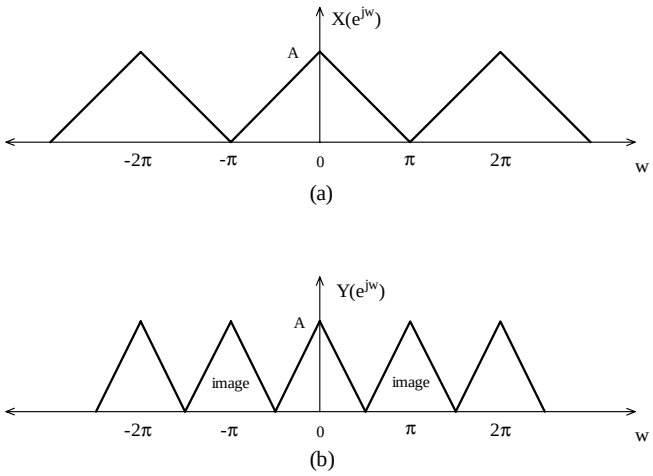

Figure 2.7: Upsampling in frequency domain.

The result of upsampling is shrinkage of the input spectrum. Due to this shrinkage, copies of the original spectrum of the input which are called *image* appear at higher frequencies for a low frequency input. Figure 2.7 illustrates upsampling in frequency domain for $L = 2$. Upsamplers are known to be sources of imaging in a filter bank.

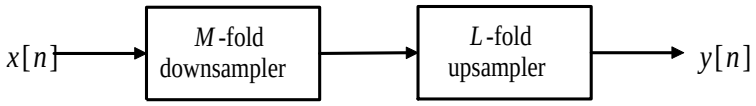

Figure 2.8: Cascade connection of an M-fold downsampler with an L-fold upsampler.

Cascade connection of an upsampler and a downsampler is used to change the sampling rate. A cascade connection of an M-fold downsampler and an L-fold upsampler is shown in Figure 2.8. For this connection, in z-domain, we have

$$Y(z) = \frac{1}{M} \sum_{k=0}^{M-1} X(z^{L/M} W_{M/L}^{k}). \tag{2.6}$$

In general, multirate operators are used together with digital filters. When multirate operators are used with digital filters, we can place them before or

after the filters. Different combinations are shown in Figure 2.9. There are two identities for these combinations which are also shown in the same figure.

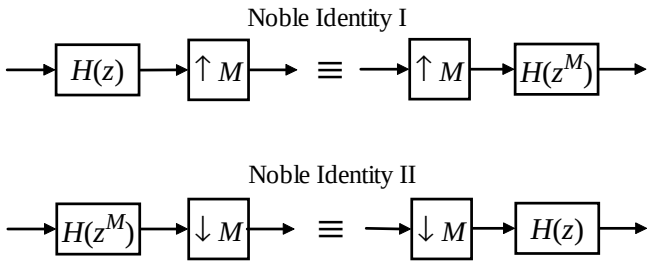

Figure 2.9: Noble Identities.

2.3 Analysis and Synthesis Filters

Analysis filters are a set of filters that operate in parallel. The main function of these filters is that they separate the input into different frequency bands. Analysis filters must be chosen to decrease the aliasing due to downsamplers that follows them. Therefore, sometimes they are called anti-aliasing filters. Similarly, synthesis filters must be determined so that they do not introduce images. Many different ways of separating the frequency band is possible and the choice depends on the type of application. The important point is to cover the whole input spectrum, i.e., prevent data loss. Uniform partition of the spectrum is an example. It is done with equal bandwidth band-pass filter. Figure 2.10 shows two different uniform separation. Filters $H_k(e^{j\omega})$, $k = 1, 2, .., M$, are analysis filters for an M-channel filter bank. In Figure 2.10a, non-overlapping filters are used. However, in such cases there are very severe attenuations at the frequencies multiples of $\frac{\pi}{M}$ for an M-channel filter bank. Therefore, the situation in Figure 2.10b is preferred most of the time. By such a choice analysis filters produce aliasing but it is possible to cancel the aliasing due to analysis part by a proper selection of synthesis filters.

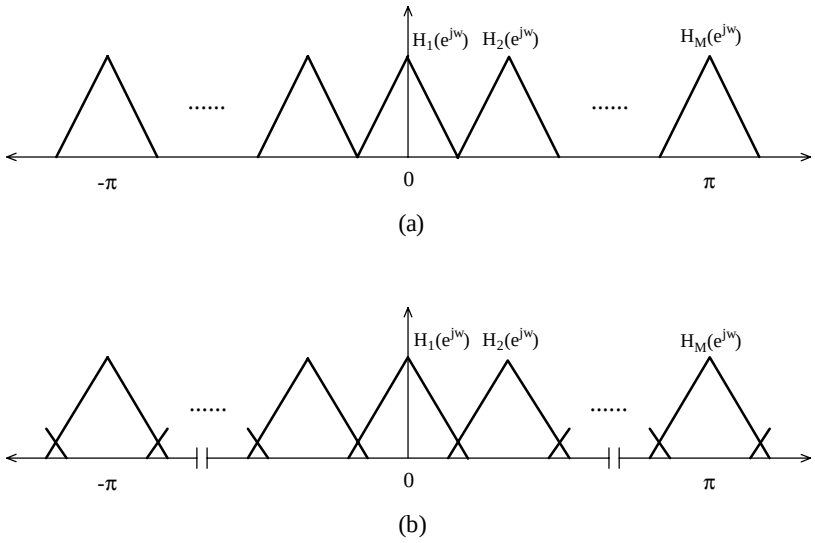

Figure 2.10: Uniform partition of the spectrum (a) non-overlapping partition of the spectrum, (b) overlapping partition.

Chapter 3

PERFECT RECONSTRUCTION FILTER BANKS

In the previous chapter, the building blocks of a two-channel filter bank have been introduced. The time domain and the frequency domain input-output relation of these blocks have been given. Using this information, it is possible to write the input-output relation of the overall system. The input signal is first filtered by the analysis filters and then decimated. This process produces so called subband signals $v_k[n]$, $k = 1, 2$, of Figure 2.1. Although subband signals $v_k[n]$ are quantized and then coded, we assume in defining PR that the subband signals enter the synthesis part without any further processing like quantization and coding. In the synthesis part subband signals are first upsampled and then filtered by synthesis filters. PR is achieved when the output signal $\hat{x}[n]$ is the same as the input signal $x[n]$ except possibly some delay in time. Croiser [3] showed that is it is possible to achieve PR using the freedom in choosing the analysis and the synthesis filters. This chapter explains how to use this freedom to achieve PR. The relation between the input and the output of the filter bank

can be analyzed in time domain or in the z-domain. The z-domain analysis is simpler and appropriate from the point of view of assigning zeros, so we will proceed in the z-domain. The reader may consult [1, 21] for the analysis in the time domain.

This chapter is organized as follows: Section 3.1 exposes the input-output relation of the two-channel filter bank. The errors created in the system are discussed together with an assessment of how to avoid these errors. Section 3.2 contains some examples to PR systems: Croiser's design, Smith and Barnwell design, and filter banks with Daubechies' maximally flat filters.

3.1 PR in a Two-Channel Filter Bank

The reconstruction at the output of a filter bank of Figure 2.1 differs from its input due to disturbances influencing the system or distortions introduced inside the system. There are four basic sources of distortion:

i. aliasing,

ii. imaging,

iii. amplitude distortion,

iv. phase distortion.

Aliasing is mainly due to downsamplers and overlapping filters. Aliasing due to downsamplers can be eliminated if the output of analysis filters are band limited to a frequency band of $\frac{\pi}{M}$ where M is the decimation factor (which is 2 for maximally decimated two-channel filter bank). In the ideal case this can be achieved using ideal bandpass filters. However, in practice filters have nonzero transition band and stopband gain. Another solution is non-overlapping

spectrum partition as seen in Figure 2.10a. However, in that case, there is severe data loss at frequencies multiples of $\frac{\pi}{M}$ where M is the number of subbands. In the light of these, the optimal solution is to use overlapping analysis filters that allow aliasing and then cancel the aliasing in the synthesis part by a proper design of synthesis filters. How this can be achieved will be explained in this section.

Imaging occurs in the synthesis part due to upsamplers as mentioned in Section 2.2.2. Images, just like aliasing, can be removed by a proper choice of synthesis filters.

Amplitude distortion and phase distortion can be easily seen from the input output relation of the overall system in the z-domain. For a two-channel filter bank the output $\hat{X}(z)$ can be written in terms of the input $X(z)$ as follows:

$$\hat{X}(z) = \frac{1}{2}\big[T(z)X(z) + S(z)X(-z)\big], \tag{3.1}$$

where

$$T(z) = H_1(z)K_1(z) + H_2(z)K_2(z)$$

and

$$S(z) = H_1(-z)K_1(z) + H_2(-z)K_2(z).$$

Transfer functions $T(z)$ and $S(z)$ result from (2.6). The term with $X(-z)$ in (3.1) is called the *aliasing term* and $T(z)$ is knows as *distortion transfer function* [20]. In order to achieve PR the aliasing term must be removed, i.e., $S(z)$ must be zero. However, even when $S(z) = 0$, $\hat{X}(z)$ is

$$\hat{X}(z) = \frac{1}{2}T(z)X(z). \tag{3.2}$$

On the unit circle we can write $T(z)$ as

$$T(e^{j\omega}) = |T(e^{j\omega})|e^{j\phi(\omega)}. \tag{3.3}$$

Therefore, $\hat{X}(e^{j\omega}) = \frac{1}{2}|T(e^{j\omega})|e^{j\phi(\omega)}X(e^{j\omega})$. If $|T(e^{j\omega})|$ is not allpass, i.e., $|T(e^{j\omega})| = c \neq 0$, then amplitude distortion is inevitable. Likewise, if $\phi(\omega)$

is not a linear function of ω which means $T(z)$ is not linear phase, then phase distortion is a direct consequence. If a filter bank system is free from aliasing and moreover there is no phase and no amplitude distortion, then we say PR is achieved. The output $\hat{X}(z)$ is given as

$$\hat{X}(z) = \frac{1}{2} c z^{-n_0} X(z) \tag{3.4}$$

for some constant c and an odd integer n_0. In time domain this corresponds to $\hat{x}[n] = \frac{1}{2} c x[n - n_0]$.

As mentioned previously, by proper design of synthesis filters aliasing cancellation is possible. By a proper design we mean the following selection

$$\begin{aligned} K_1(z) &= H_2(-z)V(z) \\ K_2(z) &= -H_1(-z)V(z) \end{aligned} \tag{3.5}$$

for some stable $V(z)$. This is a consequence of the condition $S(z) = 0$ provided $H_1(z)$, $H_2(z)$ have no common zeros. This selection completely cancels aliasing. Distortion transfer function $T(z)$ becomes

$$T(z) = \big[H_1(z)H_2(-z) - H_2(z)H_1(-z)\big]V(z) = cz^{-n_0}. \tag{3.6}$$

Equation (3.6) will be referred to as the PR equation. After defining $P_0(z) = H_1(z)H_2(-z)$, equation (3.6) becomes

$$\big[P_0(z) - P_0(-z)\big]V(z) = cz^{-n_0}. \tag{3.7}$$

For exact reconstruction c is chosen to be 2. There are different designs that satisfy equation (3.7). When $V(z)$ is 1, equation (3.7) turns out to be

$$P_0(z) - P_0(-z) = 2z^{-n_0}. \tag{3.8}$$

The left hand side in equation (3.8) is an odd function, therefore n_0 must be an odd integer. If we multiply both sides in equation (3.8) by z^{n_0} and define $P(z) = z^{n_0} P_0(z)$, we obtain

$$P(z) + P(-z) = 2. \tag{3.9}$$

Any filter $P(z)$ satisfying (3.9) is called a *halfband filter*. All even indexed samples of $p[n]$ are zero except $p[0]$ which is 1. Some authors first design a halfband filter $P(z)$ and then factor it into $H_1(z)$ and $H_2(-z)$. Moreover, it is possible to build other filters multiplying the particular filters $H_1(z)$ and $H_2(z)$ by an allpass filter $V(z)$ as in [22]. However, from this point on, for simplicity, $V(z)$ in (3.7) will be assumed to be 1.

3.2 Different Designs

It is possible to design different types of filter banks using the freedom in $P_0(z)$ of (3.8). In this section we will consider Croiser's design, Smith and Barnwell's design, and Daubechies maximally flat filter design.

3.2.1 A Simple Alias Free QMF System

If two analysis filters $H_1(z)$ and $H_2(z)$ satisfy the property

$$|H_2(e^{j\omega})| = |H_1(e^{j(\pi-\omega)})|, \tag{3.10}$$

then the pair is called a *quadrature mirror filter* (QMF) since the highpass filter $|H_2(e^{j\omega})|$ is the mirror image of $|H_1(e^{j\omega})|$ with respect to quadrature frequency $\frac{2\pi}{4}$. Figure 3.1 shows a QMF pair. There are two different types of filter selection satisfying this property. One is introduced by Croiser [3] and the other by Smith and Barnwell [17] and Mintzer [15], independently. Croiser's selection relates the analysis filters as

$$H_2(z) = H_1(-z). \tag{3.11}$$

If $H_1(z)$ is a good lowpass filter, then $H_2(z)$ is a good highpass filter. In time domain $h_2[n]$ is constructed from $h_1[n]$ by modulating it with $(-1)^n$, that is, $h_2[n] = (-1)^n h_1[n]$; so this method is also called the *alternating sign method*. In

Croiser's design, PR equation (3.6) in terms of analysis filter $H_1(z)$ with aliasing cancellation choice is

$$H_1(z)^2 - H_1(-z)^2 = 2z^{-n_0}. \tag{3.12}$$

Any $H_1(z)$ satisfying (3.12) achieves PR. There is a severe limitation on FIR solutions to Equation (3.12). It is easy to see this limitation with the polyphase structure introduced by Vaidyanathan [20]. Analysis lowpass filter $H_1(z)$ can be written in the polyphase form as

$$H_1(z) = H_{10}(z^2) + z^{-1}H_{11}(z^2)$$

where polyphase component $H_{10}(z)$ is

$$H_{10}(z) = \sum_{k=-\infty}^{\infty} h_1[2k]z^{-k}$$

and polyphase component $H_{11}(z)$ is

$$H_{11}(z) = \sum_{k=-\infty}^{\infty} h_1[2k+1]z^{-k}$$

Let us rewrite equation (3.12) in terms of polyphase components of $H_1(z)$, then we have

$$4z^{-1}H_{10}(z^2)H_{11}(z^2) = 2z^{-n_0}. \tag{3.13}$$

If $H_1(z)$ is FIR, then so are $H_{10}(z)$ and $H_{11}(z)$. However, under this condition, (3.13) holds if and only if $H_{10}(z)$ and $H_{11}(z)$ are pure delays, i.e., $H_{10}(z) = a_{n_1}z^{-n1}$ and $H_{11}(z) = a_{n_2}z^{-n2}$. Analysis filters become

$$H_1(z) = a_{n_1}z^{-2n_1} + a_{n_2}z^{-2n_2-1}, \quad H_2(z) = a_{n_1}z^{-2n_1} - a_{n_2}z^{-2n_2-1}.$$

Therefore, FIR solutions are limited to only two nonzero coefficients which results in poor stopband attenuation and smooth transition band. Although, choosing $H_{10}(z) = 1/H_{11}(z)$ may give better filters, with such a choice the filters become IIR.

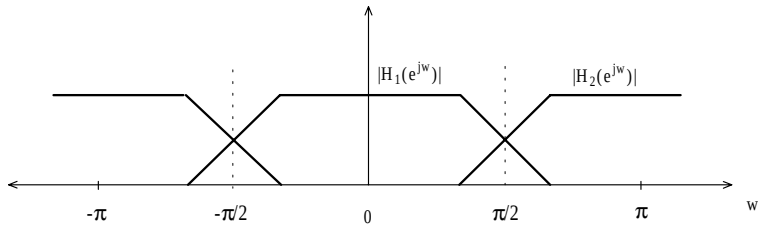

Figure 3.1: QMF pair.

3.2.2 FIR PR System with Better Filters

Smith and Barnwell [17] and Mintzer [15], improving the design of Croiser, came up with another type of QMF filters which are also known as *conjugate quadrature filters* (CQF). After satisfying (3.5) with $V(z) = 1$, they relate analysis filters as

$$H_2(z) = -z^{-N} H_1(-z^{-1}). \tag{3.14}$$

where N is an odd integer. This design is also called as *alternating flip design* [19], because in time domain this selection corresponds to first flipping the sequence $h_1[n]$ with respect to origin and then changing the sign of odd indexed samples. The term $-z^{-N}$ is used to make $H_2(z)$ causal by shifting the new sequence to the right by N when $H_1(z)$ is FIR. Letting $n_0 = N$, these new filters satisfy the following PR equation

$$\left[H_1(z)H_1(z^{-1}) + H_1(-z)H_1(-z^{-1})\right] z^{-N} = 2z^{-N}. \tag{3.15}$$

Thus the halfband filter $P(z)$ defined by equation (3.9) has a special form, $P(z) = H_1(z)H_1(z^{-1})$. The *product filter* $P(z)$ in that special form is an autocorrelation function. A CQF filter bank has two properties that are worth mentioning: power complementarity and orthogonality.

i. **Power Complementarity:**

Any two filters $H_1(z)$ and $H_2(z)$ satisfying

$$|H_1(e^{j\omega})|^2 + |H_2(e^{j\omega})|^2 = c$$

for some constant c are called *power complementary filters* [20]. PR equation (3.6) for $V(z) = 1$ and $c = 2$ becomes

$$H_1(z)H_2(-z) - H_1(-z)H_2(z) = 2z^{-n_0}. \tag{3.16}$$

From (3.14) we can get $H_1(-z) = -z^{-N}H_2(z^{-1})$. Substituting $H_1(-z)$ and $H_2(-z)$ in (3.16) we have

$$z^{-N}H_1(z)H_1(z^{-1}) + z^{-N}H_2(z)H_2(z^{-1}) = 2z^{-n_0}. \tag{3.17}$$

Taking $n_0 = N$ in (3.17) and evaluating the expression on the unit circle we reach

$$H_1(e^{j\omega})H_1(e^{-j\omega}) + H_2(e^{j\omega})H_2(e^{-j\omega}) = 2$$
$$|H_1(e^{j\omega})|^2 + |H_2(e^{j\omega})|^2 = 2.$$

Therefore, Smith and Barnwell's choice results in power complementary filters.

ii. **Orthogonality:** Any two-channel filter bank satisfying (3.14) and (3.15) with $n_0 = N$ is called an orthogonal filter bank. Sometimes they are also called *lossless* or *paraunitary* filter banks [22]. Orthogonality we mention here is *double-shift orthogonality*. In time domain, it means that two sequences $h_1[n]$ and $h_2[n]$ satisfy

$$\sum_{n=-\infty}^{\infty} h_1[n]h_2[n-2k] = 0, \qquad \forall k \in \mathbf{Z}, \tag{3.18}$$

$$\sum_{n=-\infty}^{\infty} h_1[n]h_1[n-2k] = \delta[k], \qquad \forall k \in \mathbf{Z}, \tag{3.19}$$

$$\sum_{n=-\infty}^{\infty} h_2[n]h_2[n-2k] = \delta[k], \qquad \forall k \in \mathbf{Z}. \tag{3.20}$$

Writing Equation (3.15) in time domain for $n_0 = N$, we can see that the sequence $h_1[n]$ satisfies

$$\sum_{n=-\infty}^{\infty} h_1[n]h_1[n-k] + \sum_{n=-\infty}^{\infty} (-1)^n(-1)^{n-k}h_1[n]h_1[n-k] = 2\delta[k]$$
$$\sum_{n=-\infty}^{\infty} h_1[n]h_1[n-2k] = \delta[k]. \tag{3.21}$$

n	Filter coefficients
0	0.04935260
1	-0.01553230
2	-0.08890390
3	0.31665300
4	0.78751500
5	0.50625500
6	-0.03380010
7	-0.10739700

Table 3.1: 8-tap Smith & Barnwell filter coefficients.

Therefore, Smith and Barnwell filters satisfies (3.19). Following the same steps we can show that $h_2[n]$ satisfies (3.20).

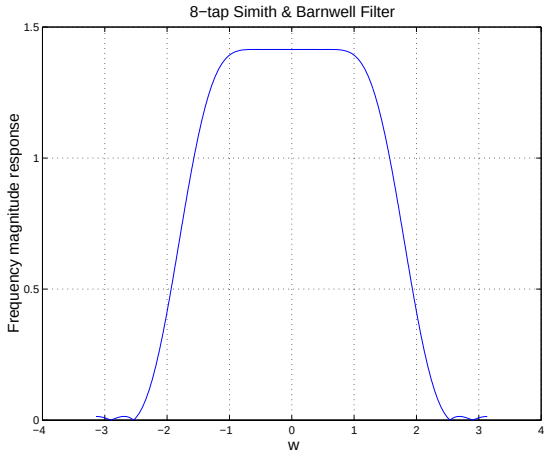

Figure 3.2: Frequency Magnitude Response of 8-tap Smith & Barnwell Filter.

Table 3.1 gives an example to filters that Smith and Barnwell designed. This filter is known as 8-tap lowpass Smith and Barnwell filter. It was widely used in speech and image processing. The frequency magnitude response is shown in Figure 3.2. In Section 4.4, this filter will be used to generate wavelet function.

3.2.3 Daubechies' Maximally Flat Filters

Daubechies' filters were first designed to construct orthogonal wavelets. These are FIR filters that have zeros[1] at $w = \pi$ and/or $w = 0$ with multiplicity at least 1. Daubechies chooses synthesis filters to cancel aliasing and relates analysis filters by Equation (3.14), i.e., she uses alternating flip design of Smith and Barnwell so that the resulting filters are orthogonal. Daubechies' filters are named according to number of zeros they have at $w = \pi$. Daubechies' filter with N zero at $w = \pi$ is named as D_N. She concentrates on an analysis lowpass filter $H_1(e^{j\omega})$ in the form

$$H_1(e^{j\omega}) = \Big(\frac{1 + e^{-j\omega}}{2}\Big)^N \mathcal{L}(e^{j\omega})$$

with $N \geq 1$ for some $\mathcal{L}(e^{j\omega})$. Then PR equation (3.6) on the unit circle is given by

$$\begin{aligned} |H_1(e^{j\omega})|^2 + |H_1(e^{j(\omega+\pi)})|^2 &= 2 \\ \Big(\cos^2\frac{\omega}{2}\Big)^N L(e^{j\omega}) + \Big(\cos^2\frac{\omega+\pi}{2}\Big)^N L(e^{j(\omega+\pi)}) &= 2 \end{aligned} \tag{3.22}$$

where $L(e^{jw}) = |\mathcal{L}(e^{jw})|^2$. Cosine terms come from $\left|\frac{1+e^{-jw}}{2}\right|^{2N}$. Since filter coefficients are real, $L(e^{j\omega})$ can be written as a polynomial in $\cos\omega$. However, writing $L(e^{j\omega})$ as a polynomial in $\sin^2\frac{\omega}{2} = \frac{1-\cos\omega}{2}$ is more convenient [6]. After a change of variable from ω to $\sin\frac{\omega}{2}$ and defining $y = \sin\frac{\omega}{2}$, the equation (3.22) becomes

$$(1-y)^N P(y) + y^N P(1-y) = 2 \tag{3.23}$$

where

$$P(y) = L(e^{j\omega})\Big|_{\sin\frac{\omega}{2}=y}. \tag{3.24}$$

The explicit solution of (3.23) turns out to be

$$P(y) = \sum_{k=0}^{N-1} \binom{N+k-1}{k} y^k + y^N R(\frac{1}{2} - y) \tag{3.25}$$

[1]Lowpass filters have zeros at $w = \pi$ and highpass filters have zeros at $w = 0$.

n	N=2	N=3	N=4
0	0.48296	0.33267	0.23038
1	0.83652	0.80689	0.71485
2	0.22414	0.45988	0.63088
3	-0.12941	-0.13501	-0.02798
4		-0.08544	-0.18703
5		0.03523	0.03084
6			0.03288
7			-0.01059

Table 3.2: Daubechies synthesis lowpass filters for $N = 2$, $N = 3$ and $N = 4$.

where $R(\cdot)$ is an odd polynomial chosen such that $P(y) \geq 0$ for $y \in [0, 1]$. This is the set of all solutions. Individual filters come from the spectral factorization of $P(y)$. First, $L(e^{jw})$ is calculated using (3.24). Then, $L(e^{jw})$ is factored into $L(e^{jw}) = \mathcal{L}(e^{jw})\mathcal{L}(e^{-jw})$. Finally, the minimum phase zeros generated from factorization are assigned to $H_1(z)$, [6]. Table 3.2 shows coefficients of D_2, D_3 and D_4 synthesis lowpass filters. We will obtain the above design of Daubechies as a corollary to our main result in Chapter 5.

Chapter 4

WAVELETS AND MULTIRESOLUTION ANALYSIS

In signal processing, one needs to perform series expansion of signals for analysis and synthesis purposes. Sometimes, it is necessary to have both time and frequency information. In such cases, the Fourier transform is not sufficient and the short-time Fourier transform does not have both good time and good frequency localization. Thus, the wavelet transform which has good time locality at high frequencies and good frequency localization at low frequencies is introduced. There are very efficient algorithms to compute the wavelet transform. These algorithms are provided by the multiresolution analysis (MRA) techniques which use two-channel PR filter banks as a tool for computations. Among the methods of constructing wavelets, the construction using the two-channel PR filter banks is very popular. In this chapter, we give the formal definition of the wavelet transform and focus on the relation between discrete-time wavelet transform and the two-channel PR filter banks.

This chapter is organized as follows: Section 4.1 introduces two different tools for time-frequency analysis, namely the short-time Fourier transform and the wavelet transform. The advantages of the wavelet transform in comparison with the short-time Fourier transform (STFT) is discussed. Section 4.2 is devoted to MRA where an axiomatic definition of MRA is given. In Section 4.3, it is shown how every orthogonal wavelet transform corresponds to an orthogonal filter bank. Conversely, under certain conditions, an orthogonal filter bank corresponds to an orthogonal wavelet transform. These conditions and an algorithm to compute the wavelet from the filter bank are given in Section 4.4.

4.1 Time Frequency Analysis

There are several ways of decomposing a signal for analysis. One of them is Fourier transform. Although it is a powerful tool for signal analysis, it only gives limited information about the signal to be analyzed. Formally Fourier transform of a function $f(t)$ is given as

$$F(\omega) = \int_{-\infty}^{\infty} f(t)e^{-j\omega t}dt.$$

Since integration is an averaging operation, the analysis obtained using the Fourier transform is in some sense an average analysis. The averaging interval is all of time. By looking at the Fourier transform of a signal we can say which frequencies are involved in the signal, what are their relative weight, etc. However, we cannot say when a particular frequency occurred. If we have a very non-stationary signal, then we need time information adjoined with a particular frequency, since it is required to know not only which frequency components occur but also when a particular frequency occurs. Fourier transform of a function is perfectly localized in frequency, on the other hand, the function $f(t)$ itself is perfectly localized in time. Although $f(t)$ and $F(\omega)$ represent the same function,

they are two extremes in time and frequency localization. One way of obtaining this information is to use STFT which is also known as *Gabor transform* or *windowed Fourier transform.*

4.1.1 Short-Time Fourier Transform

STFT was introduced in 1946 by Gabor [8] to measure localized frequency components of sounds. In STFT, a real symmetric window function $g(t)$ with unit norm is used. Transform is calculated by translating and modulating the fixed window function $g(t)$. Modulated and translated $g(t)$ is written as

$$g_{u,\Omega}(t) = e^{j\Omega t} g(t-u),$$

which is also of unit norm for any u and Ω. STFT of a function $f(t)$ is given as

$$F(u,\Omega) = \langle f, g_{u,\Omega} \rangle = \int_{-\infty}^{\infty} f(t) g_{u,\Omega}(t-u) e^{-j\Omega t} dt,$$

and inverse transform is

$$f(t) = \frac{1}{2\pi} \int_{-\infty}^{\infty} \int_{-\infty}^{\infty} F(u,\Omega) g(t-u) e^{j\Omega t} du d\Omega.$$

$F(u,\Omega)$ is a continuous function of u and Ω. Information provided by $F(u,\Omega)$ is represented in time-frequency plane by a region whose location and width depends on the time-frequency spread of $g_{u,\Omega}(t)$. Since $g_{u,\Omega}(t)$ has unit norm, $|g_{u,w}(t)|^2$ can be interpreted as a probability distribution with mean

$$u_\gamma = \int_{-\infty}^{\infty} t |g_{u,\Omega}(t)|^2 dt. \tag{4.1}$$

The spread around the mean u_γ is given by the variance

$$\sigma_u^2 = \int_{-\infty}^{\infty} (t-u_\gamma)^2 |g_{u,\Omega}(t)|^2 dt. \tag{4.2}$$

By Parseval formula, $\int_{-\infty}^{\infty} |G_{u,\Omega}(\omega)|^2 dt = 2\pi ||g_{u,\Omega}(t)||^2$ where $G_{u,\Omega}(\omega)$ is the Fourier transform of $g_{u,\Omega}(t)$. Now we can interpret $\frac{1}{2\pi}|G_{u,\Omega}(\omega)|^2$ as a probability density function. Similarly, for the frequency variable Ω, the mean of

$\frac{1}{2\pi}|G_{u,\Omega}(\omega)|^2$ is given as

$$\Omega_\gamma = \frac{1}{2\pi}\int_{-\infty}^{\infty} \omega |G_{u,\Omega}(\omega)|^2 d\omega \tag{4.3}$$

and the spread around Ω_γ is

$$\sigma_\Omega^2 = \frac{1}{2\pi}\int_{-\infty}^{\infty} (\omega - \Omega_\gamma)^2 |G_{u,\Omega}(\omega)|^2 d\omega. \tag{4.4}$$

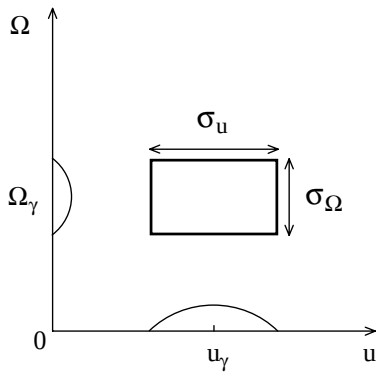

Figure 4.1: Time-frequency atom centered at $(u_\gamma, \Omega_\gamma)$.

Time-frequency resolution of $g_{u,\Omega}(t)$ is represented in the time-frequency plane (u, Ω) by a Heisenberg box centered at $(u_\gamma, \Omega_\gamma)$ whose width is σ_Ω and σ_u along frequency and time, respectively, as seen in Figure 4.1. By the Heisenberg uncertainty theorem, the area satisfies

$$\sigma_u \sigma_\gamma \geq \frac{1}{2}$$

Therefore there is a trade off between time resolution and frequency resolution. Since $g_{u,\Omega}(t)$ is an even function of t, time spread around u is independent of u. Similar argument holds for $G_{u,\Omega}(\omega)$, because $G_{u,\Omega}(\omega)$ is also an even function since $g_{u,\Omega}(t)$ is real. As a result, for a fixed window function, dimensions of the Heisenberg box is fixed which means we have the same resolution all over the time-frequency plane. Figure 4.2 shows the uniform tiling of time-frequency plane for STFT. Example 1 and 2 explain two extreme cases.

Example 1. A complex sinusoid $f(t) = e^{j\Omega_0 t}$ is very well localized in frequency. Its Fourier transform is $F(\omega) = 2\pi\delta(w - \Omega_0)$, an impulse at $w = \Omega_0$. Taking STFT of

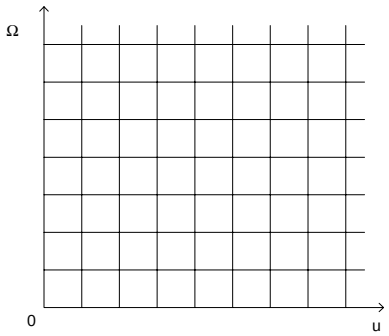

Figure 4.2: Uniform tiling of time-frequency plane.

$f(t)$ we reach

$$F(u,\Omega) = \int_{-\infty}^{\infty} e^{j\Omega_0 t} g(t-u) e^{-j\Omega t} dt = e^{-ju(\Omega-\Omega_0)} G(\Omega-\Omega_0).$$

Therefore, in time-frequency plane the energy is concentrated along a horizontal strip around the frequency Ω_0 and the width of the strip is determined by the window function's Fourier transform variance σ_Ω^2. This is illustrated in Figure 4.3.

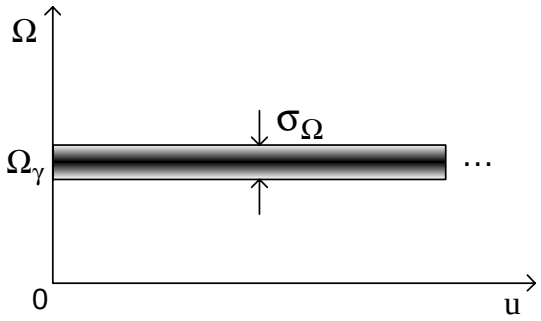

Figure 4.3: STFT of a complex sinusoid with frequency Ω_0.

Example 2. Contrary to complex sinusoids a Dirac function $f(t) = \sigma(t-u_0)$ is very well localized in time. Its Fourier transform is $F(\omega) = e^{-j\omega u_0}$. Taking the STFT we have

$$F(u,\Omega) = \int_{-\infty}^{\infty} \delta(t-u_0) g(t-u) e^{-j\Omega t} dt = e^{-j\Omega u_0} g(u_0-u).$$

In that example, energy of $F(u,\Omega)$ is concentrated around u_0 with a width of σ_u. This is shown in Figure 4.4.

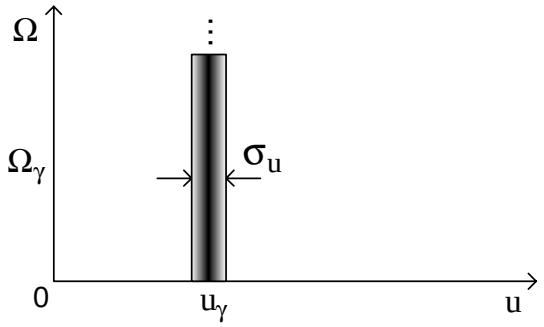

Figure 4.4: STFT of a Dirac delta function at $\delta(t - u_0)$.

Uniform tiling of time-frequency plane is a limited representation since the resolution is the same for all frequencies. In Figure 4.5, there are four different cases. In each case, sinusoids with different frequencies are multiplied by a fixed Gaussian window. In Figure 4.5a, window function cannot capture one period of the sinusoid, therefore sinusoid cannot be detected correctly. On the other extreme, in Figure 4.5d, there are more than one period of the sinusoid in the support of window function, therefore time locality is poor. Because, for example, if there is only one period of a sinusoid inside the window and the window's support is very large compared to the period of the sinusoid, we can only say that there is a sinusoid inside the window. Time information of this sinusoid is specified as being in the support of the window. A narrower window will give better time locality since its support is narrower than the previous one. In the light of these, we can conclude that we need a variable size window. At low frequencies window size will be comparatively large in order to detect low frequencies accurately and at high frequencies we need a narrower window in order to have good time locality. Wavelet transform is a good solution to this problem.

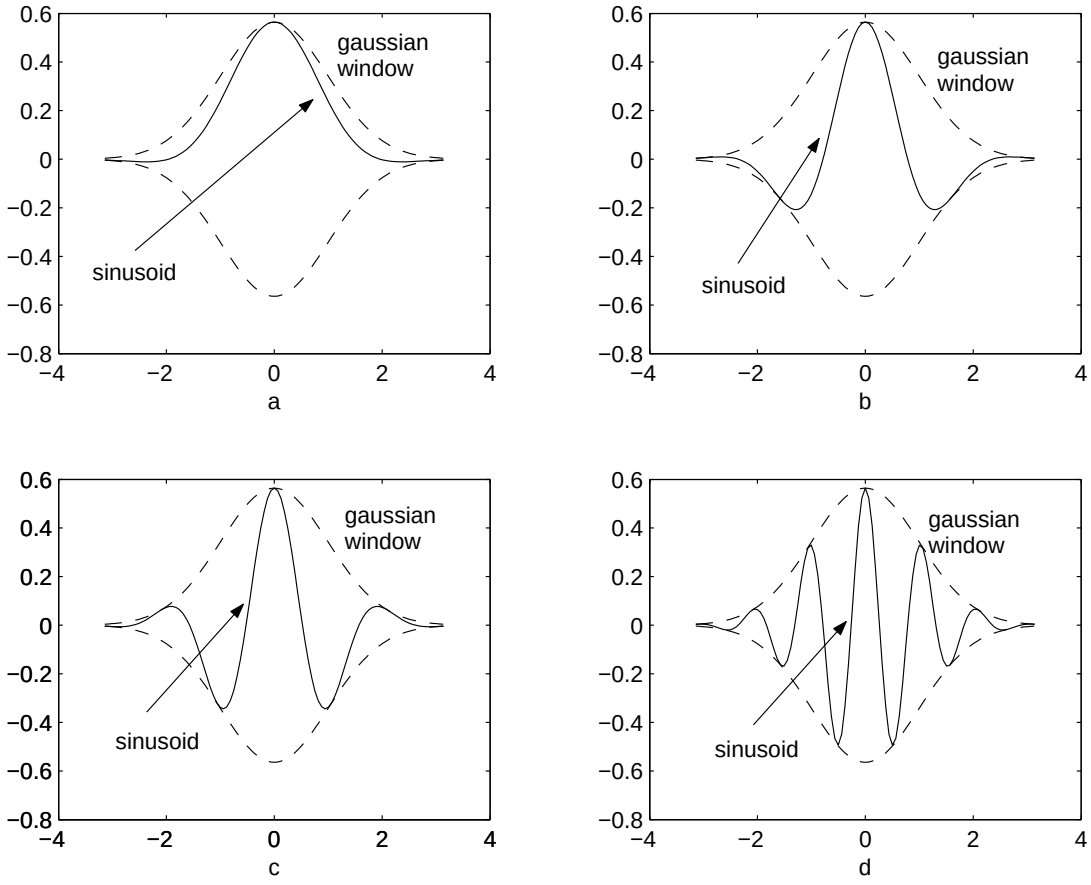

Figure 4.5: windowed.

4.1.2 Wavelet Transform

Wavelets were introduced at the beginning of the eighties. First, Morlet, a French geophysicist, used them as a tool for an analysis of seismic data. His success prompted Grossmann [9] to make a more detailed mathematical analysis of wavelets. In 1985 Meyer became aware of this theory and he recognized many classical results inside it. He pointed out to Grossmann and Morlet that there was a connection between their signal analysis methods and existing powerful techniques in the mathematical study of singular integral operators. Then Ingrid Daubechies became involved. It was also the start of cross fertilization between the signal analysis and the purely mathematical aspects of techniques based on dilations and translations. After Mallat [13] and Meyer [14] introduced

multiresolution analysis, in 1988 Daubechies provided a major breakthrough by constructing families of orthonormal wavelets with compact support [4].

In the two following subsections, we summarize the fundamentals of continuous and discrete wavelet transforms.

Continuous Wavelet Transform

Wavelets constitute a family of functions derived from one single function $w(t)$ which is called *mother wavelet*. In wavelet transform, dilation and translation of this mother wavelet instead of modulation and translation of a fixed window is used. Therefore, the window function has a variable support which gives a zooming ability to wavelet transform. Wavelet transform has good time localization at high frequencies and good frequency localization at low frequencies. Dilated and scaled mother wavelet is written as

$$w_{a,b}(t) = \frac{1}{\sqrt{|a|}} w(\frac{t-b}{a}), \quad a \neq 0, \quad b \in \mathbb{R}.$$

The mother wavelet is chosen such that the wavelet function has unit norm, that is,

$$||w_{a,b}(t)||^2 = \int_{-\infty}^{\infty} |w_{a,b}(t)|^2 dt = 1, \tag{4.5}$$

for all $a, b \in \mathbb{R}$.

The Wavelet transform of a function $f(t)$ is written in terms of $w_{a,b}$ and is given as

$$F(a,b) = \int_{-\infty}^{\infty} f(t) w^*_{a,b}(t) dt \tag{4.6}$$

where * denotes complex conjugation. Equation 4.6 is known as a *continuous wavelet transform* (CWT), as $F(a,b)$ is a continuous function of a and b. The variable a replaces the frequency Ω in STFT and it is called the *scale parameter*. The variable b, is the analogue of the translation parameter u in STFT. The

inverse CWT is

$$f(t) = \frac{1}{C_w} \int_{-\infty}^{\infty} \int_{-\infty}^{\infty} F(a,b) w_{a,b}(t) \frac{da}{a^2} db. \tag{4.7}$$

where

$$C_w = \int_0^{\infty} \frac{|W_{a,b}(\omega)|^2}{\omega} < \infty \tag{4.8}$$

is written in terms of the Fourier transform $W_{a,b}(\omega)$ of $w_{a,b}(t)$. Inequality in (4.8) is known as the *admissibility condition* [13]. For the integral in (4.8) to exist, $|W_{a,b}(0)| = 0$ must hold, since otherwise, there will be a singularity at $\omega = 0$. Note that $W_{a,b}(0)$ is the average value of $w_{a,b}(t)$, so that the wavelet function must have a zero average. Note also that since $|W_{a,b}(0)| = 0$, $W_{a,b}(\omega)$ must be either nonzero only for frequencies larger than certain frequency or nonzero only for a band of frequencies. However, since $w_{a,b}(t)$ has unit norm, by Parseval's relationship

$$\frac{1}{2\pi} \int_{-\infty}^{\infty} |W_{a,b}(\omega)|^2 d\omega = 1, \tag{4.9}$$

so that $W_{a,b}(\omega)$ is nonzero only for a band of frequencies.

Time-frequency analysis of wavelet transform can be carried out as in STFT. The mother wavelet $w(t)$ has unit norm specified by (4.5). Therefore, we can interpret $|w(t)|^2$ as a probability distribution with mean

$$t_\gamma = \int_{-\infty}^{\infty} t |w(t)|^2 dt$$

and a spread around t_γ, specified by the variance

$$\sigma_t^2 = \int_{-\infty}^{\infty} (t - t_\gamma)^2 |w(t)|^2 dt.$$

Similarly, by (4.9), the Fourier transform $\frac{1}{2\pi}|W(\omega)|^2$ of the mother wavelet could be interpreted as a probability distribution with mean

$$\omega_\gamma = \frac{1}{2\pi} \int_{-\infty}^{\infty} \omega |W(\omega)|^2 d\omega$$

and variance

$$\sigma_\omega^2 = \frac{1}{2\pi} \int_{-\infty}^{\infty} (\omega - \omega_\gamma)^2 |W(\omega)|^2 d\omega$$

around the mean ω_γ. The mother wavelet defines an Heisenberg box in the time-frequency plane with dimensions $\sigma_t \times \sigma_\omega$. The dimension of the Heisenberg box corresponding to dilated and translated wavelet function $w_{a,b}(t)$ is different from the mother wavelet's. Let $t_{a,b,\gamma}$ denote the mean of $w_{a,b}(t)$. The mean is equal to

$$\begin{aligned} t_{a,b,\gamma} &= \int_{-\infty}^{\infty} t|w_{a,b}(t)|^2 dt, \\ &= \int_{-\infty}^{\infty} t\Big|\frac{1}{\sqrt{a}} w(\frac{t-b}{a})\Big|^2 dt, \\ &= \int_{-\infty}^{\infty} (ax+b)|w(x)|^2 dx \quad \text{where } t = ax+b, \\ &= a\int_{-\infty}^{\infty} x|w(x)|^2 dx + b\int_{-\infty}^{\infty} |w(x)|^2 dx, \\ &= at_\gamma + b. \end{aligned} \tag{4.10}$$

The variance of $w_{a,b}(t)$ around $t_\gamma^{a,b}$ is given by

$$\begin{aligned} \sigma_{a,b,t}^2 &= \int_{-\infty}^{\infty} (t - t_{a,b,\gamma})^2 |w_{a,b}(t)|^2 dt \\ &= \int_{-\infty}^{\infty} (t - t_{a,b,\gamma})^2 \Big|\frac{1}{\sqrt{a}} w(\frac{t-b}{a})\Big|^2 dt \\ &= \int_{-\infty}^{\infty} (ax + b - t_{a,b,\gamma})^2 |w(x)|^2 dx \quad \text{where } t = ax+b, \\ &= \int_{-\infty}^{\infty} [ax + b - (at_\gamma + b)]^2 |w(x)|^2 dx, \\ &= a^2 \int_{-\infty}^{\infty} (x - t_\gamma)^2 |w(x)|^2 dx, \\ &= a^2 \sigma_t^2. \end{aligned} \tag{4.11}$$

We have thus determined the dimension of the Heisenberg box along the time axis. We have to follow the same procedure in order to determine the dimension along the frequency axis. The Fourier transform $W_{a,b}(\omega)$ of $w_{a,b}(t)$ is also a

probability distribution with mean

$$\begin{aligned}
\omega_{a,b,\gamma} &= \frac{1}{2\pi}\int_{-\infty}^{\infty} \omega |W_{a,b}(\omega)|^2 d\omega, \\
&= \frac{1}{2\pi}\int_{-\infty}^{\infty} \omega |\sqrt{a}e^{-j\omega b}W(a\omega)|^2 d\omega, \\
&= \frac{a}{2\pi}\int_{-\infty}^{\infty} \omega |W(a\omega)|^2 d\omega, \\
&= \frac{1}{2\pi a}\int_{-\infty}^{\infty} \Omega |W(\Omega)|^2 d\Omega \quad \text{where } \omega = \frac{\Omega}{a}, \\
&= \frac{\omega_\gamma}{a}.
\end{aligned} \tag{4.12}$$

The next step is to calculate the variance $\sigma^2_{a,b,\omega}$ around the mean $\omega_{a,b,\gamma}$

$$\begin{aligned}
\sigma^2_{a,b,\omega} &= \frac{1}{2\pi}\int_{-\infty}^{\infty} (\omega - \omega_{a,b,\gamma})^2 |W_{a,b}(\omega)|^2 d\omega, \\
&= \frac{1}{2\pi}\int_{-\infty}^{\infty} (\omega - \omega_{a,b,\gamma})^2 |\sqrt{a}e^{-j\omega b}W(a\omega)|^2 d\omega, \\
&= \frac{a}{2\pi}\int_{-\infty}^{\infty} (\omega - \frac{\omega_\gamma}{a})^2 |W(a\omega)|^2 d\omega, \\
&= \frac{1}{2\pi}\int_{-\infty}^{\infty} (\frac{\Omega}{a} - \frac{\omega_\gamma}{a})^2 |W(\Omega)|^2 d\Omega \quad \text{where } \omega = \frac{\Omega}{a}, \\
&= \frac{1}{a^2}\Big[\int_{-\infty}^{\infty} (\Omega - \omega_\gamma)^2 |W(\Omega)|^2 d\Omega\Big], \\
&= \frac{\sigma^2_\omega}{a^2}.
\end{aligned} \tag{4.13}$$

As a result, an Heisenberg box with dimensions $a_0\sigma_t \times \frac{\sigma_\omega}{a_0}$ corresponds to any dilated and modulated wavelet $w_{a_0,b}(t)$. Dimensions of the Heisenberg box are independent of translation parameter b, only the scale parameter a is effective. However, the area of Heisenberg box stays constant independent of a. Figure 4.6 shows time-frequency atoms for wavelet transform for different scales and Figure 4.7 shows the tiling of time-frequency plane. In Figure 4.7, zooming ability of wavelet transform is very obvious.

In CWT variables a and b run from $-\infty$ to ∞. Even when a and b are in bounded intervals, we have to calculate the wavelet transform for infinitely many values of a and b. This is not good for practical applications. It may also be the case that the wavelet transform $F(a,b)$ is known for some $a < a_0$ only. In such situations we need a complement of information corresponding to $F(a,b)$

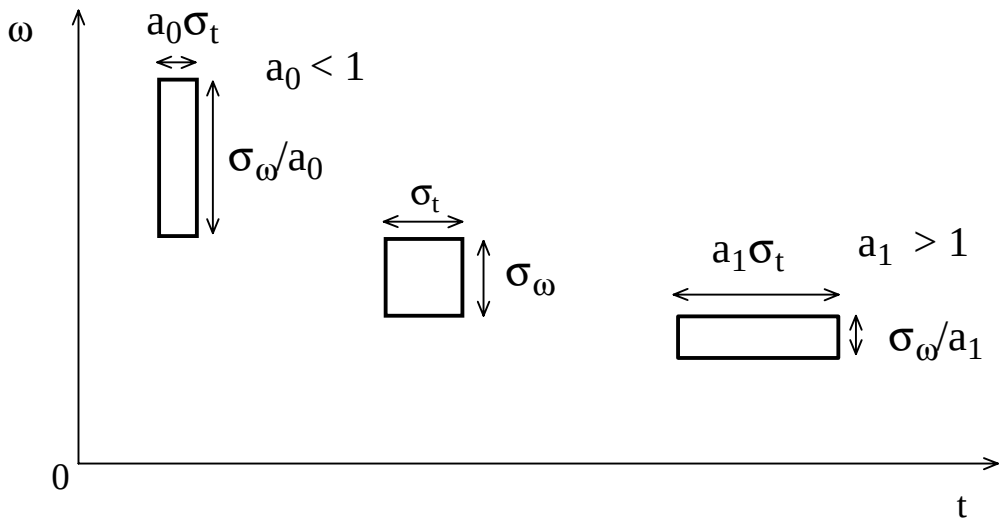

Figure 4.6: Time-frequency atoms for wavelet transform.

for $a \geq a_0$. This is obtained by introducing a *scaling function* $\phi(t)$ which is an aggregation of wavelets at scales larger than 1 [13]. Modulus of Fourier transform of scaling function is defined by

$$|\Phi(\omega)|^2 = \int_1^\infty |W(a\omega)|^2 \frac{da}{a},$$

and the complex phase of $\Phi(\omega)$ can be arbitrarily chosen. Scaling function $\phi(t)$ has unit norm like wavelet function. Since scaling function is an aggregation of wavelet functions $w_{a,b}(t)$ for $a \geq 1$, it is low pass in nature. Because, as a gets larger, $w_{a,b}(t)$ slows down. This means that $\phi(t)$ is a lowpass function compared to $w_{a,b}(t)$. Therefore, low frequency approximation of any function $f(t)$ at scale a_0 can be written in terms of $\phi(t)$ and contains all the information contained in $f(t)$ for scales larger than a_0. Let $F_\phi(a_0, b)$ be the low frequency approximation of a signal $f(t)$. It is given as

$$F_\phi(a_0, b) \ = \langle f(t), \frac{1}{\sqrt{a_0}} \phi(\frac{t-b}{a_0}) \rangle = \ \int_{-\infty}^{\infty} f(t) \frac{1}{\sqrt{a_0}} \phi^*(\frac{t-b}{a_0}) dt.$$

As a result, wavelet transform of a function can be written in terms of a wavelet function up to some scale a_0 plus the low frequency approximation which covers

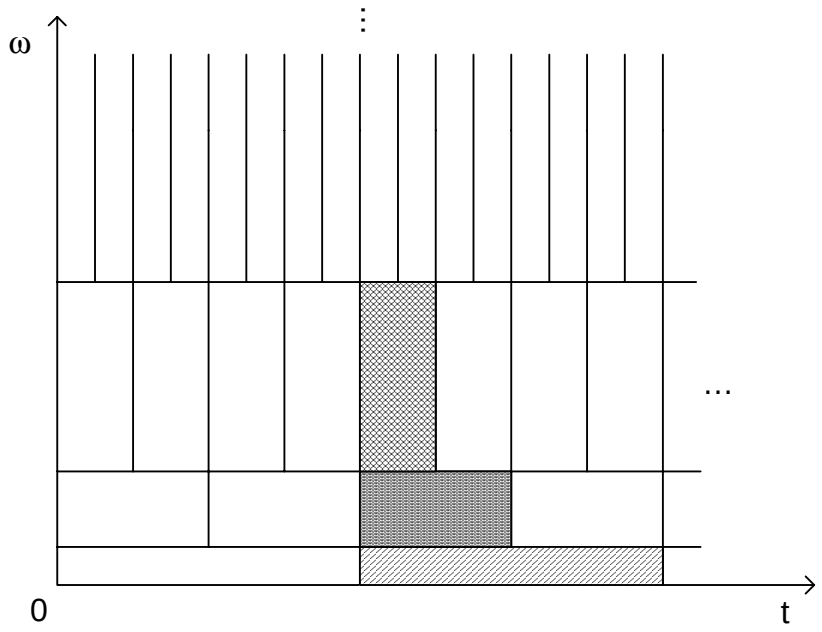

Figure 4.7: Tiling of the time-frequency plane for wavelet transform.

scales larger than a_0. Then, the inverse transform given by equation 4.7 becomes

$$f(t) = \frac{1}{C_w}\int_{-\infty}^{\infty}\int_{-\infty}^{a_0} F(a,b)w_{a,b}(t)\frac{da}{a^2}db + \frac{1}{C_w}\int_{-\infty}^{\infty} F_\phi(a_0,b)\frac{1}{\sqrt{a_0}}\phi(\frac{t-b}{a_0})dt.$$

Low frequency approximation $F_\phi(a_0, b)$ is also known as the coarse approximation for lowpass signals (most natural signals including speech and image). This type of thinking gives rise to so called *multiresolution analysis* (to be explained in section 4.2) introduced by Mallat [13] and Meyer [14] .

Discrete-Time Wavelet Transform

Discrete-time wavelet transform (DTWT) is obtained from CWT by special choices of a, b. We obtain a series representation where the basis functions $w_{a,b}(t)$ and $\phi_{a,b}(t) = \frac{1}{\sqrt{a}}\phi(\frac{t-b}{a})$ have discrete scaling and translating parameters a and b. The discrete version of the scaling and translating parameters have to be dependent on each other because if the scale a is such that the basis functions are narrow, the translation step b should be correspondingly small and vice versa.

There are different ways of choosing these parameters. The most popular approach is to select a and b according to

$$a = a_0^{-m}, \qquad b = nb_0a_0^{-m}$$

where m and n are integers. This selection gives us the following basis set

$$w_{m,n}(t) = a_0^{m/2} w(a_0^m t - nb_0),$$
$$\phi_{m,n}(t) = a_0^{m/2} \phi(a_0^m t - nb_0), \qquad m, n \in \mathbb{Z}.$$

In terms of these new wavelet bases, wavelet transform of a function $f(t)$ becomes

$$F[m, n] = a_0^{m/2} \int_{-\infty}^{\infty} f(t) w(a_0^m t - nb_0) dt.$$

As a special case, $a_0 = 2$ and $b_0 = 1$ is chosen. This choice has a strong relation with multiresolution analysis. Discretization of CWT corresponds to sampling the time-frequency plane. Horizontal sampling is along the time axis and it depends on a_0 and b_0. For a fixed m, time axis is sampled uniformly. Vertical sampling is along the frequency axis (or scale axis) and it depends only on a_0. Vertical sampling is non-uniform. Figure 4.8 shows sampling of the time-frequency plane. By introducing DTWT, we moved from CWT where both time function $f(t)$ and its transform are continuous function to DTWT where time function $f(t)$ is still continuous but its transform is a discrete function of m and n. In order to make use of digital signal processing, $f(t)$ must also be discretized, i.e, everything must be in discrete time. By discretizing $f(t)$, we reach a discrete wavelet transform (DWT). As pointed out by Mallat [13] and Meyer [14], two-channel PR filter banks implements a fast algorithm for DWT as explained in some more detail below. Computational complexity of the algorithm is order N, i.e., the number of multiplications and additions required to take the transform are proportional to N, the length of signal to be transformed.

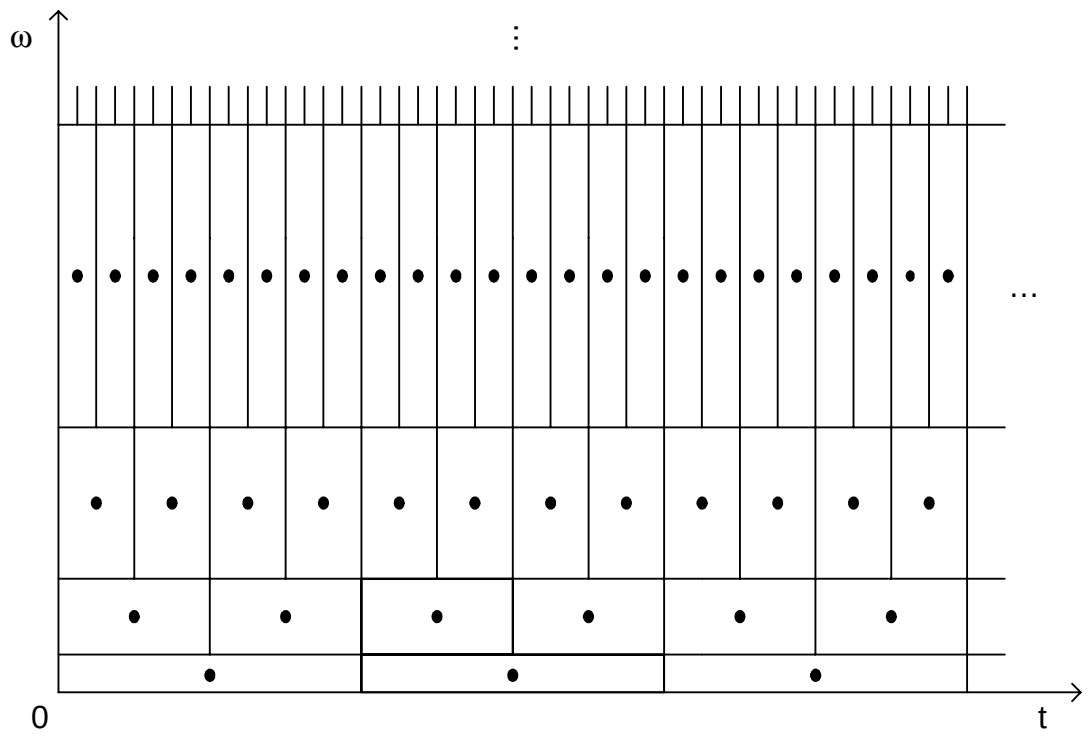

Figure 4.8: Tiling of the time-frequency plane for wavelet transform.

4.2 Multiresolution Analysis

Orthogonal wavelets dilated by 2^m carry signal variations at the resolution 2^{-m}. The construction of such bases can be related to multiresolution signal approximation by changing the resolution 2^{-m}. Examining this link between orthogonal wavelets and multiresolution analysis leads to an equivalence between wavelet bases and conjugate quadrature filters used in filter banks. These filter banks implement a fast orthogonal wavelet transform that requires only $O(N)$ operations for signals of size N. The design of CQF filter banks also provides a simpler way of constructing new orthogonal wavelets using the *cascade algorithm* introduced by Daubechies [6].

In Section 4.1.2, we introduced the scaling function in CWT. It is used to get low-frequency representation (coarse approximation) of a function $f(t)$. It contains all wavelet representations above a certain scale a_0. We can use the

same idea for DTWT. In DTWT scaling function carries all the information above a certain scale a_0^m and again it contains the low-frequency information of $f(t)$. Here, a_0 is constant and m is an integer as in Section 4.1.2. Scale is changed by changing m. By decreasing m, we can decrease the scale a_0^m and increase the resolution[1]. Let us assume that the old scale is $a_0^{m_{old}}$. Decreasing m by 1 we reach the scale $a_0^{m_{old}-1}$. Doing this, we increased the information carried by the scaling function $\phi(t)$. The difference between old and new scales are provided by the wavelet coefficients at the scale $a_0^{m_{old}}$. We call these differences as *details*. The low-frequency representation carried by $\phi(t)$ at the new scale is better than the old one. We can get better low-frequency approximations following the same procedure over and over. The idea of multiresolution is to make use of this fine and coarse approximations. Now we will introduce an axiomatic definition of multiresolution analysis developed by Mallat [13] and Meyer [14].

Definition 1. Multiresolution analysis consists of a sequence of embedded closed subspaces V_m

$$\ldots \subset V_2 \subset V_1 \subset V_0 \subset V_{-1} \subset V_{-2} \subset \ldots$$

satisfying

i. Upward completeness:

$$\bigcup_{m\in\mathbb{Z}} V_m = L_2(\mathbb{R}).$$

ii. Downward completeness:

$$\bigcap_{m\in\mathbb{Z}} V_m = \{0\}.$$

iii. Scale invariance:

$$f(t) \in V_0 \Leftrightarrow f(2^m t) \in V_{-m}, \qquad m \in \mathbb{Z}.$$

iv. Shift invariance:

$$f(t) \in V_0 \Rightarrow f(t-k) \in V_0, \quad \forall k \in \mathbb{Z}.$$

[1]Scale a_0^m corresponds to resolution a_0^{-m}.

v. Existence of a basis:

There exists $\phi(t) \in V_0$ such that

$$\{\phi(t-k)|k \in \mathbb{Z}\}$$

is an orthonormal basis for V_0. In general

$$\{2^{m/2}\phi(2^m t-k)|m,k \in \mathbb{Z}\} \tag{4.14}$$

is a basis for V_{-m}.

vi. Existence of a complementary basis:

There exists $w(t) \in W_0$ such that

$$\{w(t-k)|k \in \mathbb{Z}\} \tag{4.15}$$

is an orthonormal basis for W_0 and W_0 satisfies

$$V_{-1} = V_0 \oplus W_0,$$

that is, W_0 is orthogonal complement of V_0 in V_{-1}. In general,

$$\{2^{m/2}w(2^m t-k)|m,k \in \mathbb{Z}\}$$

is an orthonormal basis for W_{-m} and W_{-m} is an orthogonal complement of V_{-m} in V_{-m-1}. Subspaces W_{-m} and V_{-m} are coarser subspaces and V_{-m-1} is a finer subspace.

vii. Orthogonality:

$$\begin{aligned} 2^m \int_{-\infty}^{\infty} \phi(2^m t-k_1)\phi(2^m t-k_2)dt &= \delta[k_1-k_2], \\ 2^m \int_{-\infty}^{\infty} w(2^m t-k_1)\phi(2^m t-k_2)dt &= \delta[k_1-k_2], \\ 2^{(m_1+m_2)/2} \int_{-\infty}^{\infty} w(2^{m_1} t-k_1)w(2^{m_2} t-k_2)dt &= \delta[k_1-k_2]\delta[m_1-m_2] \end{aligned} \tag{4.16}$$

where $k_1, k_2, m, m_1, m_2 \in \mathbb{Z}$.

The simplest example to multiresolution analysis is the space of piecewise constant functions. The basis function of V_0 is an indicator function $\phi(t-k)$ which is one in the interval $[k, k+1)$ and zero outside the interval. The basis function $\phi(t)$ is known as the *Haar scaling function*. By (4.14), the indicator function $\phi(2^m - k)$ is one in the interval $[\frac{k}{2^m}, \frac{k+1}{2^m})$ and zero outside. Obviously, any piecewise constant function in V_0 is also in V_{-m} for all $m \geq 0$. Therefore, embedded closed subspaces requirement is satisfied. From this point on we will concentrate on the subspaces V_{-1}, V_0, and W_0. The relation between these subspaces gives rise to an unexpectedly strong relation between orthogonal wavelets and two-channel orthogonal filter banks.

4.3 Orthogonal Wavelets and Orthogonal Filter Banks

In this section, we will be dealing with expansions of continuous time signals in terms of continuous wavelet and scaling functions. It is possible to expand any function in V_{-1} in terms of basis functions of V_{-1}. Since V_0 and W_0 are contained in V_{-1}, the basis functions $w(t)$ and $\phi(t)$ of these subspaces can also be written in terms of the basis functions of the finer subspace V_{-1}. More formally, we can write

$$Dilation\ equation: \quad \phi(t) = \sqrt{2} \sum_{k=-\infty}^{\infty} k_1[k]\phi(2t-k), \tag{4.17}$$

$$Wavelet\ equation: \quad w(t) = \sqrt{2} \sum_{k=-\infty}^{\infty} k_2[k]\phi(2t-k). \tag{4.18}$$

Equations (4.17) and (4.18) are also known as *two scale equations* [21] which make a design of $w(t)$ and $\phi(t)$ satisfying the axioms of multiresolution possible. These two equations will be used to design orthogonal wavelet and scaling function using the *cascade algorithm* of Daubechies below in Section 4.4. We can calculate discrete sequences $k_1[n]$ and $k_2[n]$ making use of the orthogonality of

basis functions. Multiplying both sides of (4.17) and (4.18) by $\sqrt{2}\phi(2t-n)$ and then integrating with respect to t we have

$$\sqrt{2}\int_{-\infty}^{\infty}\phi(t)\phi(2t-n)dt = \sum_{k=-\infty}^{\infty}k_1[k]\int_{-\infty}^{\infty}2\phi(2t-n)\phi(2t-k)dt, \tag{4.19}$$

$$\sqrt{2}\int_{-\infty}^{\infty}w(t)\phi(2t-n)dt = \sum_{k=-\infty}^{\infty}k_2[k]\int_{-\infty}^{\infty}2\phi(2t-n)\phi(2t-k)dt. \tag{4.20}$$

Integrals on the right hand side of (4.19) and (4.20) are one for $k=n$ and zero otherwise by (4.16). As a result, the discrete sequences come out to be

$$k_1[n] = \sqrt{2}\int_{-\infty}^{\infty}\phi(t)\phi(2t-n)dt, \tag{4.21}$$

$$k_2[n] = \sqrt{2}\int_{-\infty}^{\infty}w(t)\phi(2t-n)dt. \tag{4.22}$$

Let $f(t)$ be a function in V_{-1}. Then, as in the previous discussion, we can expand it in terms of the basis functions of V_{-1}, i.e.,

$$f(t) = \sqrt{2}\sum_{k=-\infty}^{\infty}F_{-1}[k]\phi(2t-k). \tag{4.23}$$

Another way of expanding $f(t)$ is to express it in terms of the sum of the coarser approximation $f_c(t)$ in V_0 and the detail $f_d(t)$ in W_0, i.e., $f(t) = f_c(t) + f_d(t)$ where $f_c(t)$ and $f_d(t)$ can in turn be expanded in V_0 and W_0, respectively. We thus have

$$f_c(t) = \sum_{k=-\infty}^{\infty}F_0[k]\phi(t-k), \tag{4.24}$$

$$f_d(t) = \sum_{k=-\infty}^{\infty}D_0[k]w(t-k). \tag{4.25}$$

Combining (4.23), (4.24) and (4.25) we get

$$\sqrt{2}\sum_{k=-\infty}^{\infty}F_{-1}[k]\phi(2t-k) = \sum_{k=-\infty}^{\infty}F_0[k]\phi(t-k) + \sum_{k=-\infty}^{\infty}D_0[k]w(t-k). \tag{4.26}$$

Again multiplying both sides of (4.26) by $\sqrt{2}\phi(2t-n)$ and integrating with respect to t, we get

$$\sum_{k=-\infty}^{\infty}F_{-1}[k]\int_{-\infty}^{\infty}2\phi(2t-n)\phi(2t-k)dt =$$

$$\sum_{k=-\infty}^{\infty}F_0[k]\int_{-\infty}^{\infty}\sqrt{2}\phi(t-n)\phi(2t-k)dt + \sum_{k=-\infty}^{\infty}D_0[k]\int_{-\infty}^{\infty}\sqrt{2}w(t-n)\phi(2t-k)dt.$$

After replacing t by $t+k$ and using orthogonality

$$F_{-1}[n] = \sum_{k=-\infty}^{\infty} F_0[k] \int_{-\infty}^{\infty} \sqrt{2}\phi(t)\phi(2t+2k-n)dt + \sum_{k=-\infty}^{\infty} D_0[k] \int_{-\infty}^{\infty} \sqrt{2}w(t)\phi(2t+2k-n)dt. \tag{4.27}$$

By (4.21) and (4.22),

$$F_{-1}[n] = \sum_{k=-\infty}^{\infty} F_0[k]k_1[n-2k] + \sum_{k=-\infty}^{\infty} D_0[k]k_2[n-2k] \tag{4.28}$$

Equation (4.28) can be interpreted as a synthesis of discrete sequence $F_{-1}[n]$ from $F_0[n]$ and $D_0[n]$. In fact, equation (4.28) corresponds to upsampling $F_0[n]$ and $D_0[n]$ first and then filtering with $k_1[n]$ and $k_2[n]$. Therefore, the synthesis section of a two-channel filter bank implements the synthesis of a finer signal from its coarser approximation and its detail. Figure 4.9 visualizes this process.

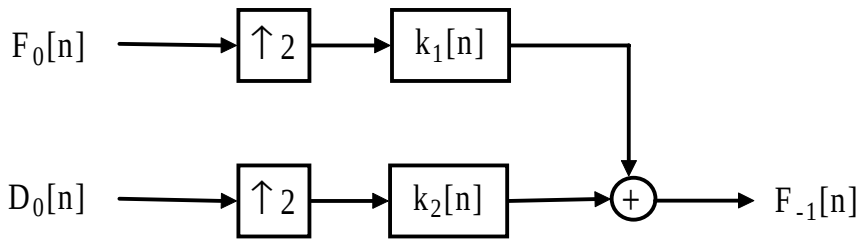

Figure 4.9: Synthesis of a fine signal $F_{-1}[n]$ from a coarse approximation $F_0[n]$ and a detail $D_0[n]$.

The natural question arising at this point is whether analysis section of a two-channel filter bank implements an inverse operation, i.e., it decomposes $F_{-1}[n]$ into $F_0[n]$ and $D_0[n]$. The answer is yes. We start with an orthogonal projection of $f(t)$ into V_0 and W_0. Coarse approximation $f_c(t)$ in terms of $f(t)$ is

$$f_c(t) = \sum_{k=-\infty}^{\infty} \Big[\int_{-\infty}^{\infty} f(t)\phi(t-k)dt \Big] \phi(t-k). \tag{4.29}$$

Equation (4.29) is the same as (4.24), so

$$F_0[k] = \int_{-\infty}^{\infty} f(t)\phi(t-k)dt. \tag{4.30}$$

Multiplying both sides of (4.23) by $\phi(t-n)$ and integrating with respect to t we get

$$\int_{-\infty}^{\infty} f(t)\phi(t-n)dt = \sum_{k=-\infty}^{\infty} F_{-1}[k] \int_{-\infty}^{\infty} \sqrt{2}\phi(2t-k)\phi(t-n)dt. \tag{4.31}$$

Then by (4.21) and (4.30)

$$F_0[n] = \sum_{k=-\infty}^{\infty} F_{-1}[k]k_1[k-2n]. \tag{4.32}$$

Following the same steps for $f_d(t)$ we can get

$$D_0[n] = \sum_{k=-\infty}^{\infty} F_{-1}[k]k_2[k-2n]. \tag{4.33}$$

Equations (4.32) and (4.33) correspond to filtering the sequence $F_{-1}[n]$ with $k_1[-n]$ and $k_2[-n]$, respectively, and then downsampling by 2. Figure 4.10 illustrates the result we have reached. We have shown that a filter bank implements an orthogonal wavelet transform. However, we have not yet answered the question of what type of filter bank it is. We now concentrate on orthogonality of wavelet basis and make use of dilation and wavelet equation in order to figure out the properties of the discrete filters $k_1[n]$ and $k_2[n]$. We first multiply both sides of the dilation equation (4.17) by $\phi(t-n)$ and integrate with respect to t to get

$$\int_{-\infty}^{\infty} \phi(t)\phi(t-n)dt = \sum_{k=-\infty}^{\infty} k_1[k] \int_{-\infty}^{\infty} \sqrt{2}\phi(2t-k)\phi(t-n)dt, \tag{4.34}$$

$$= \sum_{k=-\infty}^{\infty} k_1[k] \int_{-\infty}^{\infty} \sqrt{2}\phi(2t+2n-k)\phi(t)dt. \tag{4.35}$$

In (4.35), the left hand side is the impulse $\delta[n]$ and the integral on the right hand side is $k_1[n-2k]$, by equation (4.21). Thus

$$\sum_{k=-\infty}^{\infty} k_1[k]k_1[k-2n] = \delta[n]. \tag{4.36}$$

Following the same steps for the wavelet equation (4.18), we get

$$\sum_{k=-\infty}^{\infty} k_2[k]k_1[k-2n] = 0 \tag{4.37}$$

Finally, multiplying wavelet equation (4.18) by $w(t-n)$ and following the previous procedure we get

$$\sum_{k=-\infty}^{\infty} k_2[k]k_2[k-2n] = \delta[n]. \tag{4.38}$$

These equations are the same as (3.19), (3.18) and (3.20) of CQF filters. Therefore, an orthogonal wavelet transform is computed by an orthogonal filter bank.

In signal processing applications, in general, one likes to deal with discrete time signals. Continuous time signals are sampled and then these samples are processed. From this point of view, two-channel filter banks are very important because they provide a fast algorithm to take continuous time wavelet transform without dealing with continuous time signals themselves but rather with samples of these signals.

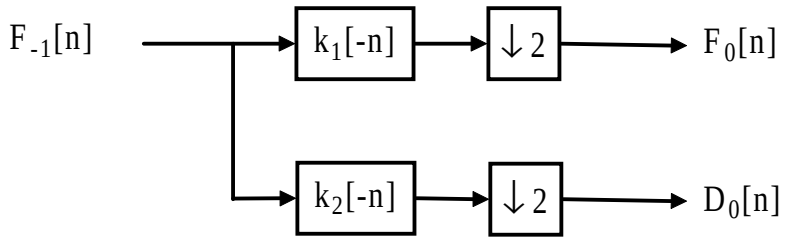

Figure 4.10: Decomposition of $F_{-1}[n]$ into a coarse approximation $F_0[n]$ and a detail $D_0[n]$.

4.4 Construction of Orthogonal Wavelets with Compact Support Using Fourier Techniques

In Section 4.2, we defined multiresolution analysis and gave the conditions on the scaling function $\phi(t)$ and the wavelet function $w(t)$. However, we did not

give any example other than the space of piecewise constant functions for which Haar wavelets are basis functions. The reason for this is that we do not have any closed form expressions for compactly supported wavelet functions except for the Haar wavelet [6]. A solution to efficient construction of wavelets is the *cascade algorithm* which uses the discrete sequences $k_1[n]$ and $k_2[n]$ to construct the scaling function and the wavelet function [6]. The algorithm uses iterated two-channel orthogonal filter bank with lowpass filter $k_1[n]$ and highpass filter $k_2[n]$ defined by (4.17) and (4.18). Figure 4.11 shows synthesis section of an iterated two-channel filter bank for wavelet-like decomposition. In this type of decomposition only outputs of the lowpass filters are decomposed further.

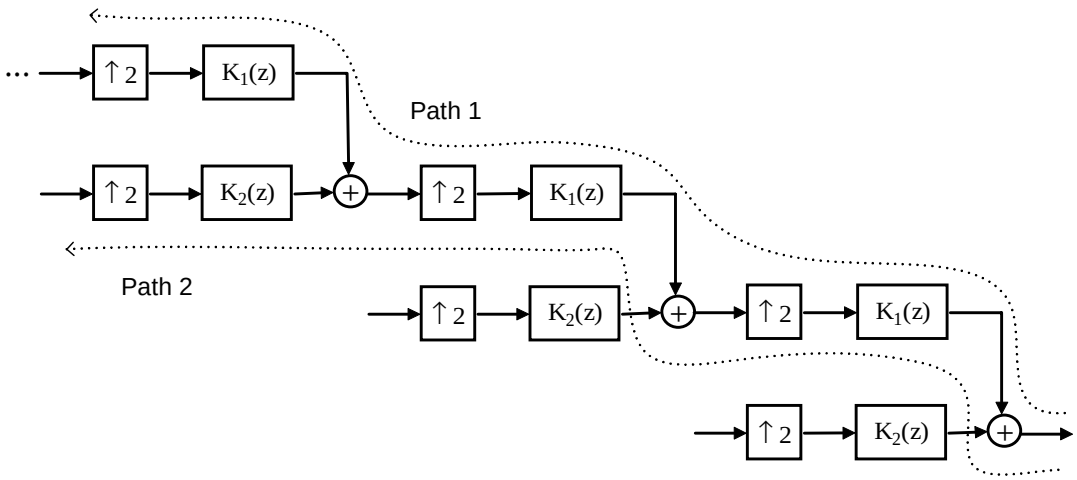

Figure 4.11: Synthesis section of iterated two-channel filter bank for wavelet-like decomposition.

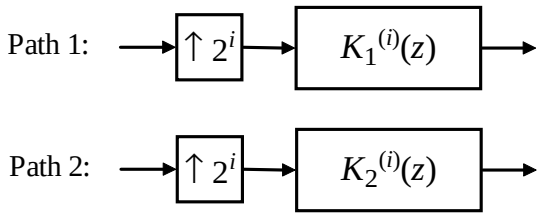

Figure 4.12: Equivalent structure of Path 1 and Path 2 after i-iterations.

Equivalent structures after i-iteration in Path 1 and Path 2 can be written as

a single upsampler followed by a single filter making use of the noble identity in Figure 2.9. Figure 4.12 shows this equivalent structures. Equivalent filters $K_1^{(i)}(z)$ and $K_2^{(i)}(z)$ are

$$\begin{aligned} K_1^{(i)}(z) &= \prod_{k=0}^{i-1} K_1(z^{2^k}) \\ K_2^{(i)}(z) &= K_2(z^{2^{i-1}}) \prod_{k=0}^{i-2} K_1(z^{2^k}) \end{aligned}$$

Let impulse responses corresponding to $K_1^{(i)}$ and $K_2^{(i)}$ be $k_1^{(i)}[n]$ and $k_2^{(i)}[n]$. Then wavelet and scaling functions are defined in terms of $k_1^{(i)}[n]$ and $k_2^{(i)}[n]$ as i goes to infinity. However, we can calculate approximations for finite i. Approximations are defined as

$$\phi^{(i)}(t) = 2^{i/2} k_1^{(i)}[n], \quad n/2^i \le t < (n+1)/2^i, \tag{4.39}$$

$$w^{(i)}(t) = 2^{i/2} k_2^{(i)}[n], \quad n/2^i \le t < (n+1)/2^i. \tag{4.40}$$

These functions are in continuous-time and they are constant in the intervals $[\frac{n}{2^i}, \frac{(n+1)}{2^i})$. As i increases, the length of the interval decreases in order to keep the support of $\phi^{(i)}(t)$ and $w^{(i)}(t)$ finite. In fact, $\phi^{(i)}(t)$ and $w^{(i)}(t)$ are nonzero in the interval $[0, N-1)$ for length N filters $k_1^{(i)}[n]$ and $k_2^{(i)}[n]$. Discrete-time filters and corresponding continuous-time functions have the same support. The normalization factor $2^{i/2}$ in (4.39) and (4.40) keeps the norm of continuous-time functions constant at 1.

Example 3. In this simple example we will construct D_2 (Daubechies' wavelet with support [0,3)) from discrete filters. Lowpass filter $k_1[n]$ and highpass filter $k_2[n]$ are

$$\begin{aligned} k_1[n] &= 0.4830 + 0.8365z^{-1} + 0.2241z^{-2} - 0.1294z^{-3}, \\ k_2[n] &= -0.1294 - 0.2241z^{-1} + 0.8365z^{-2} - 0.4830z^{-3}. \end{aligned}$$

Figure 4.13 illustrates the cascade algorithm for $N = 2$, 3, and 4 iterations.

Example 4. In Section 3.2 we introduced different types of filters that satisfy PR. We summarized some of those filters in Table 3.1 and 3.2. Figure 4.14 shows the scaling and wavelet functions corresponding to filters in those tables.

The functions in Figure 4.14a,b,c,d,e,f are really scaling functions and wavelets. However, this is not true for the functions in Figure 4.14g,h, note the wiggles at the peaks of these functions. Why discrete filters of D_2, D_3 and D_4 generate wavelets but Smith and Barnwell filter cannot is closely related to the zeros the filters have. Figure 4.15 shows the zeros of filters in Table 3.1 and 3.2. Daubechies filters have common zeros at $z = -1$ with multiplicities larger than 1 but Smith and Barnwell filter does not. Moreover, larger number of zeros at $z = -1$ gives smoother functions. This result is stated in [6] where it is shown that the discrete lowpass filter must have at least one zero at $z = -1$ and the discrete highpass filter must have at least one zero at $z = 1$. In the next chapter, we explain how to assign these and other zeros to discrete filters.

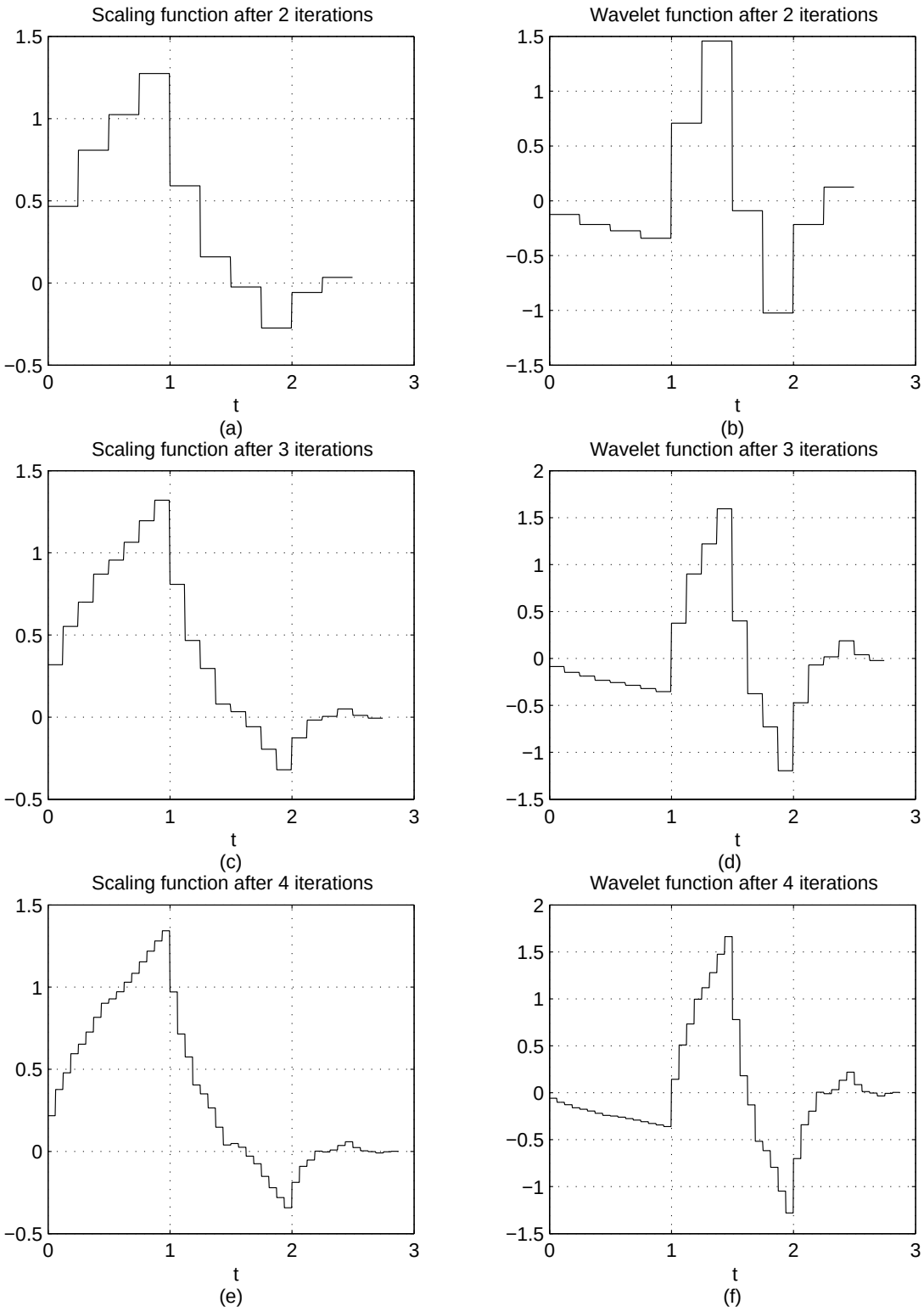

Figure 4.13: Illustration of the cascade algorithm for D_2, (a), (c), (e) Scaling functions, (b), (d), (f) Wavelet functions.

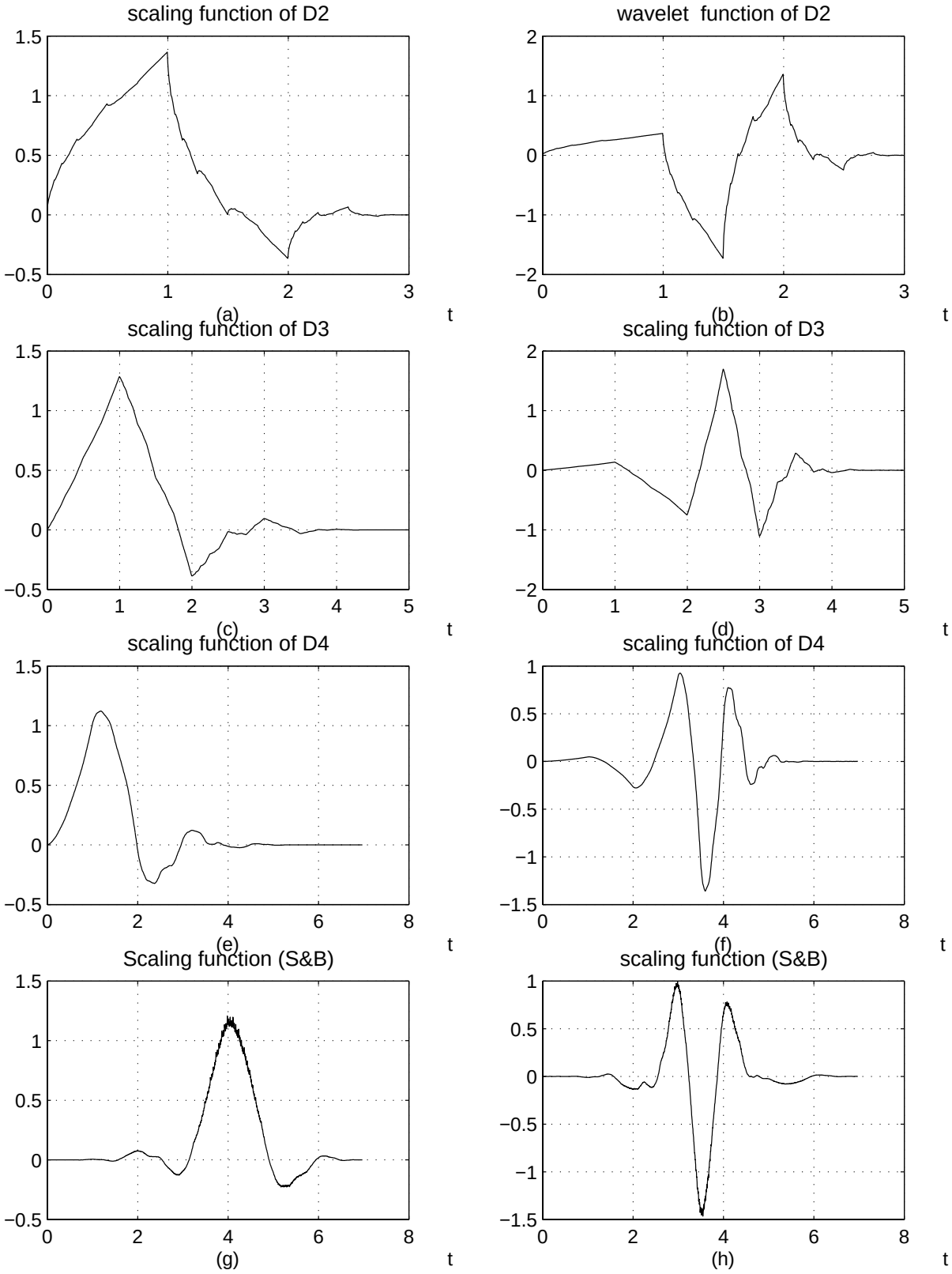

Figure 4.14: Scaling and wavelet functions constructed using cascade algorithm.

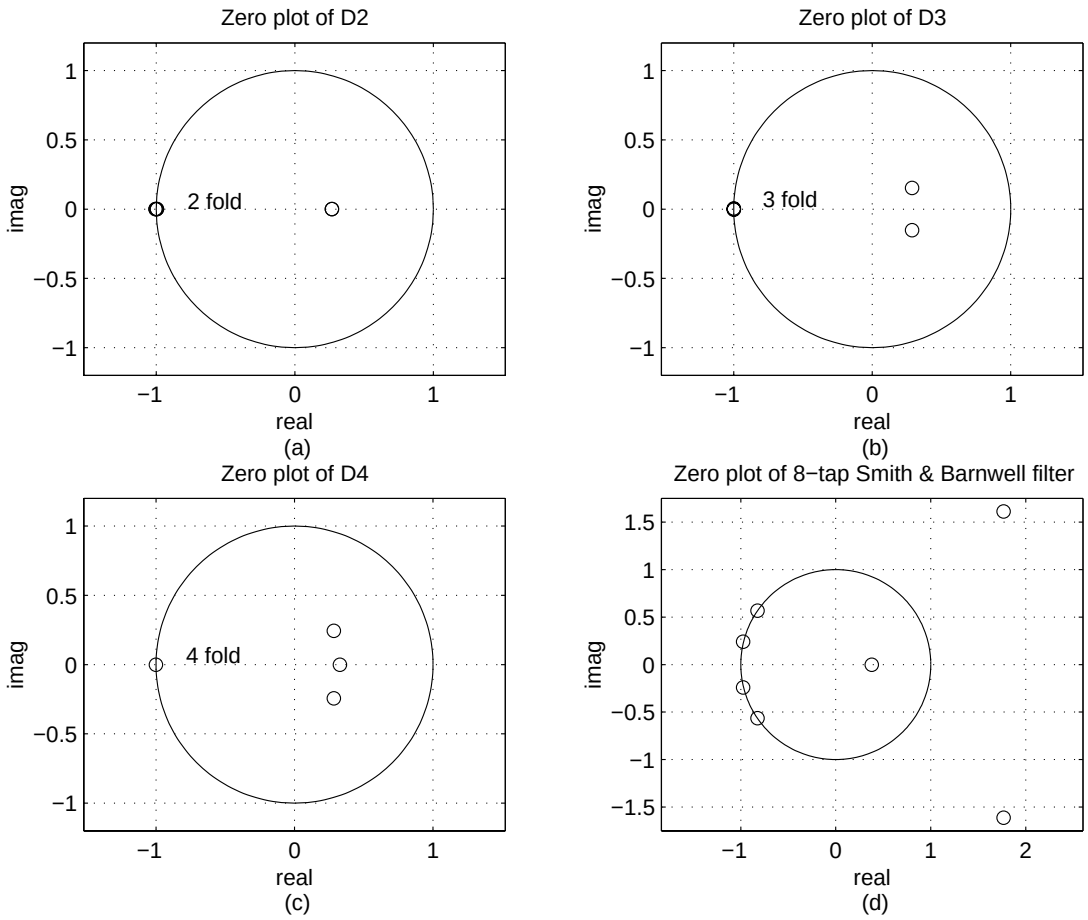

Figure 4.15: Zero plot of (a) D_2, (b) D_3, (c) D_4 and (d) Smith and Barnwell.

Chapter 5

ZERO ASSIGNMENT

Most desirable filter properties such as flatness, minimal-length, smoothness are all directly related to number and location of the zeros in the filter transfer functions. Moreover, FIR filters can be viewed as all-zero transfer functions of delay z^{-1} so that an FIR filter upto multiplication by a nonzero constant is completely characterized by its zeros. It is hence of utmost importance to be able to assign desired zeros to filter transfer functions. In this chapter, we introduce a way of assigning zeros to filter transfer functions using algebraic methods.

The main result given in Theorem 1 describes the set of all filter banks with assigned filter zeros and with poles in any desired region in the complex plane. The description is in terms of an even transfer function parameter that enters linearly into the expression for a product of filter transfer functions. Thus, every choice of an even transfer function gives a new filter bank with assigned zeros and all filter banks are obtained as such.

This chapter is organized as follows: Section 5.1 gives the mathematical preliminaries from abstract algebra. In that section, the methods of solving the equation $ax + by = c$ in a Euclidean domain is also given. Section 5.2 is the main contribution of this thesis. Theorem 1 proves that it is possible to design filter

banks with filters having assigned zeros. A construction algorithm is given in the following section, Section 5.3. Section 5.4 deals with FIR filters only. Because it is possible to design orthogonal FIR filter banks which correspond to the orthogonal wavelets when zeros at $z = 1$, and $z = -1$ exist. Theorem 2 incorporates the orthogonality condition (or conjugate symmetry) and a way of obtaining a particular orthogonal FIR solution using the free even parameter. Theorem 2 is a generalization of Daubechies' design and makes possible to assign zeros other than the ones at $z = 1$ and $z = -1$. It is hence possible to investigate the effect of perturbing the zeros at 1 and -1 on the smoothness of the wavelet and the scaling functions generated. This robustness analysis is the topic of Section 5.5.

5.1 A Brief Review of a Euclidean Domain

A brief review of a Euclidean domain, Euclidean algorithm, and the linear equation $ax + by = c$ over an arbitrary Euclidean domain is first given. The reader may consult [10] and [12] for a detailed exposition.

A commutative ring without divisors of 0, with a unit element 1, and in which every pair of elements not both zero has *a greatest common divisor* representable linearly in terms of the elements is called a *principal ideal domain*. Simplest examples of a principal ideal domain (which are not fields) are the rings of integers and polynomials of one variable, with real coefficients. In a principal ideal domain, a divisor of 1 is called a *unit*. A common divisor of a, b in a principal ideal domain $\mathbf{D}$ is $c \in \mathbf{D}$ such that $a = c\bar{a}$ and $b = c\bar{b}$ for some $\bar{a}, \bar{b} \in \mathbf{D}$. A greatest common divisor of (a, b) is a common divisor which includes any other common divisor as a factor and it is unique upto multiplication by a unit of $\mathbf{D}$.

An important instance of a principal ideal domain is a *Euclidean domain* defined by the property that (i) associated with every nonzero element a, there is a nonnegative integer $ed(a)$ called the *Euclidean degree* of a and (ii) for every pair

of elements $a, b \neq 0$, there exists two elements q, r such that $a = bq + r$, and either $r = 0$ or $ed(r) < ed(b)$. Thus for integers, $ed(m) := |m|$ and for polynomials of u with real coefficients, the degree of a polynomial $ed(p(u)) := deg(p(u))$ serve as valid definitions of Euclidean degrees. A useful property of the ring of polynomials and D_Ω, defined below, is that $ed(a\dot{b}) = ed(a) + ed(b)$ for all nonzero elements a, b. In the ring of polynomials $ed(a + b) \leq max(ed(a), ed(b))$ is also true.

Although they share many nice properties, a Euclidean domain is superior to a principal ideal domain by the existence of an algorithm to determine a greatest common divisor. The *Euclidean algorithm* is based on the property (ii) above: Let $\mathbf{D}$ be a Euclidean domain and let $a, b \in \mathbf{D}$, with say $b \neq 0$, be given. Consider the algorithm

$$\begin{aligned}
&a = bq_1 + r_1, && ed(r_1) < ed(b),\\
&b = r_1 q_2 + r_2, && ed(r_2) < ed(r_1),\\
&\vdots && \vdots\\
&r_{n-3} = r_{n-2} q_{n-1} + r_{n-1}, && ed(r_{n-1}) < ed(r_{n-2}),\\
&r_{n-2} = r_{n-1} q_n + r_n, && r_n = 0.
\end{aligned} \tag{5.1}$$

The algorithm stops at the first zero remainder r_n. A greatest common divisor of a, b is then r_{n-1}. By working backwards in the algorithm, it is not difficult to construct elements $x, y \in \mathbf{D}$, in terms of quotients and remainders, satisfying

$$r_{n-1} = ax + by.$$

The Euclidean algorithm thus gives an explicit linear representation of a greatest common divisor of a, b. In Appendix A, explicit expressions for x and y are available for the polynomial ring.

Two elements a and b in $\mathbf{D}$ are called *coprime* if their greatest common divisor is a unit; (a, b) is coprime if and only if there exists $x, y \in \mathbf{D}$ such that $ax + by = 1$. Given $a, b, c \in \mathbf{D}$, let $x, y \in \mathbf{D}$ satisfy

$$ax + by = c. \tag{5.2}$$

The pair (x, y) is then called *a solution to (5.2) over* $\mathbf{D}$. A necessary and sufficient condition for a solution to exist is that a greatest common divisor g of (a, b) divides c, i.e., there exist $\hat{a}, \hat{b}, \hat{c} \in \mathbf{D}$ such that $a = g\hat{a}, b = g\hat{b}$ with $(\hat{a}, \hat{b})$ coprime and $c = g\hat{c}$. Note that a solution can be constructed by first determining $\hat{x}, \hat{y} \in \mathbf{D}$ satisfying $\hat{a}\hat{x} + \hat{b}\hat{y} = 1$ via the algorithm (5.1) and then letting $x := \hat{x}\hat{c}, y := \hat{x}\hat{c}$ so that $ax + by = g\hat{c} = c$.

The *set of all solutions* to (5.2) has a convenient description in terms of a particular solution (x, y):

$$\{(x + \hat{b}\theta, y - \hat{a}\theta) : \theta \in \mathbf{D}\}. \tag{5.3}$$

This is a very useful parameterization of all solutions since it is linear and since the parameter θ is free over the whole domain $\mathbf{D}$.

Example 5. *Consider the ring of integers and the equation* $5x + 7y = 3$. *Note that* $(x, y) = (2, -1)$ *is a particular solution. Also note that* $(5, 7)$ *is coprime. All solutions are hence obtained as* $(2 + 7\theta, -1 - 5\theta)$ *for an arbitrary integer* θ.

The algebraic structure of the Euclidean domain of *rational, causal, and stable transfer functions* (see [11] or [16]) can be examined with the objective of determining special solutions to an equation of the type (5.2).

In order to handle various different notions of stability in the same context, we introduce a *stability set* Ω, which is a set of points in the complex plane symmetric with respect to the origin. Thus, $\Omega = \{0\}$, $\Omega = \{\pm 0.5 \pm 0.5j\}$, and $\Omega =$ open unit disk are all examples of stability sets. Let D_Ω be the set of all rational functions in the indeterminate z with all their poles in Ω and such that they have finite limits as $z \to \infty$. These are transfer functions of finite-dimensional, discrete-time, causal systems which are stable to a degree determined by the stability set. If Ω is the open unit disc, then D_Ω is the set of transfer functions of filters that are stable in the usual sense. On the other hand, if $\Omega = \{0\}$, then D_Ω is the set of all FIR filters. Since it can be obtained as a quotient ring of the ring

of polynomials, D_Ω is a principal ideal domain. In fact, it is a Euclidean domain with the Euclidean degree of an element $H(z)$ defined as the number of its zeros at infinity and its finite zeros outside Ω, [16]. The units in D_Ω are those elements having their zeros all in Ω and having causal inverses (equivalently to the latter, having no zeros at infinity). If $\Omega = \{0\}$, then the units of D_Ω are nonzero real numbers. If, on the other hand, Ω is the open unit disc, then the units of D_Ω are stable, minimum-phase transfer functions devoid of zeros at infinity. It can easily be shown that a pair of elements (A, B) in D_Ω are *coprime* if and only if (i) they have no common zero outside Ω and (ii) at least one of them has no zero at infinity.

Suppose Ω contains at least one real number r. Any element $H(z) \in D_\Omega$ has the following useful representation with respect to r, [16]:

$$H(z) = U(z)\frac{\alpha(z)}{\lambda(z)^n}, \tag{5.4}$$

where $U(z)$ is a unit in D_Ω, $\alpha(z)$ is a monic polynomial in z having all its zeros outside Ω, n is a nonnegative integer, and $\lambda(z) := z - r$, a degree one polynomial with its zero at r. Such a representation is unique and is referred to as a *standard representation*, [11]. It is easy to see that, in the standard representation (5.4), $n = ed(H(z))$.

One can employ standard representations to determine solutions to an equation like (5.2) over D_Ω using polynomial algebra rather than the Euclidean algorithm over D_Ω. Let $A(z), B(z), C(z) \in D_\Omega$ be given and consider the equation

$$A(z)X(z) + B(z)Y(z) = C(z) \tag{5.5}$$

for $X(z), Y(z) \in D_\Omega$. Not showing the dependence on z, let us consider the following procedure that constructs a solution (X, Y) to (5.5). For simplicity and without loss of generality, we assume that (A, B) is coprime and that B has no zeros at infinity, i.e., B has a causal inverse. Note that by the condition for solvability of (5.5), a greatest common divisor of (A, B) should divide C, which

allows us to make the first assumption. If (A, B) is coprime, then it is necessary that either A or B is devoid of zeros at infinity; this allows the second assumption. We also assume that B is not a unit, since otherwise the construction of a solution is trivial. Let us consider the standard representations

$$A = U_a \frac{\alpha}{\lambda^n},\ B = U_b \frac{\beta}{\lambda^m},\ C = U_c \frac{\gamma}{\lambda^k}$$

of A, B, C. By the assumptions on B, we have $m = deg(\beta) \geq 1$. By the assumption of coprimeness of (A, B) over D_Ω, we also have that the polynomials (α, β) are coprime since otherwise A and B would have a common finite zero outside Ω contradicting the assumption. Define two integers $l := max\{n, m\}$ and $t := max\{l-1, k-l\}$. We now have that the pair of polynomials $(\lambda^{l-n}\alpha, \lambda^{l-m}\beta)$ is coprime so that by an application of the Euclidean algorithm (5.1) with $\mathbf{D}$ taken as the polynomial ring, there exist polynomials x, y such that $\lambda^{l-n}\alpha x + \lambda^{l-m}\beta y = \lambda^{l-k+t}\gamma$. Here one can ensure that $deg(x) \leq l - 1$. (Since if x does not satisfy this condition, by Euclidean division once more, one can write $x = \lambda^{l-m}\beta\tilde{x} + \hat{x}$ where $\hat{x}$ does satisfy $deg(\hat{x}) \leq l - 1$. Upon defining $\hat{y} := \tilde{x}\lambda^{l-n}\alpha + y$, we have a solution $(\hat{x}, \hat{y})$ satisfying the condition.) Defining

$$X = U_c U_a^{-1} \frac{x}{\lambda^t},\ Y = U_c U_b^{-1} \frac{y}{\lambda^t},$$

where $X \in D_\Omega$ by the fact that $deg(x) \leq t$, one easily verifies that (5.5) is satisfied. It remains to check that $Y \in D_\Omega$. Since all poles of Y are clearly in Ω, one only needs to verify that Y has no pole at infinity. However, $Y = B^{-1}(C - AX)$, where $C - AX$ has no pole at infinity and B has no zero at infinity. It follows that Y has no pole at infinity. Therefore, (X, Y) is a solution to (5.5). We note that the Euclidean degrees of X and Y so constructed satisfy

$$max\{ed(X), ed(Y)\} < max\{ed(A), ed(B)\} \text{ provided } ed(C) \leq 2max\{ed(A), ed(B)\} - 1. \tag{5.6}$$

We now let $\Omega := \{0\}$ and focus on a special case of the equation (5.5). Let $G(z) \in D_{\{0\}}$ have order equal to g. Suppose $(G(z), G(-z))$ is coprime over $D_{\{0\}}$.

Let n_0 be an odd integer and consider the equation

$$G(z)M(z) - G(-z)N(z) = 2z^{-n_0} \tag{5.7}$$

in the unknowns $M(z)$ and $N(z)$. If some $M(z), N(z) \in D_{\{0\}}$ satisfy (5.7), then the pair is said to be a solution to (5.7).

Fact 1. *Given any odd integer $n_0 \geq 0$, if a solution $(M(z), N(z))$ to (5.7) is such that each of $M(z), N(z)$ has order less than g, then it is unique and satisfies $M(z) = N(-z)$.*

Proof. Let $(M_i(z), N_i(z)); i = 1, 2$ be two solutions to (5.7). Then,

$$G(z)(M_1(z) - M_2(z)) = G(-z)(N_1(z) - N_2(z)).$$

By coprimeness of $(G(z), G(-z))$ over $D_{\{0\}}$, it follows that

$$M_1(z) - M_2(z) = G(-z)\Theta(z)$$

and

$$N_1(z) - N_2(z) = G(z)\Theta(z)$$

for some $\Theta(z) \in D_{\{0\}}$. Since for any two nonzero elements in $D_{\{0\}}$, the order of the multiple is equal to the sum of the order of each element, and since the order of the sum of the two elements is less or equal to the larger order, we have that $M_1(z) - M_2(z)$ has a strictly less order than $G(-z)\Theta(z)$. Thus the two are not equal unless both are identically zero. It follows that $M_1(z) = M_2(z)$ and, hence, $N_1(z) = N_2(z)$.

Now, by the fact that n_0 is odd, $(M(z), N(z))$ is a solution to (5.7) if and only if $(N(-z), M(-z))$ is a solution. Since orders of $M(z), N(z)$ being less than g implies that the orders of $N(-z), M(-z)$ are also less than g, by the uniqueness result proved in the first part it follows that $M(z) = N(-z)$. □

Fact 2. *Given any odd integer $n_0 \in [0, 2g-1]$, a solution $(M(z), M(-z))$ to (5.7), where $M(z)$ has order at most $g-1$, exists, is unique, and is a minimal order solution.*

Proof. By the construction of a solution to (5.5), a solution

$$(\hat{M}(z), \hat{N}(z))$$

to (5.7) exists and, by (5.6), satisfies

$$max\{ed(M(z), ed(N(z))\} < max\{ed(G(z)), ed(G(-z))\} = g$$

provided

$$ed(2z^{-n_0}) = n_0 \leq 2max\{ed(G(z)), ed(G(-z))\} - 1 = 2g - 1.$$

By Fact 1, $M(z) = N(-z)$ and the solution $(M(z), M(-z))$ is unique. Minimality is a direct consequence of uniqueness. □

5.2 Assignment of Arbitrary Zeros

Since PR condition (3.16) determines the synthesis filter transfer functions almost entirely in terms of the analysis filter transfer functions, we will consider the problem of assigning zeros to PR analysis filters. We assume throughout this section that $0 \in \Omega$ so that the delay element $z^{-1} \in D_\Omega$.

Suppose an odd overall delay $n_0 \geq 0$ is given. If the analysis filters $H_1(z)$ and $H_2(z)$ are to have certain zeros in Ω with desired multiplicities, then let the zeros of the causal-stable transfer functions $G_1(z)$ and $G_2(z)$ contain the desired zeros of $H_1(z)$ and $H_2(z)$, respectively.[1] The analysis filters will then have the desired zeros if and only if

$$H_1(z) = G_1(z)\hat{H}_1(z), \;\; H_2(z) = G_2(z)\hat{H}_2(z) \tag{5.8}$$

for some causal-stable transfer functions $\hat{H}_1(z)$ and $\hat{H}_2(z)$. Here, we rewrite PR equation (3.16) for convenience:

$$H_1(z)H_2(-z) - H_1(-z)H_2(z) = 2z^{-n_0}. \tag{5.9}$$

[1]Since zeros in Ω are in danger of being cancelled by poles, the stability set Ω should exclude those zeros that we desire to assign. The D_Ω-functions $G_1(z)$ and $G_2(z)$ are then formed by placing equal number of arbitrary poles in the denominator as the assigned zeros.

In what follows, we refer to $H_1(z)H_2(-z) = H_1(z)K_1(z)$ as the *product lowpass filter*. Substituting (5.8) in (5.9), we have

$$G_1(z)G_2(-z)\hat{H}_1(z)\hat{H}_2(-z) - G_1(-z)G_2(z)\hat{H}_1(-z)\hat{H}_2(z) = 2z^{-n_0}. \qquad (5.10)$$

Thus, a necessary condition on the to-be-assigned zeros is that a greatest common divisor (upto multiplication by a unit) of $\big(G_1(z)G_2(-z), G_1(-z)G_2(z)\big)$ must divide $2z^{-n_0}$ so that it must at most be a delay function of the form z^{-l_0} with $l_0 \leq n_0$. After defining $G(z) = G_1(z)G_2(-z)$, we hence assume, for simplicity, that

$$\big(G(z), G(-z)\big) \quad \text{is coprime.} \qquad (5.11)$$

Note that this assumption amounts to the restriction that there are no symmetrically located zeros (and poles) of $G(z)$ with respect to the imaginary axis. In order to construct $\hat{H}_1(z)$ and $\hat{H}_2(z)$ satisfying (5.10), we resort to the construction using the Euclidean algorithm by which there exist $F_1(z)$ and $F_2(z)$ satisfying

$$G(z)F_1(z) - G(-z)F_2(z) = z^{-n_0}. \qquad (5.12)$$

Substituting $-z$ for z in (5.12) and taking the sum of (5.12) with the resulting equality, we have

$$G(z)\hat{H}(z) - G(-z)\hat{H}(-z) = 2z^{-n_0} \qquad (5.13)$$

where $\hat{H}(z) := F_1(z) + F_2(-z)$. We have thus constructed $\hat{H}(z)$, a factorization of which would yield (5.10) and therefore a PR filter bank in which the analysis filters have assigned zeros. An application of (5.3) also yields the set of all solutions to $\hat{H}(z)$ in terms of a particular solution. Following theorem summarizes these results.

Theorem 1. *Let $G_1(z), G_2(z) \in D_\Omega$ satisfy (5.11) and let the Euclidean degree of $G(z)$ be denoted by g.*

(i) Given any odd integer $n_0 > 0$, there exists a two-channel PR filter bank of time-delay n_0 with analysis filters of the form

$$H_{1p}(z) = G_1(z)\hat{H}_{1p}(z), \;\; H_{2p}(z) = G_2(z)\hat{H}_{2p}(z)$$

for transfer functions $\hat{H}_{1p}(z),\ \hat{H}_{2p}(z) \in D_\Omega$. *If* $n_0 \in [0, 2g-1]$, *then the filters are such that the Euclidean degree of* $\hat{H}_p(z) := \hat{H}_{1p}(z)\hat{H}_{2p}(-z)$ *is at most* $g-1$.

(ii) All analysis filters giving a PR filter bank of time-delay $n_0 + l_0$ *for an even integer* $l_0 \geq 0$, *are given by* $H_1(z) = G_1(z)\hat{H}_1(z),\ H_2(z) = G_2(z)\hat{H}_2(z)$, *where*

$$\hat{H}_1(z)\hat{H}_2(-z) = \hat{H}_{1p}(z)\hat{H}_{2p}(-z)z^{-l_0} + G_1(-z)G_2(z)\Theta(z) \tag{5.14}$$

for some even $\Theta(z) \in D_\Omega$.

Proof: (i) By the construction (5.2) in Section 5.1, a particular solution $\hat{H}_p(z)$ to $G(z)\hat{H}_p(z) - G(-z)\hat{H}_p(-z) = 2z^{-n_0}$ exists and satisfies $ed(\hat{H}_p(z)) < g$ provided $n_0 \leq 2g-1$. Let $\hat{H}_p(z) = \hat{H}_{1p}(z)\hat{H}_{2p}(-z)$ be any factorization of $\hat{H}_p(z)$ into $\hat{H}_{1p}(z)$ and $\hat{H}_{2p}(z)$. Then, (5.10) is satisfied and PR is achieved. (ii) By direct substitution, it is easy to verify that any other $H_1(z)$, $H_2(z)$ related to $\hat{H}_{1p}(z)$, $\hat{H}_{2p}(z)$ by (5.14) will also satisfy (5.13), with n_0 replaced by $n_0 + l_0$, provided $\Theta(z) = \Theta(-z)$. Moreover, by the parameterization (5.3) of Section 5.1, (5.14) describes the set of all solutions to (5.10). Substituting an arbitrary solution into the equation and changing the variable z to $-z$, it is easy to see that the parameter $\Theta(z)$ is further constrained by $\Theta(z) = \Theta(-z)$. □

Every even $\Theta(z)$ *yields a unique product lowpass filter* by the linearity of the parameterization. However, nonuniqueness is still present in our scheme since in obtaining the individual analysis filters, a *(spectral) factorization* of $\hat{H}_{1p}(z)\hat{H}_{2p}(z) + G_1(-z)G_2(z)\Theta(z)$ into $\hat{H}_1(z)\hat{H}_2(-z)$ is required. For a high order product lowpass filter, there would be many different possible choices for analysis filters. This nonuniqueness may be exploited in satisfying the practical constraints of low-pass and high-pass on the filters $H_1(z)$ and $H_2(z)$. A hand-rule is to select the right half plane poles and left half plane zeros for low-pass filters and right half plane zeros and left half plane poles for high-pass filters. In low order filters, especially in FIR ones, this hand-rule works fairly well. More on the effect of pole and zero locations on frequency response may be found in [18].

The next section introduces an algorithm to find a solution to (5.13).

5.3 A Polynomial Algorithm to Construct a Filter Bank with Assigned Zeros

In the previous section, we have shown that it is possible to design filter banks with assigned zeros. There are several ways, such as Hermite polynomial interpolation or realization theory [11], of finding a solution to (5.13). In this thesis, we adopt an algorithm which uses an algebraic method and relies on the Euclidean algorithm and the preliminary work in Section 5.1. It is possible to design both FIR and IIR filters using the algorithm, however, computations occur over the ring of polynomials. The polynomial algorithm used to solve (5.5) will be used to construct a solution to PR equation formed by filters with prespecified zeros. In FIR case, Fact 1 and Fact 2 guarantee the uniqueness and minimal length property when the degree conditions required are met.

Algorithm:

Let Ω be chosen such that it contains the origin and it is symmetric with respect to the origin. Suppose $G_1(z)$ and $G_2(z)$ in D_Ω are prespecified and contain the to-be-assigned zeros, i.e., $G_1(z)$ and $G_2(z)$ has the form $G_1(z) = G_{1n}(z)/G_{1d}(z)$ and $G_2(z) = G_{2n}(z)/G_{2d}(z)$ where the zeros of the polynomials $G_{1n}(z)$ and $G_{2n}(z)$ consist only of the to-be-assigned zeros and polynomials $G_{1d}(z)$ and $G_{2d}(z)$ have their zeros arbitrary but fixed in Ω. Moreover, let $\big(G_1(z)G_2(-z), G_1(-z)G_2(z)\big)$ be coprime. Define $G(z) := G_1(z)G_2(-z)$. The PR equation (5.9), in terms of $G(z)$ and $\hat{H}_p(z)$ and for a given odd delay $n_0 > 0$, becomes

$$G(z)\hat{H}_p(z) - G(-z)\hat{H}_p(-z) = 2z^{-n_0}. \tag{5.15}$$

In order to determine a particular solution $\hat{H}_p(z)$ of (5.15), one may follow the steps below:

i. Write $G(z)$ and $G(-z)$ in the standard form

$$G(z) = \frac{G_n(z)}{G_d(z)} = U_G(z)\frac{G_n(z)}{z^g},$$

and

$$G(-z) = (-1)^g U_G(-z)\frac{G_n(-z)}{z^g}$$

where g is the Euclidean degree of $G(z)$, $U_G(z) = z^g/G_d(z)$ is a unit in D_Ω and $G_n(z) = G_{1n}(z)G_{2n}(-z)$, $G_d(z) = G_{1d}(z)G_{2d}(-z)$. (When working with FIR filters, we can take $U_G(z) = 1$.)

ii. Solve the polynomial equation

$$G_n(z)f_1(z) - G_n(-z)f_2(z) = z^{g-n_0+t} \tag{5.16}$$

with $t := max(g-1, n_0-g)$. Note that $(G_n(z), G_n(-z))$ are coprime polynomials by the coprimeness of $G(z), G(-z)$ over D_Ω.

A solution to (5.16) can be found as follows. First, solve

$$G_n(z)\alpha(z) - G_n(-z)\beta(z) = 1$$

for some polynomials $\alpha(z)$ and $\beta(z)$. A solution can be determined by the polynomial Euclidean division algorithm of Appendix A. In the next step, by Euclidean division in the polynomial ring there exist $\gamma(z)$ and $f_2(z)$ with $deg\ f_2(z) < deg\ G_n(z)$ such that

$$z^{g-n_0+t}\beta(z) = \gamma(z)G_n(z) + f_2(z).$$

Finally, $f_1(z)$ is defined as

$$f_1(z) = z^{g-n_0+t}\alpha(z) - \gamma(z)G_n(-z).$$

iii. $F_1(z)$ and $F_2(z)$ defined as

$$F_1(z) = U_G^{-1}(z)\frac{f_1(z)}{z^t}, \quad F_2(z) = (-1)^g U_G^{-1}(-z)\frac{f_2(z)}{z^t}.$$

are now a solution pair to

$$G(z)F_1(z) - G(-z)F_2(z) = 2z^{-n_0}.$$

The product filter $\hat{H}_p(z)$ satisfying (5.15) is obtained as

$$\hat{H}_p(z) = F_1(z) + F_2(-z) = \frac{U_G^{-1}(z)}{z^t}\big[f_1(t) + (-1)^{g+t} f_2(-z)\big].$$

The individual analysis filters come from a factorization of $\hat{H}_p(z)$. Let $\hat{H}_{1p}(z)$ and $\hat{H}_{2p}(z)$ be any filters in D_Ω satisfying

$$\hat{H}_{1p}(z)\hat{H}_{2p}(-z) = \frac{U_G^{-1}(z)}{z^t}\big[f_1(z) + (-1)^{g+t} f_2(-z)\big]$$

Then,

$$H_{1p}(z) = G_1(z)\hat{H}_{1p}(z)$$

and

$$H_{2p}(z) = G_2(z)\hat{H}_{2p}(z)$$

are a pair of particular analysis filters with assigned zeros. The set of all solutions with the same assigned zeros can be constructed using (5.14) in Theorem 1.

Note that this algorithm, also provides a control on the poles of the filters. Since it is possible to specify $G_{1d}(z)$ and $G_{2d}(z)$ as well. Moreover, new poles inside Ω can be added using the freedom in $\Theta(z)$.

Example 6. Let Ω be specified as $\{0\}$. Our aim is to design analysis filters that satisfy PR equation. Furthermore, filters are required to have a flat passband and ripples of magnitude 0.1 at most in the stopband. For that purpose, we choose assigned zeros such that the assigned zeros of the lowpass filter suppress frequencies around π and those of the highpass filter suppress frequencies around 0. Thus, let $\{-1, -0.97 \pm j0.2431\}$ and

n	$\hat{H}_p(z)$	$H_{1p,1}(z)$	$H_{2p,1}(z)$	$H_{1p,2}(z)$	$H_{2p,2}(z)$
0	0.017772808	0.349944392	0.050637984	0.044496347	0.398245678
1	-0.098461361	0.810135407	0.117228979	-0.087882084	-0.786551304
2	0.196628063	0.430350685	-0.117203556	-0.162218309	0.438969255
3	-0.098461281	-0.162218165	-0.438968953	0.430351615	0.117203214
4	0.017772779	-0.087881681	0.786551349	0.810135148	-0.117228958
5		0.044496155	-0.398245803	0.349943656	-0.050637885

Table 5.1: The coefficients of the filters designed in Example 6.

$\{1, 0.8 \pm j0.6\}$ be zeros of the analysis lowpass filter and the analysis highpass filter, respectively. The overall delay is given as $n_0 = 5$. Thus,

$$G_1(z) = \frac{z^3 + 2.94z^2 + .94z + 1}{z^3},$$
$$G_2(z) = \frac{z^3 - 2.9z^2 + 2.9z - 1}{z^3},$$
$$G(z) = \frac{z^6 + 5.84z^5 + 14.366z^4 + 19.052z^3 + 14.366z^2 + 5.84z + 1}{z^6}.$$

Upon running the algorithm we get a particular solution $\hat{H}_p(z)$. Table 5.1 lists the coefficients of $\hat{H}_p(z)$, $H_{1p,1}(z)$, $H_{2p,1}(z)$, $H_{1p,2}(z)$, and $H_{1p,2}(z)$. One factorization of $\hat{H}_p(z)$ gives the filters $H_{1p,1}(z)$ and $H_{2p,1}(z)$. Another factorization gives the filters $H_{1p,2}(z)$ and $H_{2p,2}(z)$. Figure 5.1 shows the frequency response magnitude plots of $H_{1p,1}(z)$ and $H_{2p,1}(z)$ and Figure 5.2 shows that of $H_{1p,2}(z)$ and $H_{2p,2}(z)$. Note that due to the zeros we have assigned filters satisfy the requirements in their passbands and stopbands.

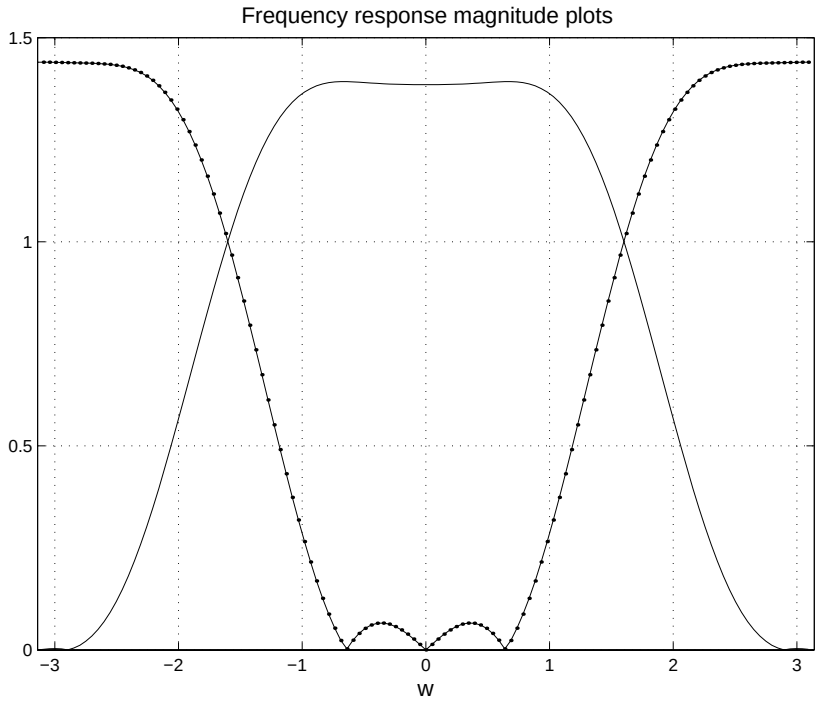

Figure 5.1: The frequency response magnitude plots of filters $H_{1p,1}(z)$ and $H_{2p,1}(z)$ designed in Example 6.

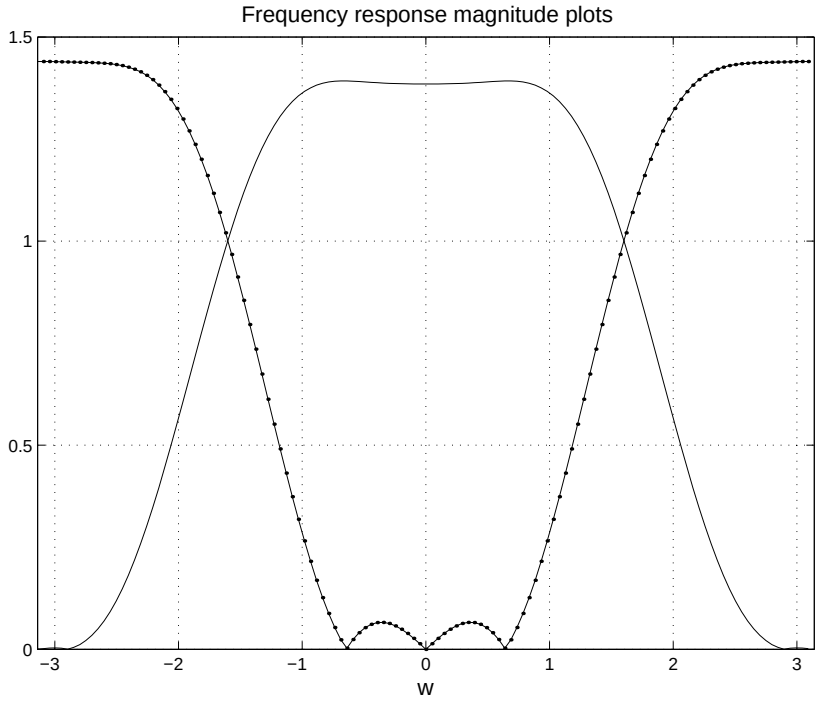

Figure 5.2: The frequency response magnitude plots of filters $H_{1p,2}(z)$ and $H_{2p,2}(z)$ designed in Example 6.

n	$\hat{H}(z)$	$H_1(z)$	$H_2(z)$
0	0.001900000	0.225795989	0.008314964
1	-0.010526000	0.668245656	0.024608235
2	0.020049595	0.653487222	-0.009336967
3	-0.005147184	0.070014279	-0.096274414
4	-0.028097603	-0.242847036	-0.017218334
5	0.005152612	-0.027964498	0.250216259
6	0.068588132	0.099797665	0.061104148
7	0.005152633	-0.008268874	-0.662232862
8	-0.028097551	-0.025666755	0.660646889
9	-0.005147227	0.008540522	-0.219827918
10	0.020049588		
11	-0.010525984		
12	0.001899995		

Table 5.2: The coefficients of the filters designed in Example 7(i).

Example 7. Let the a stability set Ω be $\{0, \pm 0.1 \pm j0.1\}$. Note that the FIR filters of Example 6 are still in Ω since $0 \in \Omega$. In this example, we will use the free parameter $\Theta(z)$ in Theorem 1 to construct more general solutions from the particular solution of Example 6.

(i) Let us first construct FIR solution with better stopband. Let

$$\Theta(z) = \frac{0.0019z^6 - 0.005z^4 - 0.005z^2 + 0.0019}{z^6},$$

and $l_0 = 4$. Then, a product filter $\hat{H}(z)$ is given as

$$\hat{H}(z) = z^{-l_0}\hat{H}_p(z) + G(-z)\Theta(z)$$

Upon factorizing $\hat{H}(z)$ such that $H_1(z)$ has the minimum-phase zeros of $\hat{H}(z)$, we get the analysis filters whose coefficients are given in Table 5.2. Figure 5.3 shows the frequency response magnitude plots of the resulting filters.

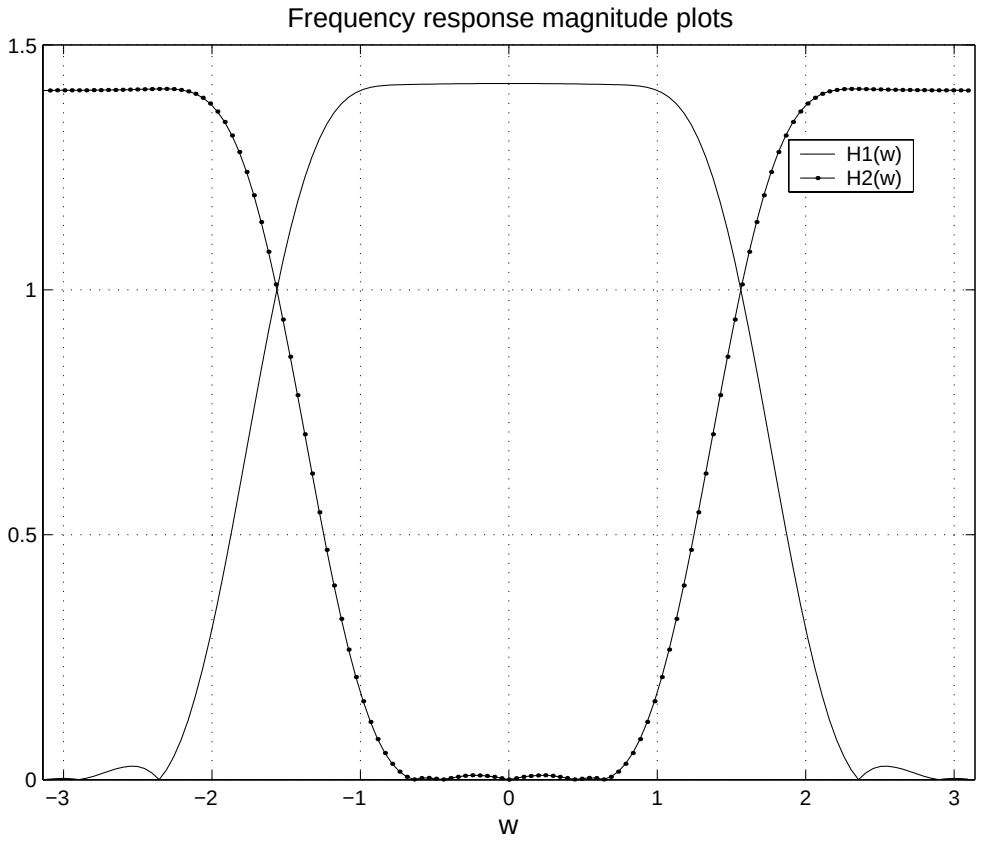

Figure 5.3: The frequency response magnitude plots of filters designed in Example 7(i).

(ii) Let us now choose $\Theta(z) = \frac{0.00342z^4+0.002897}{z^4+0.0004}$. Choosing the particular solution to be $\hat{H}_p(z)$ of Example 6 and letting $l_0 = 2$, we have

$$\begin{aligned}\hat{H}(z) &= z^{-l_0}\hat{H}_p(z) + G(-z)\Theta(z) \\ &= \frac{0.0034z^10 - 0.0189z^9 + 0.0629z^8 - 0.1576z^7 + 0.2446z^6 - 0.1335z^5}{z^6(z^4+0.0004)} \\ &\quad + \frac{0.0594z^4 - 0.0501z^3 + 0.0383z^2 - 0.0161z + 0.0029}{z^6(z^4+0.0004)}\end{aligned}$$

Upon factorizing $\hat{H}(z)$ such that the minimum-phase zeros of $\hat{H}(z)$ are assigned to the lowpass filter $H_1(z)$, the analysis filters come out to be

$$\begin{aligned}H_1(z) &= 0.3088\Big[\frac{(z+1)(z^2+1.94z+1)(z^2-0.8606z+0.20434)}{z^7(z^2-0.2z+0.02)} \\ &\quad \times (z^2-0.5712z+0.2281)(z^2+0.7926z+0.4038)\Big] \\ H_2(z) &= 0.01101\frac{(z-1)(z^2-1.6z+1)(z^2+0.3474z+7.27)(z^2+4.5514z+6.175)}{z^5(z^2-0.2z+0.02)}\end{aligned}$$

Figure 5.4 shows the frequency magnitude responses of these IIR analysis filters.

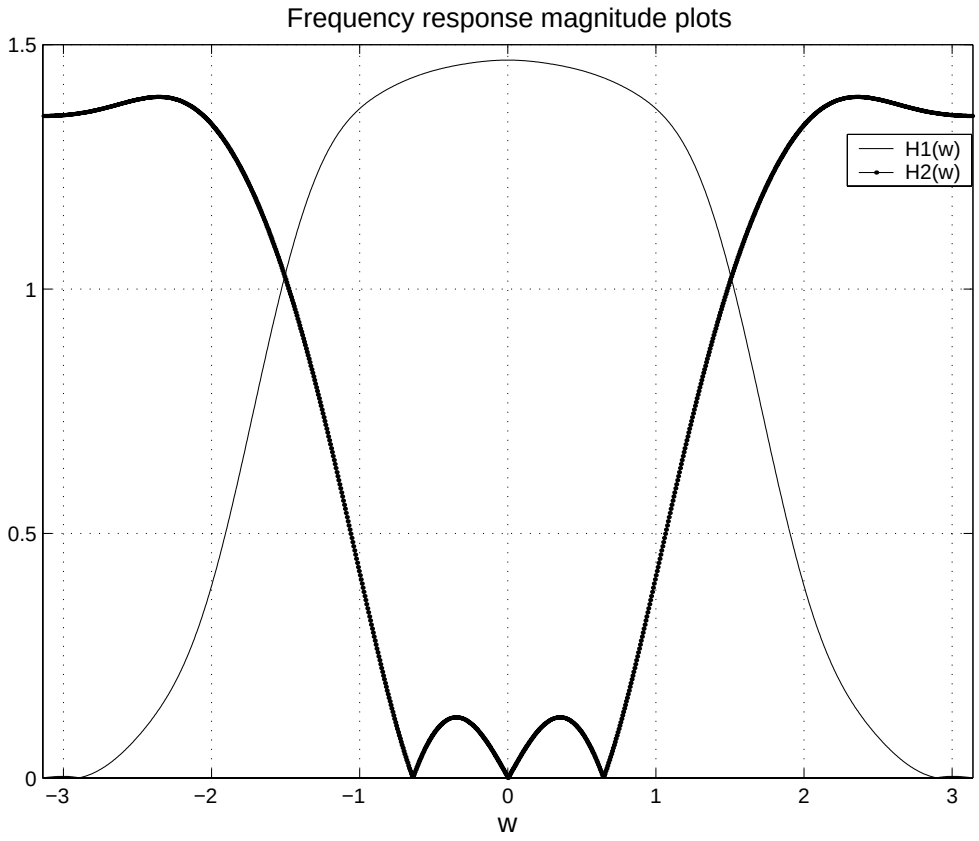

Figure 5.4: The frequency magnitude plots of filters designed in Example 7(ii).

Example 8. Let the stability set Ω be the disk with radius 0.1 and centered at the origin. It is possible to choose poles of $G_1(z)$ and $G_2(z)$ different from 0 at the outset. Let $G_1(z) = \frac{(z^2+1.6z+1)(z^2+1.84z+1)}{z^2(z^2-0.1z+0.005)}$, $G_2(z) = \frac{(z-0.9)(z^2-1.9z+1)}{(z+0.07)^3}$ and $n_0 = 7$. The algorithm gives

$$\hat{H}(z) = -\frac{(z-0.07)^3(z^2-0.1z+0.005)(z^2-3.2454+z4.7821)(z^2-0.5692z+0.1062)(z-2.4253)}{z^{10}}$$

The analysis filters are

$$H_1(z) = 0.2387\frac{(z^2+1.6z+1)(z^2+1.84z+1)(z-0.07)^3(z^2-0.5692z+0.1062)}{z^7(z^2-0.1z+0.005)},$$
$$H_2(z) = -0.0423\frac{(z-0.9)(z^2-1.9z+1)(z^2+0.1z+0.005)(z+2.4253)(z^2+3.2454z+4.7821)}{z^5(z+0.07)^3}.$$

Figure 5.5 shows the frequency response magnitude plots of the analysis filters.

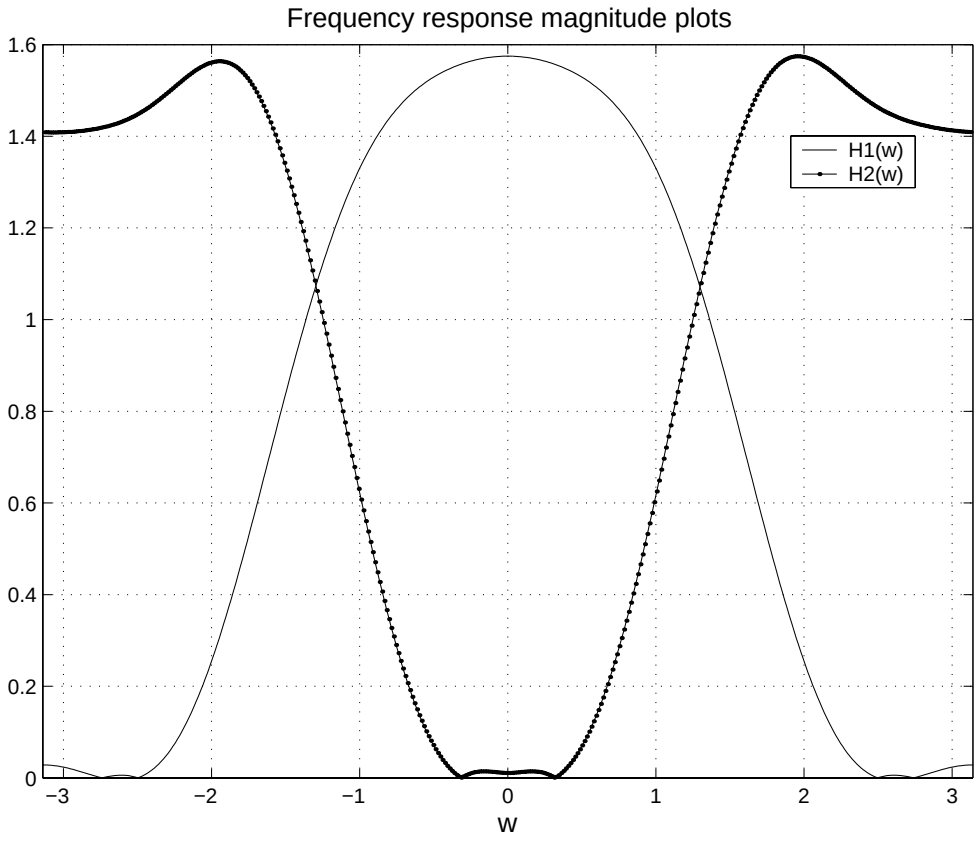

Figure 5.5: The frequency response magnitude plots of filters designed in Example 8.

5.4 FIR Filters

In this section, we will focus attention on FIR filters. Thus, we let $\Omega = \{0\}$ throughout this section so that D_Ω consists of FIR transfer functions which can be viewed as polynomials in the delay element z^{-1}. The Euclidean degree of an FIR filter is its order (i.e., its number of poles), or equivalently, the degree of the filter function considered as a polynomial in z^{-1}.

A typical need for zero assignment in FIR filters arises in designing filters with a frequency magnitude response as flat as possible. Degree of flatness of filters is determined by the number of zeros at $z = -1$ for low-pass filters and by

the number of zeros at $z = 1$ for high-pass filters. Daubechies, in her design of orthogonal wavelets with compact support, exploited the correspondence between orthogonal wavelets and PR filter banks discovered by Mallat [13]. The required filters for orthogonal wavelets are QMF and power complementary. Daubechies determined the minimum filter length for a given degree of flatness, or equivalently, the maximum degree of flatness possible for a given filter length. A characterization of all QMF, PR filters of varying degrees of flatness is another of her main results. In what follows, we show how such results, in more generality, are obtained from Theorem 1.

5.4.1 Orthogonal FIR Filter Banks

Consider the filter bank of Figure 2.1. If the synthesis filters satisfy

$$H_2(z) = -z^{-n} H_1(-z^{-1}), \tag{5.17}$$

where n is the order of the filter $H_1(z)$ and an odd integer, then the filters are said to be quadrature mirror or QMF.[2] This selection provides orthogonal filter banks as explained in Section 3.2. Substituting (5.17) in (5.9), we have

$$H_1(z)H_1(z^{-1}) + H_1(-z)H_1(-z^{-1}) = 2z^{n-n_0} \tag{5.18}$$

which implies, upon replacing z by z^{-1} and comparing the resulting equality with (5.18), $n = n_0$, i.e., *time delay in a PR filter bank with QMF property is equal to the order of the individual (analysis or synthesis) filters.*

If H_1 and H_2 have assigned zeros, then they are as in (5.8) so that

$$G_2(z)\hat{H}_2(z) = -z^{-n} G_1(-z^{-1})\hat{H}_1(-z^{-1}).$$

Let us suppose that the assigned zeros are chosen in accordance with QMF so that the transfer functions G_1 and G_2 satisfy $G_2(z) = z^{-k} G_1(-z^{-1})$, where k is the

[2] In order to distinguish this property from the more restrictive QM property $H_2(z) = H_1(-z)$, (5.17) is sometimes referred to as "conjugate quadrature property", [17], [15]. See [20] for a detailed discussion of QMF property.

order of $G_1(z)$. It follows, by the fact that the order of a multiple of elements in D_Ω is the sum of their orders, that $\hat{H}_2(z) = -z^{-\hat{n}}\hat{H}_1(-z^{-1})$, where $\hat{n}$ is the order of $\hat{H}_1(z)$, which implies that the product lowpass filter $\hat{H}(z) = \hat{H}_1(z)\hat{H}_2(-z)$ has symmetric coefficients, i.e.,

$$\hat{H}(z) = z^{-2\hat{n}}\hat{H}(z^{-1}). \tag{5.19}$$

Conversely, suppose $G(z)$ with order $2k$ has symmetry property and a solution $\hat{H}(z)$ to (5.13) also has symmetry property. Let $2\hat{n}$ be the order of $\hat{H}(z)$. Substituting z^{-1} for z in (5.13), multiplying by a suitable power of z^{-1}, and employing the symmetry conditions, we have

$$G(z)\hat{H}(z) - G(-z)\hat{H}(-z) = 2z^{-(2k+2\hat{n}-n_0)} = z^{-n_0}$$

so that $\hat{n} = n_0 - k$. Thus, the order of any symmetric solution to (5.13) is $2n_0 - 2k$. A spectral factorization of $\hat{H}(z)$ into $\hat{H}(z) = \hat{H}_1(z)\hat{H}_2(-z)$, where $\hat{H}_1(z)$ consists of zeros inside the unit disk and $\hat{H}_2(-z)$ outside, with zeros on unit circle shared appropriately, can be carried out. The analysis filters are then obtained by (5.8) and satisfy (5.17) provided $G_2(z) = z^{-k}G_1(-z^{-1})$.

We will need the following result concerning symmetric FIR filters.

Lemma 1. *Let $H(z) \in \mathbf{D}_{\{\mathbf{0}\}}$ have order n and write $H(z) = \sum_{i=0}^{n} H_i z^{-i}$ for real numbers H_i, $i = 0, 1, 2, ..., n$.*

(i) For any integer k, $z^{-k}H(z^{-1}) \in D_{\{0\}}$ if and only if $k \geq n$. If $k \geq n$, then $z^{-k}H(z^{-1})$ has order at most k.

(ii) $z^{-k}H(z^{-1}) \in \mathbf{D}_{\{\mathbf{0}\}}$ has order n if and only if $k = n$ and $H(z)$ is biproper, i.e., $H_0 \neq 0$.

(iii) $z^{-k}H(z^{-1}) = H(z)$ and $H(z)$ is biproper if and only if $k = n$ and $H_i = H_{n-i}$ for all $i = 0, ..., n$.

Proof. Since $H(z)$ has order n, $H_n \neq 0$. All claims easily follow by the expression $z^{-k}H(z^{-1}) = H_0 z^{-k} + ... + H_n z^{-(k-n)}$. □

We can now state and prove our main result on FIR filter banks with assigned zeros.

Theorem 2. *Let $G_1(z), G_2(z) \in \mathbf{D}_{\{\mathbf{0}\}}$ be of order k each and satisfy (5.11). Let CQF property $G_1(z) = z^{-k}G_2(-z^{-1})$ also hold.*

(i) For each odd integer $n_0 \in [0, 4k-1]$, a minimal order FIR solution $\hat{H}_p(z)$ to (5.13) is unique and has order at most $2k-2$. This solution has symmetry property (equivalently, a factorization of it into analysis filters satisfying the CQF property exists) if and only if $n_0 = 2k-1$ and $\hat{H}_p(z)$ has order $2k-2$.

(ii) The set of all analysis filters with assigned zeros resulting in PR-QMF filter banks are given by $H_1(z) = G_1(z)\hat{H}_1(z)$, $H_2(z) = G_2(z)\hat{H}_2(z)$, where

$$\hat{H}(z) = z^{-l_0}\hat{H}_p(z) + G(-z)\Theta(z) \tag{5.20}$$

for some even $\Theta(z)$ having symmetry property. A choice of $\Theta(z)$ with order $2(l_0 - 1)$ results in a filter bank of time delay $2k + l_0 - 1$ for even $l_0 \geq 2$ and analysis filters of order $2k + l_0 - 1$.

Proof. (i) By Theorem 1(i), where $g = 2k$, a solution of order at most $2k-1$ exists provided $n_0 \in [0, 4k-1]$. By Fact 2 of Section 5.1, it is unique and is of minimal order. Moreover, by the fact that n_0 is odd and the order of $G(z)$ is even, it must be that the order of any solution is also even. Hence, $\hat{H}_p(z)$ has order at most $2k-2$. We first show that, if $n_0 = 2k-1$, then the unique solution to (5.13) has symmetry property. Replacing z by z^{-1} in (5.13), and multiplying each term by a suitable power of z, we have

$$z^{-2k}G(z^{-1})z^{2k-2n_0}\hat{H}_p(z^{-1}) - z^{-2k}G(-z^{-1})z^{2k-2n_0}\hat{H}_p(-z^{-1}) = 2z^{-n_0}.$$

Invoking the symmetry property of $G(z)$, we obtain

$$G(z)z^{2k-2n_0}\hat{H}_p(z^{-1}) - G(-z)z^{2k-2n_0}\hat{H}_p(-z^{-1}) = 2z^{-n_0}.$$

Since the order of $\hat{H}_p(z)$ is at most $2k-2$, by Lemma 1(i), $z^{2k-2n_0}\hat{H}_p(z^{-1})$ is an FIR filter transfer function as $2n_0 - 2k = 2k-2$ is greater or equal to the order of $\hat{H}_p(z)$. By the uniqueness of a solution, we have that $\hat{H}_p(z) = z^{2k-2}\hat{H}_p(z^{-1})$ and hence, by Lemma 1(iii), the order of $\hat{H}_p(z)$ is exactly $2k-2$.

We have established prior to the statement of Lemma 1 that the order $2\hat{n}$ of any symmetric solution $\hat{H}(z)$ to (5.13) satisfies $2n_0 = 2k + 2\hat{n}$. Suppose $n_0 < 2k-1$ and a delay of n_0 gives a symmetric solution $\hat{H}(z)$. With $\hat{H}_p(z)$ being the unique solution obtained with delay equal to $2k-1$ above, We claim that $\hat{H}(z)$ is not bicausal, contradicting symmetry by Lemma 1(iii). In fact, with $l := 2k-1-n_0$, $z^{-l}\hat{H}(z)$ is clearly a solution to (5.13) with delay $2k-1$. By uniqueness of a solution for a given delay, it must be that $z^{-l}\hat{H}(z) = \tilde{H}(z)$. Thus, $\tilde{H}(z)$ is not bicausal. This argument shows that the symmetric solution $\hat{H}_p(z)$ obtained for the delay $2k-1$ is the only symmetric solution among all delays up to $2k-1$. This proves (i).

(ii) Theorem 1(ii) gives that a product lowpass filter $\hat{H}(z)$ giving a PR filter bank of time delay $n_0 + l_0$ in terms of a particular one $\hat{H}_p(z)$ giving a time delay n_0 can be written as $\hat{H}(z) = z^{-l_0}\hat{H}_p(z) + G(-z)\Theta(z)$, where $G(z) = G_1(z)G_2(-z)$. Suppose $\hat{H}_p(z)$ and $G(z)$ both satisfy the symmetry properties $\hat{H}_p(z) = z^{-2\hat{n}}\hat{H}_p(z^{-1})$ and $G(z) = z^{-2k}G(z^{-1})$. In order for $\hat{H}(z)$ also have the symmetry property, it should hold that

$$z^{-l_0}\hat{H}_p(z) + G(-z)\Theta(z) = z^{-N}[z^{l_0}\hat{H}_p(z^{-1}) + G(-z^{-1})\Theta(z^{-1})],$$

where N is the order of $\hat{H}(z)$. By the fact that the time delay is equal to the order of $H_1(z)$, N should satisfy $N+2k = 2(n_0+l_0)$ which gives $N = 2k+2l_0-2$. The order of the left hand side of the equality $\hat{H}(z) = z^{-l_0}\hat{H}_p(z) + G(-z)\Theta(z)$ is thus strictly greater than the order $l_0 + 2k - 2$ of the first term $z^{-l_0}\hat{H}_p(z)$ on the right hand side. It must be that the order of $G(z)\Theta(z)$ is equal to $2k + 2l_0 - 2$. Therefore, the order of $\Theta(z)$ is equal to $2(l_0-1)$ and gives an analysis filter $H_1(z)$

of order $2k + l_0 - 1$. $\square$

Example 9. In this example, we will design D_3, a Daubechies filter of smoothness order 3. The analysis lowpass filter has three zeros at $z = -1$. Therefore,

$$G_1(z) = \frac{(z+1)^3}{z^3}$$

which is of order $k = 3$. Choosing $G_2(z)$ according to the requirement $G_2(z) = z^{-k}G_1(-z^{-1})$, we have

$$G_2(z) = -\frac{(z-1)^3}{z^3}.$$

Using the constructive algorithm with the overall delay $2k - 1 = 5$, first we must solve the polynomial equation

$$-(z+1)^6 f_1(z) + (z-1)^6 f_2(z) = z^6.$$

Following the algorithm, we get

$$\begin{aligned}
t &= 5, \\
f_1(z) &= -0.0059z^5 + 0.0352z^4 - 0.0742z^3 + 0.0352z^2 - 0.0059z, \\
f_2(z) &= -0.0059z^5 - 0.0352z^4 - 0.0742z^3 - 0.0352z^2 - 0.0059z, \\
F_1(z) &= \frac{-0.0059z^5 + 0.0352z^4 - 0.0742z^3 + 0.0352z^2 - 0.0059z}{z^5}, \\
F_2(z) &= (-1)^6 \frac{-0.0059z^5 - 0.0352z^4 - 0.0742z^3 - 0.0352z^2 - 0.0059z}{z^5}, \\
\hat{H}_p(z) &= \frac{-0.0117z^4 + 0.0703z^3 - 0.1484z^2 + 0.0703z - 0.0117}{z^4}, \\
\hat{H}_p(z) &= -0.0117\frac{(z^2 - 5.4255z + 9.4438)(z^2 - 0.5745z + 0.1059)}{z^4}.
\end{aligned}$$

The roots of $\hat{H}_p(z)$ are $2.7127 \pm j1.4439$ and $0.2873 \pm j0.1529$. Factorizing the product filter $\hat{H}_p(z)$, we have

$$\begin{aligned}
H_{1p}(z) &= 0.3327\frac{(z+1)^3(z^2 - 0.5745z + 0.1059)}{z^5}, \\
H_{2p}(z) &= 0.0352\frac{(z-1)^3(z^2 + 5.4255z + 9.4438)}{z^5}.
\end{aligned}$$

Here, the minimum phase zeros are assigned to the lowpass filter and the non-minimum phase zeros are assigned to the highpass filter. The constant -0.0117 is factorized in

such a way that the sum of the squares of the resulting filters' coefficients is 1, i.e., the filters have unit energy. Analysis filters we designed are the same as the synthesis filters of D_3. In the cascade algorithm in Section 4.4, the synthesis section is used to generate wavelets. Thus, it is possible to construct Daubechies wavelet D_3 using the analysis section of the filter bank we have designed. Figure 5.6 shows the wavelet and the scaling function generated from $H_{1p}(z)$ and $H_{2p}(z)$.

The order of $\hat{H}_p(z)$ is $2k-2=4$ as stated in Theorem 2(i). The filter bank designed is of minimal order. It is possible to get a higher order orthogonal filter bank with the same assigned zeros. By Theorem 2(ii), this is possible if and only if an even $\Theta(z)$ of order $2(l_0-1)$ with symmetry property is used in (5.20). Let l_0 be 2 and select $\Theta(z)$ as $(0.01z^2+0.01)/z^2$ which satisfies the symmetry property. The new product filter $\hat{H}(z)$ is

$$\begin{aligned}
\hat{H}(z) &= z^{-2}\hat{H}_p(z) - \frac{(z-1)^6}{z^6}\frac{(z^2+1)}{z^2} \\
&= \frac{-0.01z^8+0.06z^7-0.1717z^6+0.3303z^5}{z^8} \\
&\quad + \frac{-0.4484z^4+0.3303z^3-0.1717z^2+0.06z-0.01}{z^8} \\
&= -\frac{(z^2-4.3548z+5.3805)(z^2-0.6432z+3.3395)}{z^8} \\
&\quad \times (z^2-0.1926z+0.2994)(z^2-0.8094z+0.1859),
\end{aligned}$$

which satisfies the symmetry property. Following the same factorization procedure, the individual filters come out to be

$$\begin{aligned}
H_1(z) &= \frac{0.424z^7+0.8472z^6+0.2693z^5-0.1529z^4}{z^7} \\
&\quad + \frac{0.0606z^3-0.0111z^2-0.0471z+0.0236}{z^7} \\
H_2(z) &= \frac{0.0236z^7+0.0471z^6-0.0112z^5-0.0605z^4}{z^7} \\
&\quad + \frac{-0.1529z^3-0.2694z^2+0.8472z-0.4240}{z^7}
\end{aligned}$$

They satisfy the orthogonality condition (5.17). Figure 5.7 shows the scaling and the wavelet functions generated from these filters.

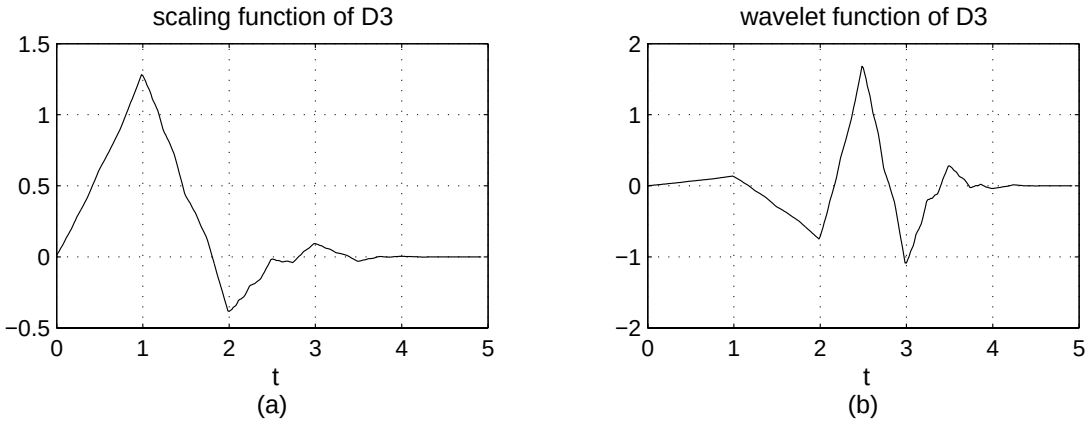

Figure 5.6: (a) The scaling function, (b) the wavelet function generated from the filters $H_{1p}(z)$ and $H_{2p}(z)$ designed in Example 9.

5.4.2 Biorthogonal FIR Filter Banks

In the absence of the relation (5.17) between analysis filters, any PR filter bank is called *biorthogonal* [21]. Biorthogonal filter banks produce biorthogonal wavelets depending on the existence of the zeros at $z = 1$ and $z = -1$. In the biorthogonal case, there are two wavelets and two scaling functions. The analysis filters $H_1(z)$ and $H_2(z)$ produce a wavelet $w(t)$ and a scaling function $\phi(t)$ and the synthesis filters produce a dual wavelet $\tilde{w}(t)$ and a dual scaling function $\tilde{\phi}(t)$ [21]. The wavelet functions satisfy the following biorthogonality relation

$$\langle w_{m,n}(t)\tilde{w}_{k,l}(t)\rangle = \delta[m-k]\delta[n-l].$$

Any function in the space spanned by these wavelets can be decomposed in two different ways, i.e.,

$$\begin{aligned} f(t) &= \sum_m \sum_n \langle w_{m,n}(t), f(t)\rangle \tilde{w}_{m,n}(t) \\ &= \sum_m \sum_n \langle \tilde{w}_{m,n}(t), f(t)\rangle w_{m,n}(t), \end{aligned}$$

since $w_{m,n}(t)$ and $\tilde{w}_{m,n}(t)$ play dual roles. In the biorthogonal case, it is possible to construct linear phase filters that satisfy PR and lead to symmetric wavelets [21]. This is not possible for the orthogonal filter banks except the Haar wavelet.

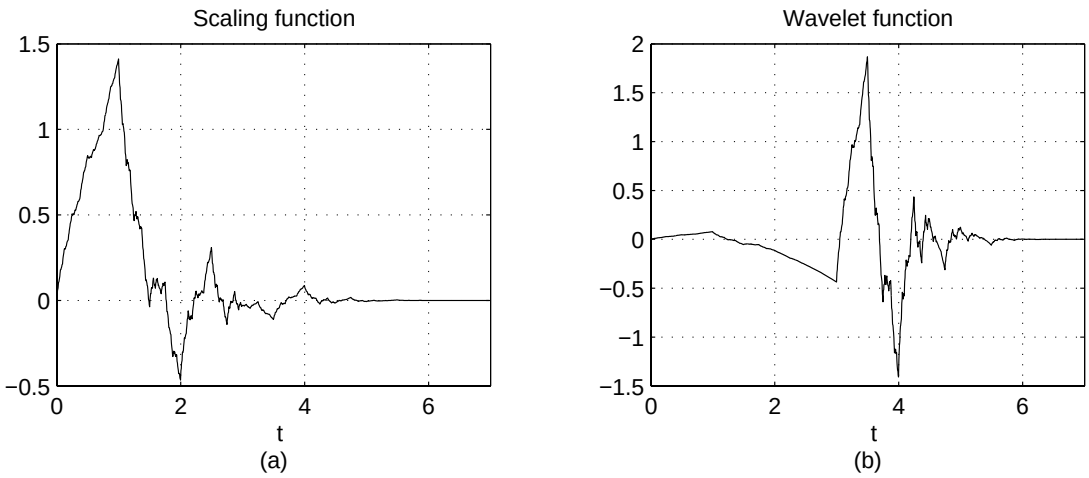

Figure 5.7: (a) The scaling function, (b) the wavelet function generated from the filters $H_1(z)$ and $H_2(z)$ designed in Example 9.

One easy way of designing biorthogonal wavelets is to design an orthogonal filter bank first and then factor it in such a way that orthogonality fails. We will illustrate this in the next example.

Example 10. Let $G_1(z) = (z+1)^2/(z^2)$ and $G_2(z) = (z-1)^2/(z^2)$. The constructive algorithm gives the following minimal order product filter.

$$\hat{H}_p(z) = (-0.0625z^2 + 0.25z - 0.0625)/z^2$$

Note that $\hat{H}_p(z)$ satisfies symmetry property. Therefore, it is possible to construct an orthogonal filter bank. In fact it gives the orthogonal filter bank that generates D_2. In this example, a factorization which gives a biorthogonal filter bank with linear phase filters will be performed. The product filter $\hat{H}_p(z)$ is assigned to the lowpass filter. The filter coefficients are adjusted so that the filters have unit norm. The filters are

$$\begin{aligned} H_1(z) &= -\frac{1}{4\sqrt{2}}\frac{(z^4 - 2z^3 - 6z^2 - 2z + 1)}{z^4}, \\ H_2(z) &= \frac{1}{2\sqrt{2}}\frac{(z^2 - 2z + 1)}{z^2}. \end{aligned}$$

Figure 5.8 shows the wavelet and the scaling functions generated.

In the previous example, the wavelet and the scaling functions generated from the analysis filters are very spiky. It is possible to improve them by increasing the

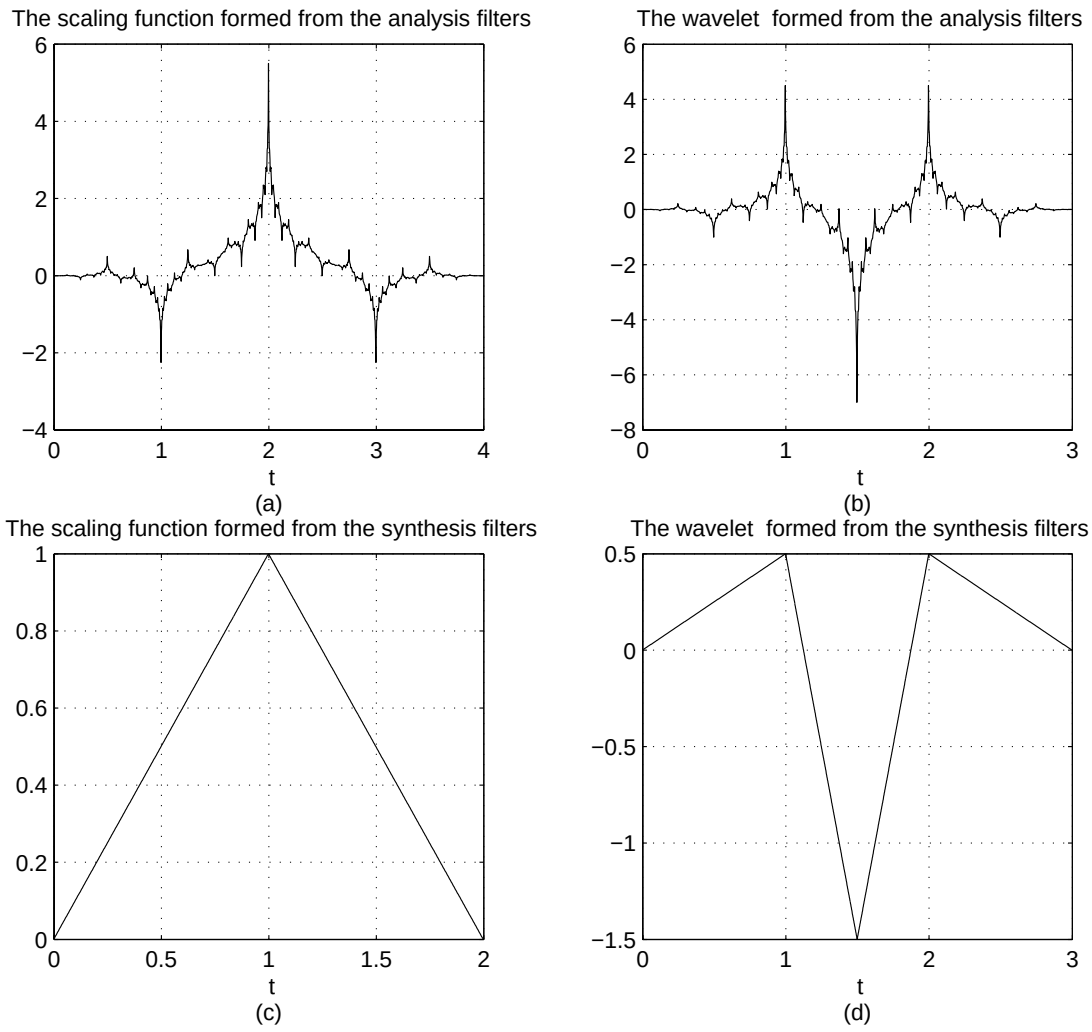

Figure 5.8: (a) The scaling function, (b) the wavelet function formed from the analysis filters. (c) The scaling function, (d) the wavelet function formed from the synthesis filters.

order of $\hat{H}_p(z)$. This is done using (5.14). It is possible to maintain the phase linearity designing a product filter with symmetry property and assigning the whole product filter to the lowpass or the highpass filter only. The next example exactly does this.

Example 11. Let $\Theta(z) = \frac{3}{64\sqrt{2}} \frac{z^2+1}{z^2}$, then by (5.14) where $\hat{H}_p(z)$ is in Example 10, the new product filter $\hat{H}(z)$ is

$$\hat{H}(z) = \frac{1}{64\sqrt{2}} \frac{3z^6 - 12z^5 + 5z^4 + 40z^3 + 5z^2 - 12z + 3}{z^6}$$

which has the symmetry property. The individual filters are

$$H_1(z) = \frac{1}{64\sqrt{2}} \frac{(3z^8 - 6z^7 - 16z^6 + 38z^5 + 90z^4 + 38z^3 - 16z^2 - 6z + 3)}{z^8},$$
$$H_2(z) = \frac{1}{2\sqrt{2}} \frac{(z^2 - 2z + 1)}{z^2}.$$

Figure 5.9 shows the wavelet and the scaling functions corresponding to this filter bank. This time there are no spikes. This illustrates the importance of the free parameter $\Theta(z)$.

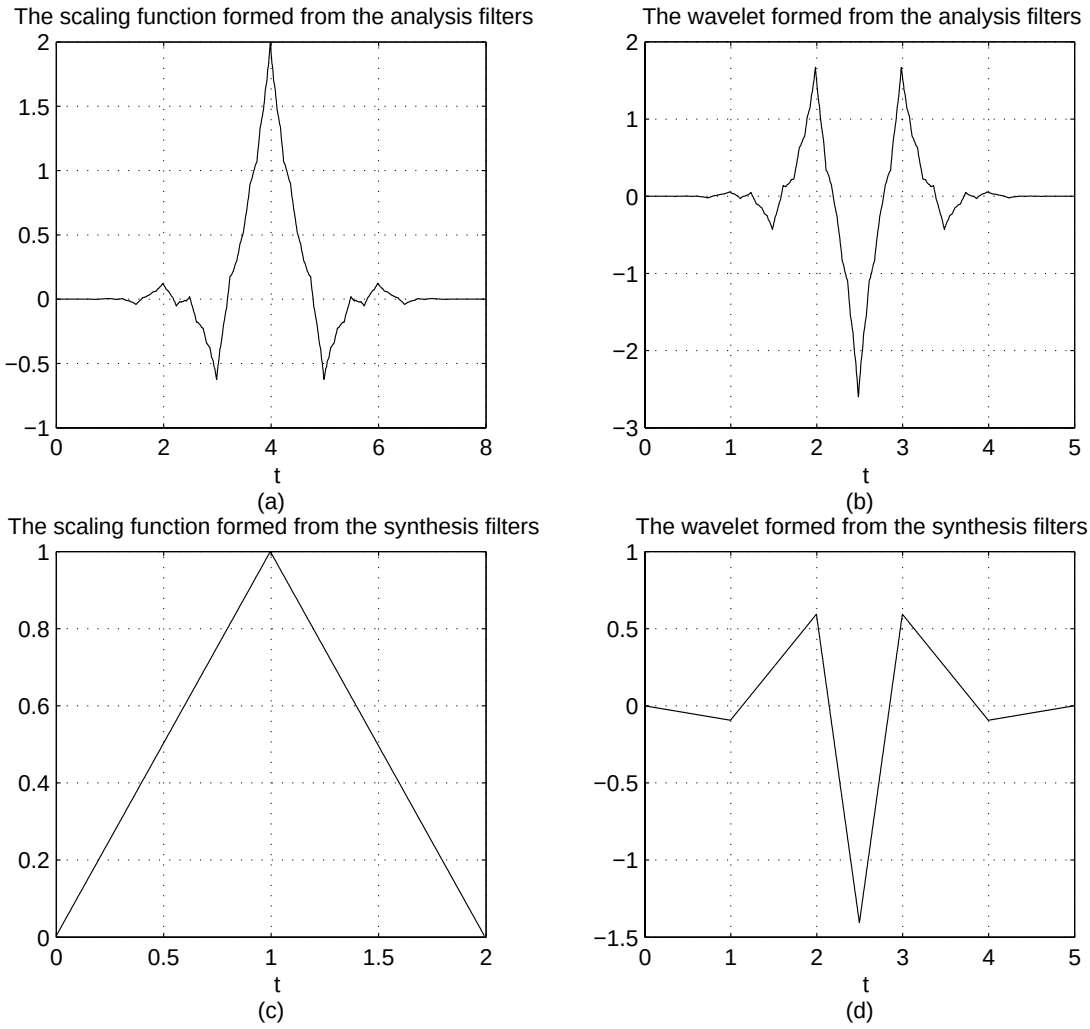

Figure 5.9: (a) The scaling function, (b) the wavelet function formed from the analysis filters. (c) The scaling function, (d) the wavelet function formed from the synthesis filters.

5.5 Robustness of Regularity of Minimal Length Wavelets

In Theorem 2, we have proved that an orthogonal FIR filter bank with analysis filters having k zeros at -1 (lowpass filter) and 1 (highpass filter) is possible and we have shown that the minimal order filters having these assigned zeros are of order $2k-1$. The wavelet and the scaling function generated from the synthesis filters corresponding to such analysis filters have k-vanishing moments, i.e.,

$$\begin{aligned} \int \phi(t)dt &= 1, \\ \int t^n \phi(t)dt &= 0 \quad \text{for } n = 1, 2, \ldots, k-1, \\ \int t^n w(t)dt &= 0 \quad \text{for } n = 0, 1, \ldots, k-1. \end{aligned}$$

These vanishing moments, for example, are important in numerical analysis applications or compression of large matrices [5]. Another important property of compactly supported wavelets is *regularity*. Regularity of a function is a measure of the differentiability of this function. Let C^n denote the space of n-times differentiable functions. Regularity of wavelet and scaling functions has a close relation to the number of zeros at -1 and 1 of the synthesis lowpass and highpass filters, respectively. If a scaling function $\phi(t)$ is compactly supported and $\phi(t) \in C^k$, then the synthesis lowpass filter[3] must have at least k-zeros at -1. The regularity of wavelet and scaling functions $\phi_N(t)$ and $w_N(t)$ generated from the minimal order synthesis filters having N zeros at -1 and 1 increases linearly as the support of these functions increases. However, $\phi_N(t) \in C^{\mu(N)}$ and $lim\ \mu(N)/N = 0.2075$ for large N, [5]. This means that, for large N, 80% of vanishing moments are wasted. Therefore, for a fixed support, it is possible to give up some vanishing moments in order to have more regular wavelet and scaling functions. Table 5.3 shows the regularity of $\phi_2(t)$, $\phi_3(t)$, and $\phi_N(t)$ for a large

[3]From this point on we will mention only the zeros of the synthesis lowpass filter because the highpass filter has a zero at $-1/z_0$ due to orthogonality. Here z_0 is a zero of the lowpass filter.

	C^0	C^1	C^2	$\cdots$	$C^{0.2075N}$
$\phi_2(t)$	$\surd$	$\times$	$\times$	$\cdots$	$\times$
$\phi_3(t)$	$\surd$	$\surd$	$\times$	$\cdots$	$\times$
$\phi_N(t)$	$\surd$	$\surd$	$\surd$	$\cdots$	$\surd$

Table 5.3: Regularity of $\phi_2(t)$, $\phi_2(t)$, and $\phi_N(t)$ for a large N.

n	Lowpass filter coef.	Highpass filter coef.
0	0.26470182888814	0.03913298187377
1	0.77142053992871	0.11406453485679
2	0.55640509458866	-0.10351113318248
3	-0.10351113318248	-0.55640509458866
4	-0.11406453485679	0.77142053992871
5	0.03913298187377	-0.26470182888814

Table 5.4: The synthesis filter coefficients corresponding to most regular scaling and wavelet functions

N. Note that even for $N = 2$ and $N = 3$, we are wasting some 2 zeros at -1 and 1 because $\phi_2(t)$ is in C^0 and $\phi_3(t)$ is in C^1.

In this section, we will investigate the regularity of compactly supported wavelet and scaling functions of support $[0, 5)$. In [5], Daubechies designs the most regular wavelet and scaling functions of support $[0, 5)$ via an optimization procedure. Since $\phi_3(t)$ is in C^1, at least one zero of the synthesis lowpass filter at -1 is necessary. However, the synthesis lowpass filter corresponding to $\phi_3(t)$ has three zeros at -1. Daubechies keeps two of them and moves the remaining in the complex plane. When the remaining zero is at $z = -1.4749$ the most regular wavelet and scaling functions are obtained. Table 5.4 gives the coefficients of the synthesis lowpass and highpass filters corresponding to these most regular functions.

In Theorem 2, we have determined how to obtain minimal-length filters for a FIR-PR filter bank with desired assigned zeros. This allows us to examine the robustness of the regularity of the obtained wavelet and the scaling functions.

We start with the most regular wavelet and scaling functions. Corresponding synthesis lowpass filter has two zeros at -1 and a zero at -1.4749. We will perturb first the zero at -1.4749 only, and then, the zero at -1.4749 together with one of the zeros at -1.

In what follows, we denote the most regular wavelet and the scaling functions of support $[0, 5)$ as $w_{reg}(t)$ and $\phi_{reg}(t)$, respectively. Denoting a perturbed wavelet and a scaling function by $w_p(t)$ and $\phi_p(t)$, respectively, we assess the regularity of these in comparison with the most regular wavelet and scaling functions $w_{reg}(t)$ and $\phi_{reg}(t)$. We use two heuristic measures in order to determine the robustness against the perturbation. The first one relies on the cross-covariance values. The cross-covariance of the functions $\phi_{reg}(t)$ and $\phi_p(t)$ is defined as

$$C_\phi = \int_0^N (\phi_{reg}(t) - \mu_{\phi_{reg}})(\phi_p(t) - \mu_{\phi_p})dt = \int_0^N \phi_{reg}(t)\phi_p(t)dt - N\mu_{\phi_{reg}}\mu_{\phi_p}$$

where ϕ_{reg} and ϕ_p are the means of ϕ_{reg} and $\phi_p(t)$, respectively, and N is the support of the scaling functions. We can write C_w for the wavelet functions using the expression of C_ϕ. One difficulty here is that we do not have these continuous time functions as they are obtained by the limiting cases of (4.39) and (4.40). Let us use discrete approximations instead of continuous functions in writing C_ϕ and C_w. Let $w_{reg}[n]$, $\phi_{reg}[n]$, $w_p[n]$, and $\phi_p[n]$ be approximated wavelet and scaling functions after eight iteration of the cascade algorithm. The cross-covariance for these discrete functions is given as

$$C_\phi = \sum_{n=0}^{N'} (\phi_{reg}[n] - \mu_{\phi_{reg}})(\phi_p[n] - \mu_{\phi_p}) = \sum_{n=0}^{N'} \phi_{reg}[n]\phi_p[n] - (N'+1)\mu_{\phi_{reg}}\mu_{\phi_p}$$

where scaling functions have support $[0, N']$.

The second measure is based on the derivative of the difference between $\phi_p(t)$ and $\phi_{reg}(t)$. If a perturbed scaling function has a regularity very close to that of the most regular one, we expect that the difference function $\phi_p(t) - \phi_{reg}(t)$ will be very smooth which means that the magnitude of the derivative of the difference function will be small. Since derivative operation is linear, derivative

of difference is the same difference of derivatives. We know that $\phi_{reg}(t)$ is in C^1, hence, it is differentiable. This means that, at any point t_0, the left and the right derivatives of $\phi_{reg}(t)$ are equal, i.e.,

$$\lim_{\Delta t \to 0} \frac{\phi_{reg}(t_0) - \phi_{reg}(t_0 - \Delta t)}{\Delta t} = \lim_{\Delta t \to 0} \frac{\phi_{reg}(t_0 + \Delta t) - \phi_{reg}(t_0)}{\Delta t}$$

and the derivative of $\phi_{reg}(t)$ at t_0 is the same the left and the right derivatives. However, as in the previous measure, we have to work with discrete (sampled) functions and hence, we do not have an expression for the derivative. Thus, we introduce the right-difference $d_r[n_0]$ and the left-difference $d_l[n_0]$ at a point n_0 as follows

$$d_l[n_0] = \phi_{reg}[n_0] - \phi_{reg}[n_0 - 1],$$
$$d_r[n_0] = \phi_{reg}[n_0 + 1] - \phi_{reg}[n_0].$$

We expect that for a high sampling rate, the difference between $d_r[n_0]$ and $d_l[n_0]$ will be very small for the samples of a differentiable continuous function. Therefore, we can approximate the derivative of $\phi_{reg}(t)$ as the average of d_r and d_l divided by the sampling period T_s. Since the sampling period is the same for all scaling functions, we can omit it in the definition. As a result, the approximate derivative of $\phi_{reg}(t)$ at n_0 can be obtained as $(d_r[n_0] + d_l[n_0])/2 = (\phi_{reg}[n_0 + 1] - \phi_{reg}[n_0 - 1])/2$. We can calculate the approximate derivative of a perturbed scaling function in the same way. Our criteria is to check the maximum differences between derivatives $d_{\phi,max}$ and $d_{w,max}$ defined as

$$\begin{aligned} d_{\phi,max} &= \max_n \Big| (\phi_p[n+1] - \phi_p[n-1]) - (\phi_{reg}[n+1] - \phi_{reg}[n-1]) \Big|, \\ d_{w,max} &= \max_n \Big| (wp[n+1] - wp[n-1]) - (w_{reg}[n+1] - w_{reg}[n-1]) \Big|. \end{aligned}$$

When $d_{\phi,max}$ and $d_{w,max}$ are small, we conclude that the perturbed scaling/wavelet function is close to the most regular scaling/wavelet function.

Table 5.5 lists the perturbed zeros of the lowpass and the highpass filters, the cross-covariance values for the associated scaling and the wavelet functions

and the maximum differences $d_{\phi,max}$ and $d_{w,max}$. There are twenty different cases. Figures 5.10, 5.11, 5.12, 5.13, and 5.14 show the wavelet and scaling functions associated to the cases (0,1,2,3), (4,5,6,7), (8,9,10,11), (12,13,14,15), and (16,17,18,19), respectively. Case 0 is the most regular one found by Daubechies [5]. It has the maximum covariance value for both the wavelet and the scaling functions. In both measures, Case 13 is the closest to the most regular case, Case 0. Among the cases 1-7 (only the zero at -1.4749 is perturbed), Case 5 is the most successful in both measures. The critical zero at -1.4749 is perturbed by as much as 25.41% but C_ϕ and C_w changed only by 2.1% and 4.3%, respectively. In Case 6, perturbing the critical zero by 35.6% results in 2.5% and 5.08% deviation in C_ϕ and C_w. When two zeros are perturbed (Case 8-19), the most successful is Case 13 in which the critical zero at -1.4749 is perturbed by 25.41% and the zero at -1 is perturbed by 10%. The cross-covariance values C_ϕ and C_w are changed by 1.01% and 2.08%. In Case 14, the perturbation of the zero at -1.4749 is very close to that of Case 13 but the zero at -1 is perturbed by 100%. This results in a very sharp decrease in the regularity. For example, the deviation in C_w becomes 48%. Therefore, the zero at -1 should not be changed too much.

In conclusion, we have observed that a change of about 20% in the critical zero location of the most regular wavelet results in at most 5% loss of regularity as measured by C_ϕ and C_w. Similarly, the same location change results in a negligible loss of smoothness as measured by $d_{\phi,max}$ and $d_{w,max}$.

Case	Lowpass filter zeros	Highpass filter zeros	C_ϕ	C_w	$d_{\phi,max}$	$d_{w,max}$
0	-1.4749	0.678	204.41	255.79	0	0
1	-0.1	10	146.14	109.71	0.08028302354797	0.20373519453968
2	-0.5	2	169.32	167.61	0.03676156368384	0.10767068890673
3	-0.75	1.333	185.63	208.52	0.01759987803525	0.05866316427791
4	-0.9	1.111	193.20	227.53	0.01089190885237	0.03913717601915
5	-1.1	0.909	200.11	244.85	0.00617007557556	0.02104485456079
6	-2	0.5	199.21	242.78	0.00921044979700	0.02440682003032
7	-5	0.2	141.23	105.83	0.04770842187740	0.11602979104981
8	-1, -1	1, 1	197.12	237.33	0.00828202658462	0.02918647207416
9	-0.1, -0.1	10, 10	71.67	-74.26	0.46592984176500	0.94873428896644
10	-0.5, -0.5	2, 2	126.84	60.82	0.11724237683618	0.28413648673457
11	-0.75, -0.75	1.333, 1.333	169.60	168.21	0.03250507255488	0.09735022995950
12	-0.9, -0.9	1.111, 1.111	188.53	215.80	0.01447789772562	0.04980649695986
13	-1.1, -1.1	0.909, 0.909	202.35	250.46	0.00464778901550	0.01357108113660
14	-2, -2	0.5, 0.5	153.28	132.31	0.03284324671261	0.06689641824730
15	-5, -5	0.2, 0.2	-26.86	-217.14	0.14784878000057	0.32921828384737
16	$-0.9 \pm j0.4359$	$0.9 \pm j0.4359$	191.69	223.84	0.01570890966185	0.04578482922494
17	$-0.8 \pm j0.6$	$-0.8 \pm j0.6$	183.06	202.59	0.02008000640811	0.05908125150989
18	$-0.7071 \pm j0.7071$	$0.7071 \pm j0.7071$	170.91	172.88	0.04776402691921	0.10090097776274
19	$-0.5 \pm j0.5$	$-1 \pm j1$	116.21	34.29	0.14240734427135	0.34756744538444

Table 5.5: The perturbed zeros of the synthesis lowpass and highpass filters, and C_ϕ, C_w, $d_{\phi,max}$, and $d_{w,max}$ for the associated scaling and wavelet functions.

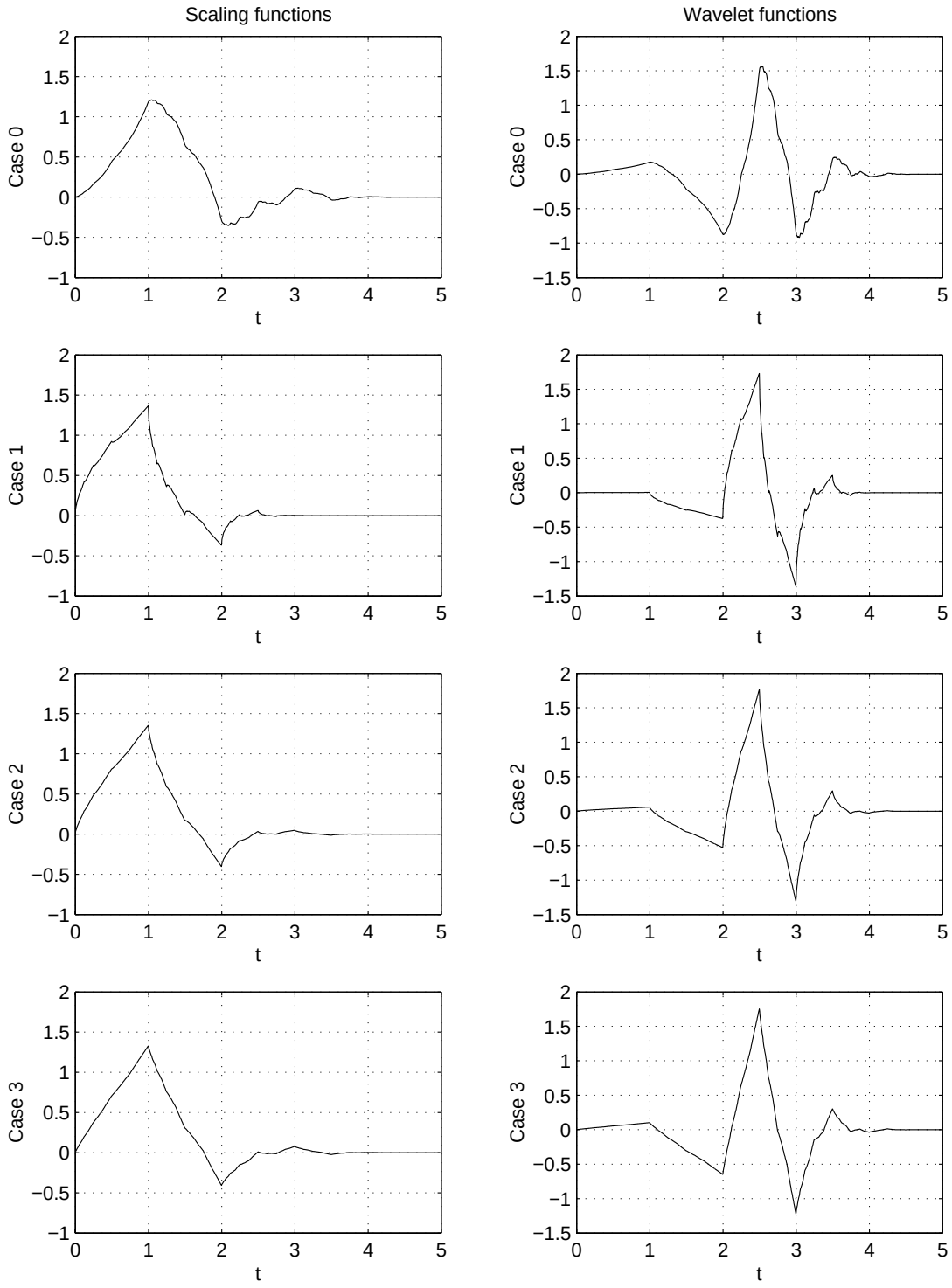

Figure 5.10: The first column shows the scaling functions and the second column shows the wavelet functions of the cases 0, 1, 2, and 3 of Table 5.5.

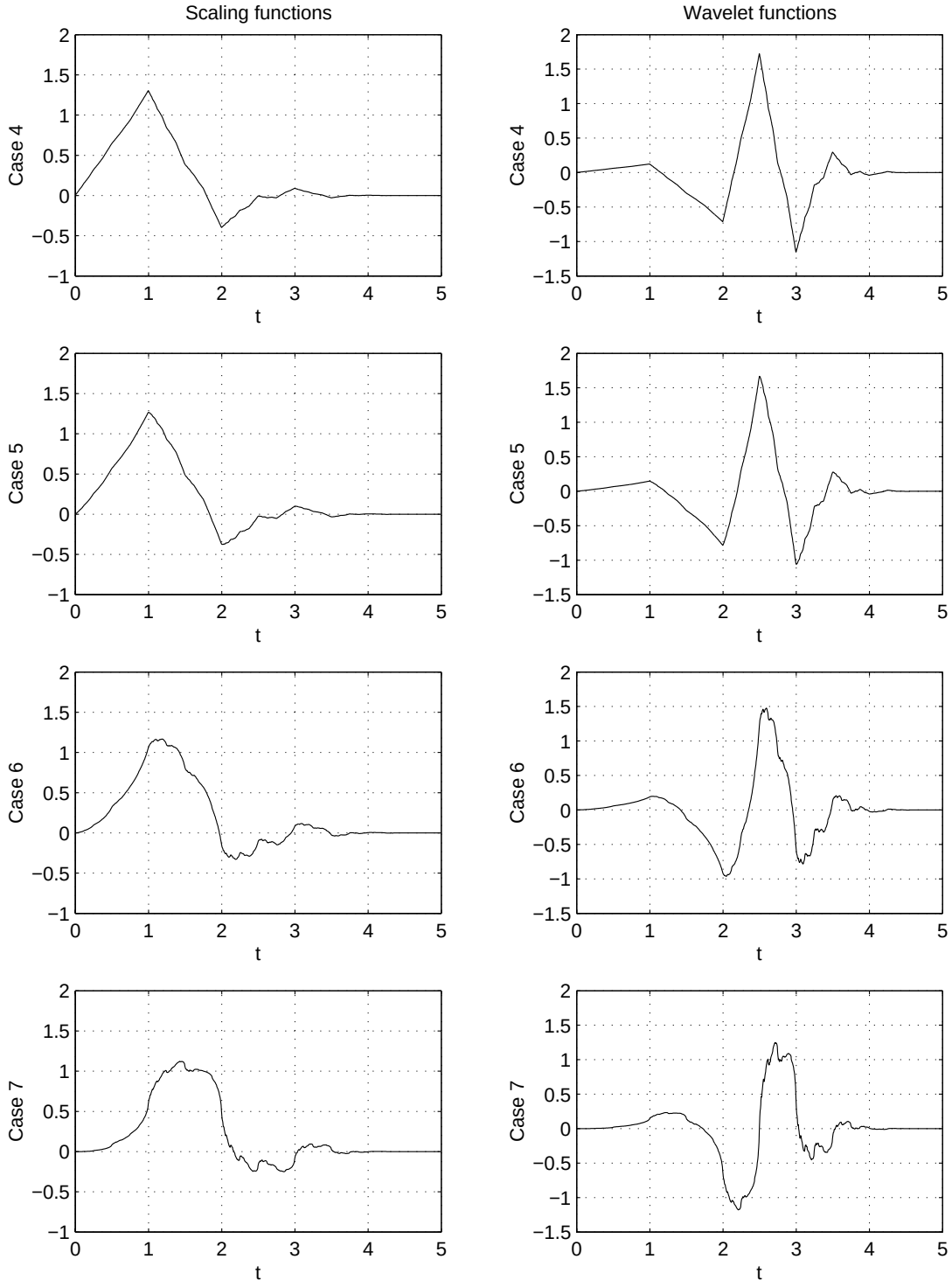

Figure 5.11: The first column shows the scaling functions and the second column shows the wavelet functions of the cases 4, 5, 6, and 7 of Table 5.5.

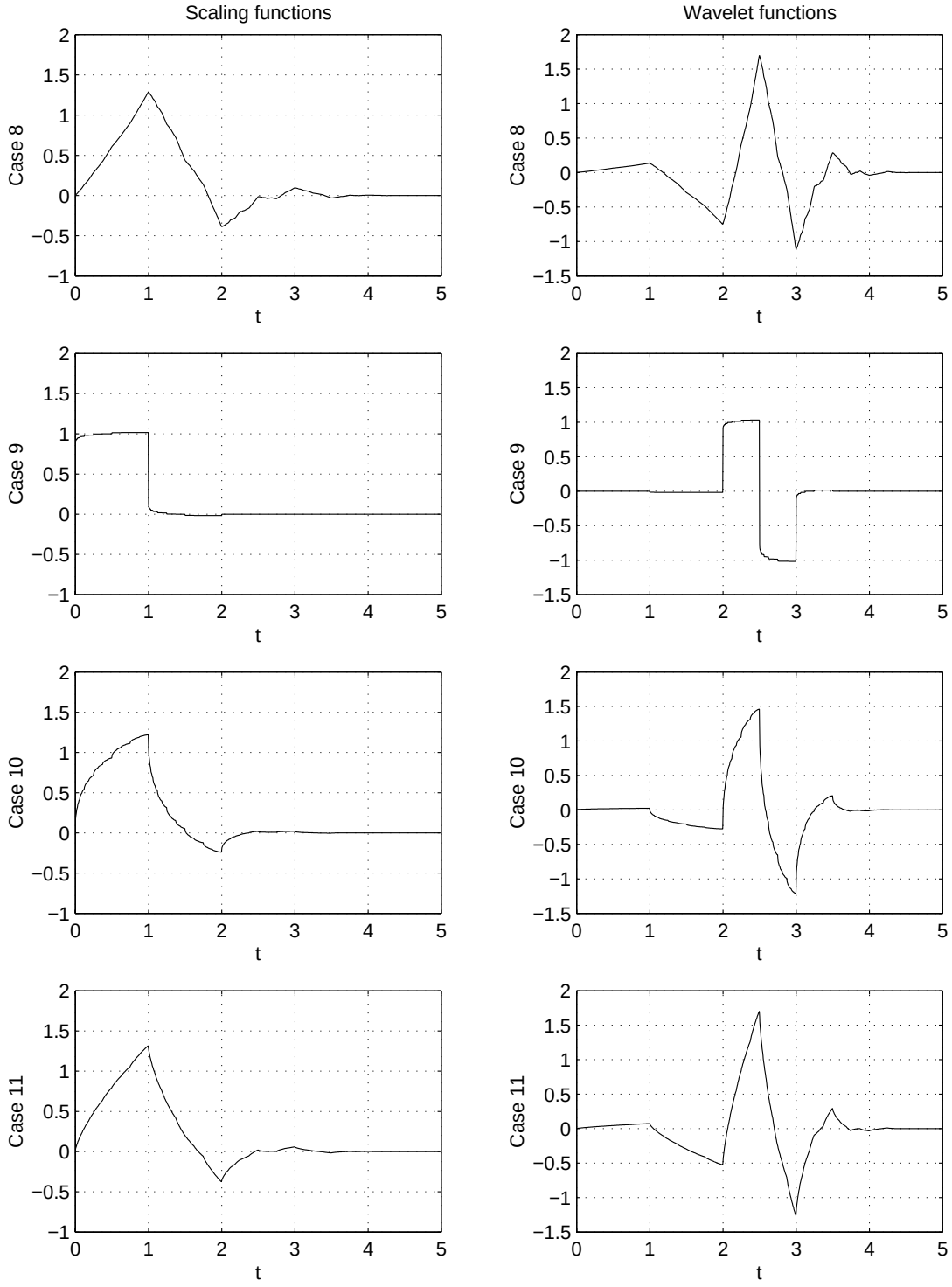

Figure 5.12: The first column shows the scaling functions and the second column shows the wavelet functions of the cases 8, 9, 10, and 11 of Table 5.5.

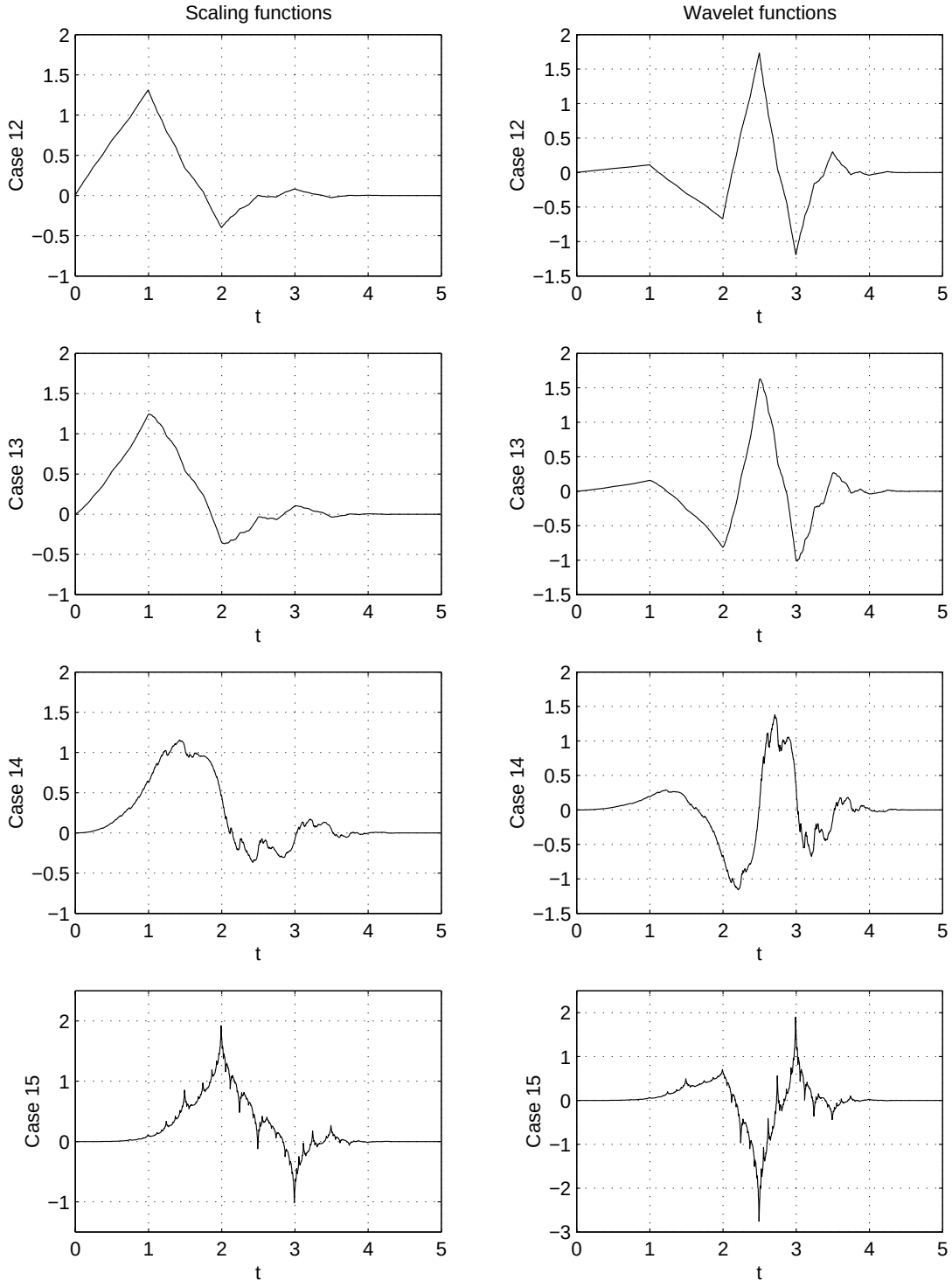

Figure 5.13: The first column shows the scaling functions and the second column shows the wavelet functions of the cases 12, 13, 14, and 15 of Table 5.5.

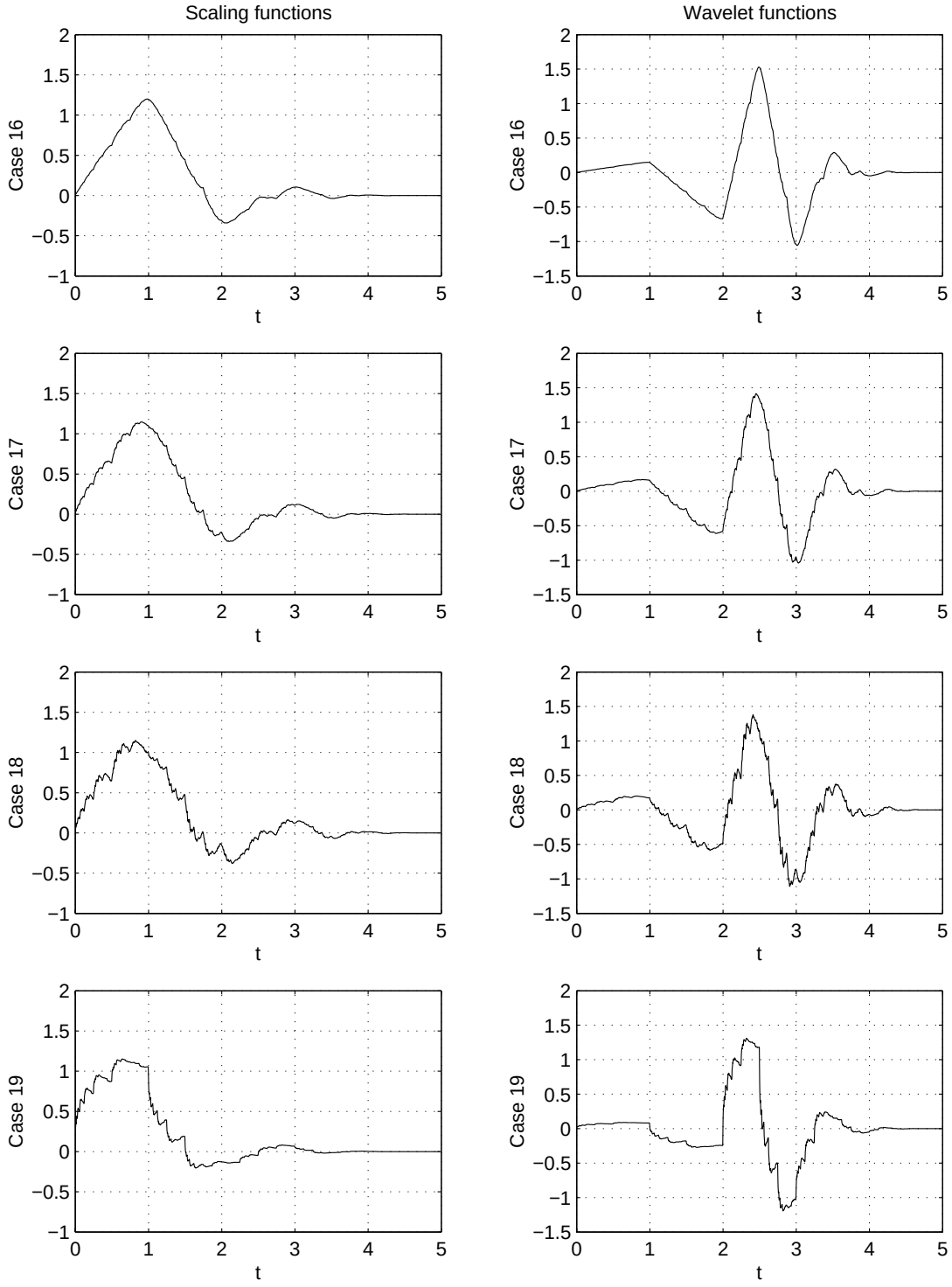

Figure 5.14: The first column shows the scaling functions and the second column shows the wavelet functions of the cases 16, 17, 18, and 19 of Table 5.5.

Chapter 6

CONCLUSION

We have considered PR filter banks and associated wavelets. The focus of our attention was on assigning zeros and poles to analysis filters. The following are the main contributions of this thesis:

(i) It is possible to assign to the analysis filters any number of desired zeros and place the poles in any desired region in the complex plane while preserving the perfect reconstruction property.

(ii) All "product lowpass filters" in a PR filter bank can be described based on a particular product filter and a free parameter $\Theta(z)$ which is an even, causal transfer function with poles in the same region as the poles of the filters.

(iii) All FIR filters having conjugate quadrature property can be described based on a particular product filter and a free parameter $\Theta(z)$ which is an even function having symmetry property.

(iv) A minimal length FIR filter with conjugate quadrature property exists for any given set of assigned zeros. Such filters have the same length as the overall delay in the filter bank.

(v) Most of Daubechies' conclusions on minimal-length compactly supported orthonormal wavelets are thus shown to hold for arbitrarily assigned zeros, not necessarily for zeros at -1 and 1.

We have also shown, using the result in (iv), how to examine the robustness of regularity of minimal-length compactly supported orthonormal wavelets with respect to perturbations of zeros at -1 (and 1). Finally, we have illustrated how the free parameter $\Theta(z)$ can be used to generate orthogonal and biorthogonal wavelets with extra desired properties.

The main result of Theorem 1 has other potential applications not considered in this thesis. Perhaps, the most promising application is in the case the distortions modelled by $d_1[n]$ and $d_2[n]$ of Figure 2.1 are present (nonzero). The reconstruction with delay will then be corrupted by terms caused by $d_i[n],\ i = 1, 2$. One open problem is thus to optimally design the analysis filters so that the "influence" of distortions on the reconstructed output is at a minimum. If the influence is quantified by an H_∞-norm, then the problem becomes one of a special H_∞-optimization problem in which the free parameter $\Theta(z)$ should be optimally chosen. This problem is currently under study.

Appendix A

Polynomial Division Algorithm

Let polynomials a and b be coprime, i.e., no zeros in common. There exists a polynomial pair (x, y) which is a particular solution of the equation

$$ax + by = 1.$$

Following algorithm finds the solution.

Step 1 We can assume that degree of a is greater than or equal to degree of b. Since $deg(a) \geq deg(b)$, we can find polynomials a_2 and b_2, with $deg(a_2) = deg(a) - deg(b)$, $deg(b_2) < deg(b)$, so that

$$a = a_2 b + b_2.$$

Step 2 Similarly, we can find a_3 and b_3 with $deg(a_3) = deg(b) - deg(b_2)$, $deg(b_3) < deg(b_2)$, so that

$$b = a_3 b_2 + b_3.$$

We keep going on this procedure, with b_{n-1} taking the role of b in this last equation, and b_n the role of b_2,

$$b_{n-1} = a_{n+1} b_n + b_{n+1}.$$

Since $deg(b_n)$ is strictly decreasing, this has to stop at some point, which is only possible if $b_{N+1} = 0$ for some N, with $b_N \neq 0$,

$$b_{N-1} = a_{N+1} b_N .$$

Step 3 Since

$$b_{N-2} = a_N b_{N-1} + b_N ,$$

it follows that b_N divides b_{N-2} as well. By induction b_N divides all the previous b_n, and b so that b_N divides both a and b. Since a and b have no zeros in common, it follows that b_N is a constant different from zero.

Step 4 By induction

$$b_N = \tilde{a}_{N,k} b_{N-k} + \tilde{b}_{N,k} b_{N-k-1},$$

with $\tilde{a}_{N,1} = -a_N$, $\tilde{b}_{N,1} = 1$, $\tilde{a}_{N,k+1} = \tilde{b}_{N,k} - \tilde{a}_{N,k} a_{N-k}$, and $\tilde{b}_{N,k+1} = \tilde{a}_{N,k}$. For $k = N - 1$, we find

$$b_N = \tilde{a}_{N,N-1} b + \tilde{b}_{N,N-1} a.$$

It follows that

$$x = \tilde{b}_{N,N-1} / b_N$$

and

$$y = \tilde{a}_{N,N-1} / b_N .$$

Bibliography

[1] Akansu, A., N., Smith, M., *Subband and wavelet transforms : design and applications*, Kluwer Academic Publishers, Boston, 1996.

[2] Cohen, A., "Ondelettes, analyses multirésolutions et filtres miroir en quadrature", Ann. Inst. H. Poincaré, Anal. non linéaire, 7, pp. 439-459, 1990.

[3] Croiser A., Estaban D. ve Galand C. "Perfect channel splitting by use of interpolation/decimation/tree decomposition techniques" Int. Symp. on Info., Circuits and Systems, Patras, Greece, 1976.

[4] Daubechies, I., "Orthonormal Bases of Compactly Supported Wavelets", Comm. Pure and Appl. Math. 41, 909-996, 1988.

[5] Daubechies, I., "Othonormal Bases of Compactly Supported Wavelets II. Variations on a Theme", SIAM J. Math. Anal., vol. 24, pp. 499-519, 1990.

[6] Daubechies, I., *Ten Lectures on Wavelets*, Capital City Press, Vermont, 1992.

[7] Daubechies, I., and Sweldens, W., "Factoring wavelet transforms into lifting steps", J. Fourier Anal. Appl., 4 (no. 3), pp. 247-269, 1998.

[8] Gabor, D., *Theory of Communation, J. IEE,* 93:429-457, 1946.

[9] Grossman, A. and Morlet, J., "Decomposition of Hardy Functions into Square Integrable Wavelets of Constant Shape", SIAM J. Math, Anal. 15, 723-736, 1984.

[10] Herstein, I.N., *Topics in Algebra*, John Wiley & Sons Inc., New York, 1975.

[11] Khargonekar, P. P. and Özgüler, A. B., "System-theoretic and algebraic aspects of the rings of stable and proper stable rational functions", *Linear Algebra and its Applications*, 66: 123-167, 1985.

[12] MacDuffee, C. C., *The Theory of Matrices*, Chelsea Pub. Com., New York, 1946.

[13] Mallat S., *A Wavelet Tour of Signal Processing*, Academic Press, San Diego, USA, 1998.

[14] Meyer, Y., *Wavelets and Operators*, Advanced Mathematics, Cambridge University Press, 1992.

[15] Mintzer F., "Filters for distortion-free two-band multirate filter banks," IEEE Trans. Acoust., Speech, Signal Processing, 33(3):626-630, June 1985.

[16] Morse, A. S., "System invariants under feedback and cascade control", in *Lecture Notes in Economics and Mathematical Systems*, 131, Springer, New York, 1976.

[17] Smith M., ve Barnwell T. P., "A procedure for designing exact reconstruction filter banks for tree-structured subband coders," Proc. IEEE Int. Conf. Acoust., Speech, Signal Processing, San Diego, CA, March 1986.

[18] Oppenheim A. V. ve Schafer R. W., *Discrete-Time Signal Processing*, Prentice Hall, New Jersey, USA, 1989.

[19] Strang, G., *Wavelets and Filter Banks*, Wellesly-Cambridge Press, Boston, 1996.

[20] Vaidyanathan, P.P., *Multirate Systems and Filter Banks*, Prentice Hall, New Jersey, 1993.

[21] Vetterli, M., *Wavelets and Subband Coding*, Prentice Hall, New Jersey, 1995.

[22] Vetterli, M., Heyley, C., "Wavelets and Recursive Filter Banks", IEEE Tran. on Signal Proc., 2536-2556, August 1993. Press, Boston, 1996.

[23] Vidyasagar M., *Control System Synthesis: A Factorization Approach*, The MIT Press, Massachusetts, USA, 1985.